BULLETIN OF THE ASTRONOMICAL INSTITUTES OF THE NETHERLANDS

1957 MAY 29 VOLUME XIII NUMBER 475

COMMUNICATIONS FROM THE NETHERLANDS FOUNDATION FOR RADIO ASTRONOMY AND THE OBSERVATORY AT LEIDEN

A CATALOGUE OF 21-CM LINE PROFILES

BY C. A. MULLER AND G. WESTERHOUT

This paper presents a catalogue of profiles of the 21-cm line of neutral hydrogen in 694 points in a strip approximately 20° wide around the galactic equator, from $l = 318°$ to $l = 220°$. The profiles are presented in the form of drawings giving the intensity as a function of radial velocity; a loose scale is added to facilitate reading the curves.
A description of the receiver and the method of observation is given. The frequency and intensity calibrations are discussed; the accuracies in absolute intensity (temperature scale) are ± 20%, in relative intensity ± 5% and in radial velocity ± 0.4 km/sec. The extinction at 21 cm was found to be 0.037 ± 0.003 db at the zenith. The profiles in the catalogue have been corrected for it.

1. *Introduction.*

The earlier large-scale survey of the emission of neutral hydrogen in the Galactic System, made at Kootwijk with a 7.5 m mirror, was finished in June 1953. This survey was limited to the galactic plane and has led to the establishment of the spiral structure in the outer parts of the Galactic System. The results were described in *B.A.N.* No. 452 [1]), in which paper also a brief account of the history of 21-cm research in the Netherlands was given, and the persons and institutions who took part in the development of the project were mentioned.

The present set of papers describes the results of a new survey, not limited to the galactic plane, made with improved equipment from November 1953 till August 1955. The work described was carried out under the auspices of the Netherlands Foundation for Radio Astronomy. All financial support was provided by the Netherlands Organization for Pure Research (Z.W.O.).

During the present investigation, continued use could be made of the 7.5-m Würzburg paraboloid of the P.T.T. Many thanks are due to Mr DE VOOGT, to the Director General of the P.T.T., and to the director of the Kootwijk transmitting station for their courtesy in making all facilities of the P.T.T. at Kootwijk available to us. In August 1955 the equipment was moved to the new observatory at Dwingeloo.

Brief summaries of the results reported in this paper have been given by OORT [2]), WESTERHOUT and SCHMIDT [3]) and VAN DE HULST [4]).

Of the authors, MULLER has been chiefly responsible for the instrument and the observations, and WESTERHOUT for most of the reductions. In total, about 45 persons assisted in some phase of the observations or reductions. Mr TEBRA and Mr HIN assisted in the construction and maintenance of the receiver, Mr KIEL did the largest share of the reductions and many students assisted as volunteers with the observations. Mr WOLTJER supervised the reductions for five months during the absence of WESTERHOUT. The total time during which the instrument was used for actual observations for the present programme was 7500 hours. The corresponding reduction has taken about 23500 man-hours.

We are greatly indebted to Prof. J. H. OORT and

[1]) H. C. VAN DE HULST, C. A. MULLER and J. H. OORT, *B.A.N.* **12**, 117 (No. 452), 1954.

[2]) J. H. OORT, *Mitt. A. G.*, 83, 1955.

[3]) G. WESTERHOUT and M. SCHMIDT, Radio Astronomy Symposium 1955, I.A.U. Symposium No. 4, Ch. 4–6, Cambridge University Press, 1957.

[4]) H. C. VAN DE HULST, I.A.U. Symposium, No. 5, Cambridge University Press, 1957.

CONTENTS

Prof. H. C. VAN DE HULST, who did the original planning and gave invaluable help and advice. Many discussions with them, and their constant encouragement have led to the successful completion of this investigation.

2. *Antenna and receiver.*

This section gives a brief description of antenna and receiver as used during the last part of the measurements in 1955. This receiver is the outcome of a gradual development during several years. Earlier versions of the receiver have been described in *B.A.N.* Nos. 452 and 458.

The antenna used in all measurements was a reflector of the Würzburg type, with an aperture of 7.5 metres and a focal length of 1.70 metre. The feed antenna at the focus consisted of a half-wave dipole with a reflector disk. The antenna system was carefully matched to a low-loss air-insulated rigid coaxial line of 2 metre length, which connected the antenna to the front end of the receiver mounted behind the reflector. The main lobe of the antenna beam had an elliptical cross section with half-power widths of 1°.85 and 2°.78. The pointing accuracy of the antenna system was 0°.1, in both azimuth and elevation.

The receiver is based on the switching principle, first introduced by DICKE. The receiver is being switched between two frequencies 1080 kc/s apart, at a rate of 400 c/s, one of the frequencies being at or near the 21-cm line frequency, the other away from it. As the signal at the line frequency is stronger than the other, we find in the output voltage after rectification a 400 c/s square wave component whose amplitude is a measure of the line intensity.

Since the receiver is tuned to a frequency outside the spectral line for half the switching period the information on the line profile is received for only half the observing time. The reduction in sensitivity due to this loss of information is overcome by using behind the wide-band front end of the receiver a parallel arrangement of two intermediate-frequency amplifiers, which are tuned to frequencies differing from each other by again 1080 kc/s. Two measurements are now carried out simultaneously (Figure 1). When the receiver is in the one switching position, the first i.f. amplifier receives the comparison frequency f_2, while the second receives the spectral line frequency f_1. In the other switching position the first i.f. amplifier is tuned to frequency f_1 and the second to a comparison frequency f_3 1080 kc/s to the other side of f_1. In both channels we find in the output after rectification a 400 c/s square wave component. The two 400 c/s components, which are in antiphase, are subtracted and their combined amplitude is measured. In this way the line radiation is measured during the full switching cycle and compared to the average power at the two comparison frequencies f_2 and f_3.

FIGURE 1

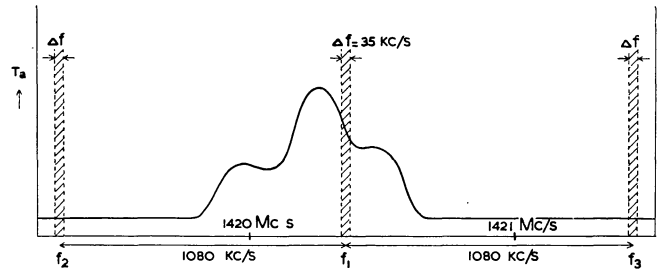

Schematic diagram of a line profile.

During a measurement of the line profile the three frequencies are slowly displaced together so that f_1 traverses the spectral line and f_2 and f_3 remain outside the profile, while the frequency differences between the three frequencies remain constant.

A receiver built on this principle must satisfy two stringent requirements:

a. The receiver must be identical in the two switching positions, as otherwise a spurious 400 c/s component may be measured due to a change in receiver properties.

b. The switching process should not influence the measurements, i.e. it must not cause spurious 400 c/s output voltages.

Both requirements have been adequately met. The receiver (see block diagram Figure 2) is of the superheterodyne type with triple frequency conversion. It has been described by one of us elsewhere [1]), so only the main features need be repeated.

The frequency switching is done in the first local oscillator of the receiver. An electronic switch driven by a 400 c/s oscillator alternately connects two crystal-controlled oscillators with a frequency difference of 5 kc/s at about 6.43 Mc/s to a frequency multiplier (216 ×), thus providing two frequencies near 1390 Mc/s, 1080 kc/s apart. The last stage of the multiplier, a tripler, is mounted together with the crystal mixer and the first three stages of the i.f. amplifier in a box behind the reflector surface. The 30 Mc/s i.f. amplifier has an overall bandwidth of 5 Mc/s.

The slow tuning of the receiver is done with the variable second local oscillator, which can be tuned over a range of about 5 Mc/s around 35 Mc/s either by hand or by motor at a rate of 0.6 Mc/s per hour.

Behind the wide-band second i.f. amplifier at 5 Mc/s the signal goes into two separate i.f. amplifiers operating at 4.96 and 6.04 Mc/s. The third crystal-

[1]) C. A. MULLER, *Philips Technical Review* **74**, 305 and 351, 1956.

FIGURE 2

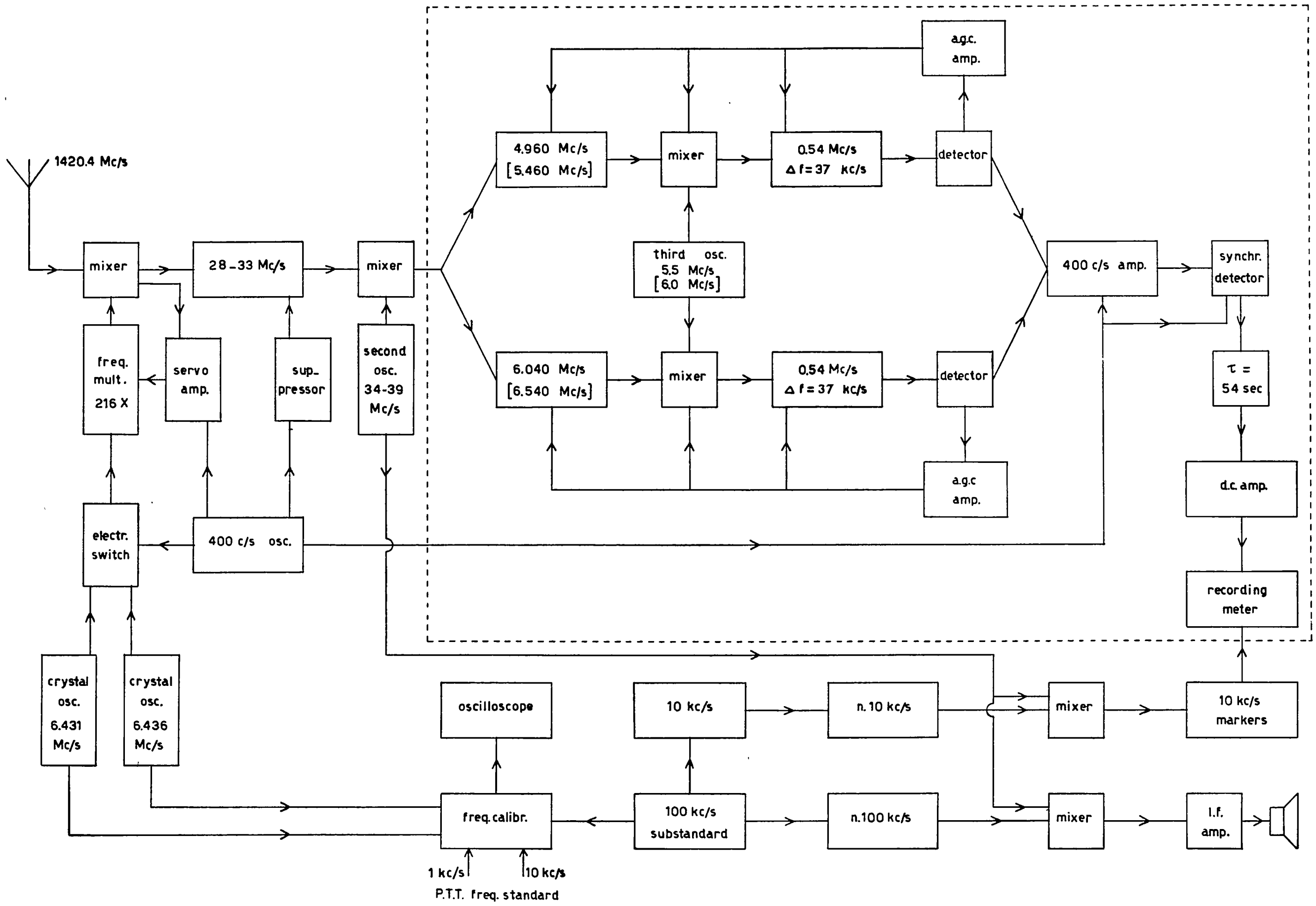

Block diagram of the receiver. The part of the receiver inside the dotted line is present in duplicate; specifications for the second set that differ from those for the first set are given in parentheses.

controlled local oscillator at 5.5 Mc/s is used for both channels simultaneously. The third i.f. amplifiers are both at 0.540 Mc/s and have a bandwidth of 37 kc/s. They determine the overall passband of the two receiver channels.

The d.c. output current of the linear diode detector in both channels is kept constant by means of an automatic gain control system which regulates the amplification of the second and third i.f. amplifiers.

The output of the linear detector contains a 400 c/s square wave voltage, if the energies received on the two switching frequencies differ. The voltages from the two channels, which are in antiphase, are subtracted and amplified in a 400 c/s selective amplifier and converted into direct current in a synchronous detector. Behind the synchronous detector follows the integrating network, consisting of a two-section low-pass filter which has the properties of a slightly undercritically damped filter and a time constant [as defined by ZECHLEBA [1]] of 54 sec. The bandwidth is 0.005 c/s. Via a d.c. amplifier the signal is fed into a Brown recorder.

The two requirements mentioned above have been met in the following way. The first requirement means that the output admittance of the antenna system including the coaxial line should change only slightly with frequency both on signal and image frequencies, (and also on a number of other frequencies, though the influence of admittance change is smaller), and that the properties of the crystal mixer do not change with frequency. To meet the requirement of constant output admittance the antenna system has been very carefully matched to the coaxial line on both 1420 and 1360 Mc/s. To keep the mixer properties the same on both switching frequencies it is necessary to keep the power of the first local oscillator equal on its two frequencies. This was done by means of a servo-system, tuning the last multiplier stage so that the d.c. crystal current is the same in both switching positions.

The second requirement was satisfied by connecting a suppressor circuit to the last stages of the first i.f.

[1]) F. ZECHLEBA, *Elektrotechn. Z.* **74**, 98, 1953.

amplifier. This suppressor circuit is triggered by 800 c/s pulses derived from the 400 c/s switching voltage and cuts out the i.f. amplifier during 60 microseconds just before and during the moment of switching. Since this circuit operates effectively at 800 c/s, no 400 c/s component occurs due to the switching.

From the double second i.f. channel onwards the receiver was built double, as indicated in the block-diagram by a dotted line. The second double channel uses second i.f. frequencies 500 kc/s higher than the first double channel, i.e. 5.46 and 6.54 Mc/s and a third local oscillator of 6.00 Mc/s. The rest of this channel, including 0.54 Mc/s third i.f. amplifiers, 400 c/s amplifier, synchronous detector, integrating network, d.c. amplifier and recorder is identical to the first channel. Its effect is to measure simultaneously on a second recorder a part of the line profile displaced 500 kc/s from the part of the profile measured by the first recorder. The time necessary for a complete tracing of the line profile is reduced to about 60% of the time necessary with one double channel allowing for some overlap between the two parts of the record.

3. *Frequency calibration.*

The frequency calibration of the receiver has been divided into three independent calibrations:

1. Calibration of the two crystal frequencies of the first local oscillator.

2. Calibration of the second local oscillator frequency.

3. Calibration of the passband of the four i.f. channels on 4.96, 5.46, 6.04 and 6.54 Mc/s.

The local primary frequency standards used in these calibrations were the 1 and 10 kc/s frequencies derived from the P.T.T. primary frequency standard in The Hague and transmitted by telephone line to Kootwijk Radio Station. The accuracy and stability of these two frequencies was of the order of 1 in 10^8. As a secondary standard a 100 kc/s crystal oscillator has been used, which was compared at regular intervals with the 10 kc/s primary standard on an oscilloscope. The accuracy of this comparison and the short-time constancy of the oscillator were of the order of 10^7.

The calibration of the two crystal frequencies of the first oscillator is done by mixing the third harmonic of the two frequencies (19.293 and 19.308 Mc/s) with the 193rd harmonic of the standard frequency and comparing the frequency difference of 7 or 8 kc/s with the 1 kc/s primary standard on an oscilloscope. A continuous check on these calibrations was made by the observer, so the two first oscillator frequencies were held constant within 1 part in 3.10^6 or 0.5 kc/s on 1390 Mc/s. The most important source of error was the frequency cycle due to the temperature cycle in the simple thermostats of the crystals.

As the second local oscillator frequency is continuously varied during the measurements, a different method of calibration had to be adopted. The frequency of this oscillator is compared with harmonics of a frequency of 10 kc/s in the interval around 35 Mc/s. When the difference between the oscillator frequency and one of these harmonics becomes less than about 50 c/s, a marker is automatically put on the record by short-circuiting the recorder input for a short, constant interval.

Another comparison between the local oscillator frequency and harmonics of 100 kc/s or 1 Mc/s permitted the observer to distinguish between the markers. In this case the low-frequency difference was made audible.

The shape and frequencies of the four i.f. channels were checked about once a week. They were found to be practically constant; no larger fluctuations than 1 kc/s have been observed.

4. *Intensity scale.*

Direct absolute calibration of the intensity scale is not possible as no noise source is available that emits radiation in a spectral line and whose intensity can be determined, independently of radio measurements, by a well-known physical relation. Absolute calibration of the intensity therefore has to be done indirectly by calibrating the various receiver constants concerned, such as noise figure, the noise rectification characteristic of the detectors and the sensitivity of the 400 c/s voltmeters.

Of these the determination of the noise figure is the most difficult. A well-known method for the determination of noise figures is the replacing of the antenna system by a noise source whose noise output is variable. As noise diodes cannot be used as a primary noise source on these high frequencies, the only available primary noise source is a hot body, for instance a hot resistor. However, a fundamental difficulty in the case of a wide-band crystal mixer is, that it is impossible to give the noise source the same admittance characteristics as the antenna system on all the frequencies that are important for the conversion- and admittance characteristics of the mixer. This makes accurate calibrations not well possible.

We have tried to use the earth as a noise source in order to include the entire instrument, with the antenna system, in the calibration. With the antenna first pointed to the zenith and then to the earth at an elevation of $-3°$ (a hill covered with a pine wood north of the antenna), the increase of the output energy has been measured. Assuming the pine wood to radiate as a black body at about 290°K and estimating the energy received in the side and back lobes of the antenna pattern, we arrive at a difference in antenna temperature in the two positions of about 270°K, giving a noise figure $N' = 3.0$ for reception on both signal and image frequencies (no image rejection is used in the high-frequency part of the receiver). Assuming equal sensitivity on signal and image frequencies, the noise figure for reception on the signal frequency alone is twice as large, giving a noise figure for line measurements of $N = 2\ N' = 6.0$. The noise figure so determined is an upper limit, as it is unlikely that the difference in antenna temperature is larger than the value given, but it may be somewhat smaller. The accuracy in the noise figure is judged to be about 20%, taking into account that some radiation may be received at harmonics of signal and image frequencies. The absolute intensity scale has the same order of accuracy.

The intensity scale of the recorded profiles given in this catalogue is not quite linear due to two different causes:

1. With the linear detector used, the detector current is proportional to the square root of the energy input. In the two switching positions the detector currents may be written as

$$i_1 = C.\sqrt{2(N'-1)\,T_\circ}$$

and $$i_2 = C.\sqrt{2(N'-1)\,T_\circ + \Delta T}$$

where $2(N' - 1)\,T_\circ$ is the effective noise temperature of the receiver, ΔT is the increase in antenna temperature due to line radiation and C is a constant. The square-wave output voltage is proportional to $(i_2 - i_1)$ and in first approximation proportional to ΔT. In second approximation the voltage is proportional to

$$\Delta T.\left(1 - \tfrac{1}{4}\Delta T/2\,(N'-1)\,T_\circ\right) \quad (1)$$

2. The automatic gain control keeps the average d.c. output current of the detector constant. It would have no influence if it kept the current i_1 constant but now it reduces the amplitude of the square-wave voltage with a factor

$$\left(1 - \tfrac{1}{4}\Delta T/2\,(N'-1)\,T_\circ\right) \quad (2)$$

Due to these effects we find that the deflection of the recorder is not quite proportional to ΔT, but is in effect proportional to

$$\Delta T\,.\left(1 - \tfrac{1}{2}\Delta T/2\,(N'-1)\,T_\circ\right) \quad (3)$$

Since $2(N' - 1)\,T_\circ$ is about 1200°K, we find that the deflection of the recorder for $\Delta T = 100$°K is about 4% less than it would be if the deflection were proportional to ΔT.

The automatic gain control may also influence the recorded intensity when the effective temperature, which includes both receiver and antenna noise, increases by an increase in antenna temperature on both signal and image frequencies because of the reception of continuous radiation from the galaxy, point sources or the earth. When the antenna temperature increases by an amount $\Delta T'$, the a.g.c. system reduces the gain and thus the deflection of the recorder with a factor of

$$1 - \Delta T'/(N'-1)\,T_\circ \quad (4)$$

This effect is particularly noticeable near the horizon, and the profiles obtained at low altitudes have been corrected for it (section 6).

The line profiles in the catalogue have not been corrected for the alinearity in the intensity scale. With $\Delta T = 100$°K as unit intensity the alinearity correction in the conversion from recorder deflection h to ΔT ranges from 1.01 at $\Delta T = 120$°K and 0.98 at $\Delta T = 50$°K to 0.96 at $\Delta T = 5$°K. In the reductions described in the subsequent articles in this series the alinearity correction has also been omitted. In view of the large uncertainties arising from other causes, this does not influence the density distribution of neutral hydrogen derived from the profiles.

The intensity scale of the receiver was checked daily by measuring the recorder deflection for the unit intensity ($\Delta T = 100$°K, i.e. the main top of the profile at $l = 50°$, $b = 0°$), which should be $h = 129$ mm on the record. The recorder deflection was plotted against time, thus providing a continuous check on the performance of the receiver. It was found that there was a slow drift from time to time, amounting to 1.5% per day, which must have been due to slow fluctuations in the noise figure of the receiver, since this is used as a constant reference by the a.g.c. system. Sometimes sudden jumps of about 3 to 10% occurred, for which no clear explanation can be given. In such cases a double check was made by comparing the relative deflections in other line profiles obtained at other moments when no jumps occurred.

When the deflection of the recorder differed by more than 7.5% from the adopted value of 129 mm it was brought to this value by changing the gain of the 400 c/s selective amplifiers. This was necessary only at rare occasions.

The correction factors obtained from the daily check record were applied to all profiles. It was found from the comparison of profiles far apart in time that the error in the relative intensities of the profiles due to variations in the intensity scale cannot be more than 5%.

5. *Sensitivity.*

According to accepted usage, the smallest difference in antenna temperature between signal and comparison frequencies that is still considered measurable is equal to the effective value of the noise fluctuations, expressed in antenna temperature, on the record. In our case, where the signal is small compared to the internal receiver noise and where a double i.f. channel is used, we find the following expression for the theoretical sensitivity

$$\Delta T = 1.03 \frac{\pi}{\sqrt{2}} (N' - 1)\, T_0 . \left[F . \Delta f . \tau\right]^{-1/2} . \quad (5)$$

In this relation N' is the noise figure for simultaneous reception in both signal and image channels, $T_0 = 293°K$, Δf is the noise bandwidth of the i.f. amplifiers, F is a factor determined by the shape of the i.f. passband ($F = 1.53$) and τ is the time constant of the integrating network. For this receiver we find $\Delta T = 0.73°K$. Comparing the sensitivity of this receiver with the theoretical sensitivity of a simple receiver we find that it is inferior by a factor of 1.57. This loss in sensitivity is amply offset by the much greater stability obtained in the comparison method.

From the formula given for ΔT it would appear that in principle it is possible to achieve any sensitivity by increasing the time constant or the i.f. bandwidth. The latter is not desirable in this case as it entails the loss of details in the spectrum of the hydrogen line. An increase in the time constant necessitates a corresponding reduction in the tuning rate; the tuning rate should be about one i.f. bandwidth in 4τ seconds when all details observable with this i.f. bandwidth should be recorded. The tuning rate of 0.6 Mc/s per hour used in the present receiver satisfies this requirement.

In practice the zero stability during the measurements decides the maximum sensitivity obtainable with a receiver. In this receiver the zero stability was excellent, but the sensitivity was restricted by interference from the neighbouring transmitters of the Kootwijk Radio Station to a limit of about 1°K.

FIGURE 3

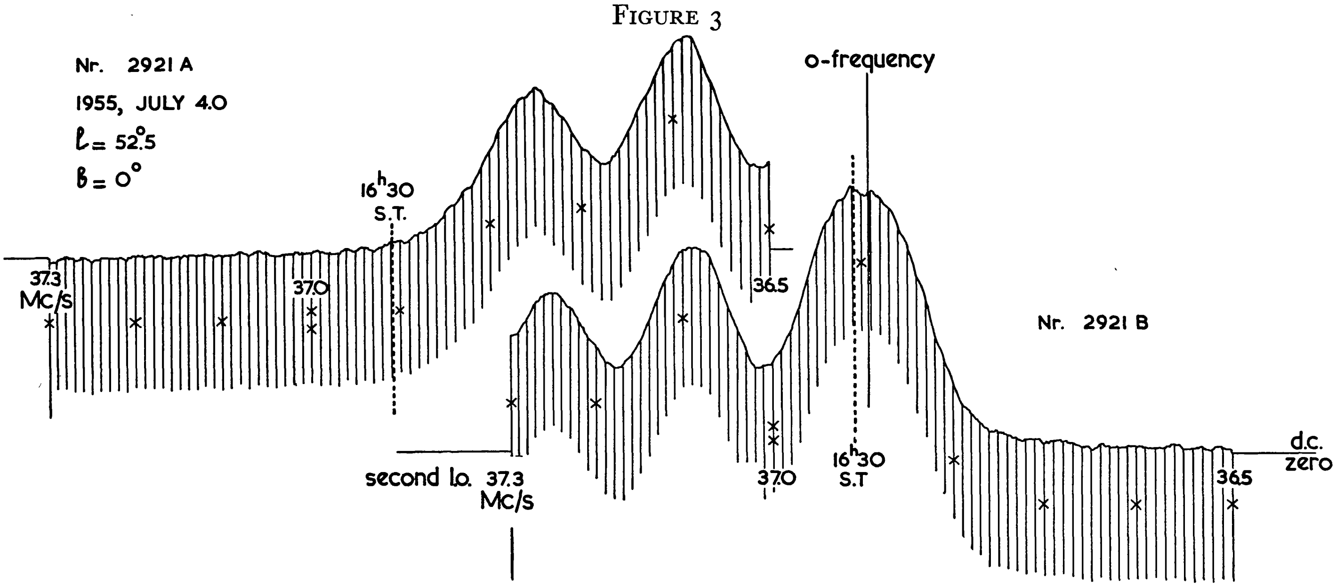

Example of a double recording. The two simultaneously recorded profiles are displaced by 500 kc/s relative to each other. The vertical lines, separated by 10 kc/s, indicate the frequency of the second local oscillator.

6. *Extinction.*

The radiation received at the antenna has been attenuated during its passage through the earth's atmosphere. Although the extinction at radio wavelengths is much smaller than in the optical region, allowance has to be made for its effect at low altitudes. The extinction was measured by tuning the receiver to the frequency of a flat, high-intensity part of a line profile, and noting the decrease of recorder deflection h, while following a point from altitude 30° down to the horizon. Mostly, points near $l = 340°$ were used, which rise and set less than 90° from South. The curves thus obtained were combined with a curve obtained by guiding the telescope for 24 hours on the position $l = 50°$, $b = 0°$, with the receiver tuned to the frequency of the main top.

The final reduction into a mean curve of h versus altitude was made by Mr L. WOLTJER. From it the correction factor as a function of altitude was read. It was taken as 1 at altitude 35°; no correction factor was applied to profiles obtained at altitudes higher than 25°, because the correction needed was < 1%.

The decrease of the recorder deflection is due to two causes, namely the extinction and the sky radiation. The latter raises the noise level in the continuum, and the automatic gain control then decreases the gain to keep the detector output constant. The incoming energy at a given frequency may be expressed by

$$\Delta T = T_l p^{F(z)}, \qquad (6)$$

where T_l is the brightness temperature in the line outside the earth's atmosphere, p the extinction per unit air mass and $F(z)$ the air mass as a function of zenith distance z. The sky radiation raises the antenna temperature by an amount

$$\Delta T' = (1 - p^{F(z)})\, T_\circ \qquad (7)$$

and thereby decreases the gain by a factor $1 - 2\Delta T'/T$, where T is the effective noise temperature, $T = 2(N' - 1)\, T_\circ$. The deflection may thus be written as

$$h = c \,.\, \Delta T\left(1 - \frac{\Delta T}{2T}\right)\left(1 - \frac{2\Delta T'}{T}\right). \qquad (8)$$

Inserting the values of ΔT and $\Delta T'$ we find, for a zenith distance $z < 85°$

$$h = c' T_l p^{F(z)}\left\{1 - \frac{T_l}{2T} p^{F(z)}\right\}\left\{1 - \frac{2T_\circ}{T}(1 - p^{F(z)})\right\}. \qquad (9)$$

For $z > 85°$ the wings of the antenna beam pick up radiation from the earth, thereby increasing $\Delta T'$ still further.

As the value of $p^{F(z)}$ is close to 1, we may develop (9) into powers of $(1 - p^{F(z)})$. Omitting higher orders, we find

$$\log h = a + b\, F(z) \log p, \qquad (10)$$

where a and b are functions of the receiver constants and T_l. The observed log h plotted against $F(z)$ gave a straight line, from which log p was determined. We found $p = 0.9915 \pm .0008$. This value corresponds to an extinction of 0.037 ± 0.003 db in the zenith, or in the units of optical astronomy to an extinction coefficient of $k = -2.5 \log p = 0.009 \pm .001$ magnitudes. The sky radiation then corresponds to $\Delta T' = 13°$ K at $z = 80°$ and $\Delta T' = 3°$K at the zenith.

Another way of determining p is to measure the sky radiation separately with a continuum receiver, and inserting the values of $\Delta T'$ found in equation (8). This method gave results in good agreement with the other determination, but the measured values of $\Delta T'$ were systematically higher than the computed values. For instance, the measured value at $z = 80°$ was $\Delta T' = 23°$K. The larger temperatures observed probably arise from earth radiation in the far side lobes and back lobes of the antenna pattern.

7. *Observing procedure.*

A complete coverage of all information obtainable in the 21-cm line is reached if the intensity of this radiation is known as a function of position and frequency. Common ways of reaching this are either sweeping in frequency at a fixed position, or sweeping in position (for example letting the sky drift past a fixed antenna) at a fixed frequency. The observations described in this paper have been made by the first method.

Line profiles were obtained, sweeping in frequency by means of automatic tuning of the second local oscillator. For each point observed the galactic co-ordinates are given, based on the standard pole at $12^h40^m.0$, $+ 28°.0$ (1900). Conversion to equatorial co-ordinates was made with the aid of OHLSSON's tables [1]). Tables of azimuth and altitude as a function of sidereal time were computed for all points observed, at $\frac{1}{2}$ hour intervals. The telescope was guided on a point by hand-setting in a and h every $2\frac{1}{2}$ minutes, with values interpolated between the half-hour computed values. The a and h scales on the telescope were accurate to 0°.1, and were rechecked on point sources with a continuum receiver halfway and towards the end of the observing period. Optical refraction corrections were applied to the altitude settings. From point source observations, this appeared correct for the accuracy reached here.

The performance of the receiver was such that the observations could be made by an inexperienced observer. Observing a line profile involved the following tasks: *a*. Guiding of telescope, setting in a and h. *b*. Setting of second l.o. on a given frequency (outside the line) and starting the tuning motor. *c*. Marking every tenth frequency mark on the record, when an audible signal indicated a multiple of 100 kc/s. *d*. Occasional checking of the frequency of the first l.o. against the standard oscillator on an oscilloscope.

The telescope was used 24 hours per day in three shifts. Most observations were carried out by students in various fields, who had a 2-day training period and stayed for a fortnight at the observatory.

8. *Radial-velocity corrections.*

For each record the displacement of the zero frequency due to the motion of the earth and the motion of the sun with respect to the local standard of rest was computed. A table has been prepared giving at 5-degree intervals in longitude, at $b = 0°$, the component of the combined earth-sun radial velocity at intervals of five days. It also gives this radial velocity for points on declination circles through the longitudes at $b = 0°$, but displaced by $\pm 15°$ in right ascension. The latter part of the table was used only for the profiles between $l = 40°$ and $l = 320°$, that were obtained along declination circles.

For the profiles with $b \neq 0°$, $l > 40°$ a table was used

[1]) *Lund Annals* No. 3, 1932.

giving for each day the components of the earth-sun radial velocity in a rectangular equatorial co-ordinate system, A, B and C. The radial velocity of a point (α, δ) was found from

$$v_r = A \cos \alpha \cos \delta + B \sin \alpha \cos \delta + C \sin \delta. \quad (11)$$

The direction cosines in (11) were computed for each point for which a line profile was obtained. The factors A, B and C, which are functions of the ecliptical longitude of the sun and include the motion of the sun, of 20 km/sec towards $\alpha = 270°$, $\delta = +30°$ (1900), were taken from tables kindly put at our disposal by Dr H. L. HELFER [1]).

The frequency of the second l.o., which corresponds to the zero frequency in the line profile in a given direction, was computed for each profile from the formula $f_0 = f' + a + b$. Here, f' is the uncorrected l.o. frequency, given by

$$f' = 1420.4056 - 216 f_{\text{first l.o.}} + f_{\text{second i.f.}}$$

Further, a is the radial velocity correction, converted into frequency, and b is a correction due to the time constant. The displacement of the profile in time by 54 sec at a sweep speed of -0.6 Mc/s per hour, corresponds to $b = -9.0$ kc/s. Corrections for the barycentric motion ($\pm$ 0.07 kc/s) and for the diurnal motion of the earth (maximum $\pm$ 1.3 kc/s) were omitted.

The final accuracy of the zero frequency of a line profile is of the order of $\pm$ 2.0 kc/s ($\pm$ 0.4 km/sec).

9. *Construction of mean profiles.*

The recordings of the line profiles were smoothed if necessary, and zero lines were drawn. The zero lines appeared to be straight lines throughout the observations. Often they could be interpolated between the zero intensities on both sides of the profiles. They were always compared with the zero lines of adjacent profiles, and with the positions of the zero of the d.c. amplifier. Generally, the position of the zero lines was certain within $\pm$ 1°K.

As the sweep speed was not constant during one measurement, it was necessary to replot all profiles on a uniform scale. This was done by two persons, one reading the intensities above zero from the recording, the other plotting them on transparent graph paper.

The receiver sensitivity at the time of the measurement was found from a graph based on measurements of the top intensity at $l = 50°$, $b = 0°$. A table with this sensitivity and the mean altitude at which the profile was obtained as entries, then gave the correction factor for the combined effect of extinction and sensitivity. All ordinates were multiplied by this factor. The zero frequency was drawn into the curve, and the two or three curves obtained at the same position were compared by superposition. If the intercomparison showed serious differences, the original recordings were checked and, if necessary, a measurement was repeated. The intercomparison also revealed errors as small as 2 to 4 kc/s in the computation of the zero frequency.

Finally, a mean curve was drawn on a separate transparent sheet of graph paper. These curves formed the basis for the further reduction and are given in the catalogue. The estimated overall accuracy of the profiles in the catalogue is

in absolute intensity (temperature scale):	$\pm$20%,
in relative intensity:	$\pm$5%,
in radial velocity:	$\pm$0.4 km/sec.

10. *Catalogue.*

The catalogue on the following pages contains all line profiles obtained with the Kootwijk instrument in the galactic survey programme described in the following articles. The intensities are given in a slightly non-linear scale (p. 161); the main top of $l = 50°$, $b = 0°$ has been taken as 100°K. The vertical lines are at intervals of 20 km/sec, and the thick vertical lines give the position of the zero velocity. To facilitate the reading of velocities or frequencies of details in the profiles, a loose scale has been added to this number of the *B.A.N.*

The catalogue contains the following series of profiles.

a. Region $l = 318° - 45°$. The line profiles were obtained at the positions given in Table 1. These points are in groups along declination circles with intervals of 10^m in right ascension, which corresponds to about 2° in b. Each declination circle cuts the galactic equator at l = a full multiple of 2°.5; the (a, h) tables for these points were used for other points on the circle with an offset $\Delta\alpha$ given also in Table 1. Maximum intensity in each group was usually reached at $b = -1°.5$.

b. Region $l = 45° - 120°$. The profiles were taken at 2°.5 intervals in longitude (with the exception of $l = 112°.5$ and 117°.5) and 2°.5 intervals in latitude, from $b = +10°$ to $b = -10°$. The declination circles in this region run almost parallel to the galactic equator.

c. Region $l = 125° - 220°$. The profiles were taken at longitude intervals of approximately 5° and latitude intervals of approximately 2°.5, at the exact positions given by Table 2. These points, chosen in order to avoid the computation of more a and h tables, differ

[1]) New tables of A, B and C, at $^1/_4$ day intervals, and of the direction cosines at 1 degree intervals in l and b, computed by Dr A. REIZ and Dr D. A. MACRAE, have been published by the Observatory, Lund, Sweden. In the same publication, conversion tables are given of (l, b) into (α, δ) for 1958.0, based on the standard pole, at intervals of 1 degree in l and b.

by less than 1°.3 from the mean longitudes at intervals of 5° and by less than 0°.3 from the mean latitudes $b = \pm 2°.5$, $b = \pm 5°$, etc. The negative latitudes at $l = 220°$ do not rise above the horizon at Kootwijk.

d. Between $l = 60°$ and $l = 110°$ a number of profiles at higher latitudes, $b = \pm 12°.5$ and $b = \pm 15°$, have been taken in order to follow some details visible at lower latitudes.

e. Between $l = 112°.5$ and $l = 217°.5$ extra line profiles were taken at $b = 0°$ to fill in the 2°.5 points. Lack of time prevented the extension of this programme to higher latitudes.

TABLE I

Galactic longitude and latitude for the observed points between $l_0 = 318°$ and $l_0 = 45°$. The points are situated on declination circles passing through the points at l_0, $b = 0°$, and are shifted in right-ascension by an amount $\Delta\alpha$.

l_0	$\Delta\alpha$						
		-30^{m}	-15^{m}	$-2^{\mathrm{m}}.5$	$+10^{\mathrm{m}}$	$+22^{\mathrm{m}}.5$	$+35^{\mathrm{m}}$
318°		314°.3 +4°.7	316°.2 +2°.4	317°.7 +0°.4	319°.1 −1°.6	320°.5 −3°.7	321°.9 −5°.8
		-25^{m}	-15^{m}	$-2^{\mathrm{m}}.5$	$+10^{\mathrm{m}}$	$+20^{\mathrm{m}}$	$+30^{\mathrm{m}}$
320		316.9 +4.1	318.2 +2.5	319.7 +0.4	321.1 −1.7	322.2 −3.4	323.3 −5.2
322.5		319.4 +4.4	320.7 +2.6	322.2 +0.4	323.6 −1.7	324.7 −3.6	325.8 −5.4
		$-22^{\mathrm{m}}.5$	$-12^{\mathrm{m}}.5$	$-2^{\mathrm{m}}.5$	$+7^{\mathrm{m}}.5$	$+17^{\mathrm{m}}.5$	$+27^{\mathrm{m}}.5$
325		322.2 +4.1	323.5 +2.2	324.7 +0.4	325.9 −1.3	327.0 −3.3	328.1 −5.0
327.5		324.7 +4.3	326.0 +2.3	327.2 +0.5	328.8 −1.4	329.5 −3.3	330.6 −5.1
330		327.2 +4.4	328.5 +2.4	329.7 +0.5	330.8 −1.4	332.0 −3.4	333.1 −5.3
332.5		329.7 +4.5	331.0 +2.4	332.2 +0.5	333.4 −1.4	334.5 −3.4	335.6 −5.4
335		332.2 +4.5	333.5 +2.5	334.7 +0.5	335.9 −1.5	337.0 −3.5	338.1 −5.6
337.5		334.8 +4.5	336.0 +2.5	337.2 +0.5	338.4 −1.5	339.5 −3.6	340.6 −5.7
340		337.3 +4.6	338.5 +2.5	339.7 +0.5	340.9 −1.6	342.0 −3.7	343.1 −5.8
342.5		339.8 +4.6	341.0 +2.6	342.2 +0.5	343.4 −1.6	344.5 −3.8	345.6 −5.9
345		342.3 +4.7	343.5 +2.6	344.7 +0.5	345.9 −1.6	347.0 −3.8	348.1 −6.0
347.5		344.8 +4.8	346.0 +2.6	347.2 +0.5	348.4 −1.6	349.5 −3.8	350.6 −6.0
350		347.3 +4.8	348.5 +2.7	349.7 +0.5	350.9 −1.6	352.0 −3.8	353.2 −6.0
352.5		349.8 +4.9	351.0 +2.7	352.2 +0.5	353.4 −1.6	354.5 −3.8	355.7 −6.0
355		352.3 +4.9	353.5 +2.8	354.7 +0.6	355.9 −1.6	357.0 −3.8	358.2 −6.0
357.5		354.8 +5.0	356.0 +2.8	357.2 +0.6	358.4 −1.6	359.5 −3.8	0.7 −6.0
0		357.3 +5.0	358.5 +2.8	359.7 +0.6	0.9 −1.6	2.1 −3.8	3.2 −6.0
2.5		359.8 +5.0	1.0 +2.8	2.2 +0.6	3.4 −1.6	4.6 −3.8	5.7 −6.0
5		2.4 +5.0	3.5 +2.8	4.7 +0.6	5.9 −1.6	7.1 −3.8	8.2 −6.0
7.5		4.9 +5.0	6.0 +2.8	7.2 +0.6	8.4 −1.6	9.6 −3.8	10.8 −6.0
10		7.4 +5.0	8.5 +2.8	9.7 +0.6	10.9 −1.6	12.1 −3.8	13.3 −5.9
12.5		9.9 +4.9	11.0 +2.7	12.2 +0.6	13.4 −1.6	14.6 −3.8	15.8 −5.9
15		12.4 +4.8	13.5 +2.7	14.7 +0.6	15.9 −1.6	17.1 −3.7	18.3 −5.8
17.5		14.9 +4.8	16.0 +2.6	17.2 +0.5	18.4 −1.6	19.6 −3.7	20.8 −5.7
20		17.4 +4.7	18.5 +2.6	19.7 +0.5	20.9 −1.5	22.1 −3.6	23.3 −5.6
22.5		19.9 +4.6	21.0 +2.5	22.2 +0.5	23.4 −1.5	24.6 −3.6	25.8 −5.5
25		22.4 +4.5	23.5 +2.5	24.7 +0.5	25.9 −1.5	27.2 −3.5	28.4 −5.4
27.5		24.9 +4.5	26.1 +2.5	27.2 +0.5	28.4 −1.5	29.7 −3.5	30.9 −5.4
30		27.4 +4.4	28.6 +2.4	29.7 +0.5	30.9 −1.4	32.2 −3.4	33.4 −5.3
32.5		30.0 +4.3	31.1 +2.4	32.2 +0.5	33.4 −1.4	34.7 −3.2	35.9 −5.1
	-35^{m}	-25^{m}	$-12^{\mathrm{m}}.5$	$-2^{\mathrm{m}}.5$	$+7^{\mathrm{m}}.5$	$+20^{\mathrm{m}}$	$+30^{\mathrm{m}}$
35	31.1 +6.4	32.2 +4.6	33.6 +2.3	34.7 +0.4	35.9 −1.4	37.5 −3.6	38.7 −5.4
37.5	33.7 +6.3	34.8 +4.5	36.1 +2.2	37.2 +0.4	38.4 −1.4	39.9 −3.4	41.2 −5.2
	$-37^{\mathrm{m}}.5$	$-27^{\mathrm{m}}.5$	-15^{m}	$-2^{\mathrm{m}}.5$	$+10^{\mathrm{m}}$	$+22^{\mathrm{m}}.5$	$+35^{\mathrm{m}}$
40	35.9 +6.6	37.0 +4.7	38.4 +2.6	39.7 +0.4	41.2 −1.7	42.7 −3.7	44.3 −5.7
	-40^{m}	$-27^{\mathrm{m}}.5$	-15^{m}	$-2^{\mathrm{m}}.5$	$+10^{\mathrm{m}}$		
42.5	38.2 +6.8	39.5 +4.6	40.9 +2.5	42.2 +0.4	43.7 −1.6		
	-45^{m}	-30^{m}	-15^{m}				
45	40.2 +7.3	41.7 +4.8	43.4 +2.4				

TABLE 2

Galactic longitude and latitude of the points in the region $l = 125° - 220°$.

l	b	l	b	l	b	l	b	l	b	l	b	l	b	l	b	l	b
124°.2	9°.9	124°.4	7°.4	124°.7	5°.0	124°.8	2°.5	125°.0	0°.0	125°.1	−2°.7	124°.9	−5°.1	125°.5	−7°.6	125°.8	−10°.0
130.5	10.2	129.9	7.5	129.1	5.0	129.5	2.4	130.0	0.0	130.4	−2.5	131.0	−5.0	131.1	−7.7	131.9	−9.9
134.7	10.2	135.3	7.5	136.3	5.4	134.4	2.6	135.0	0.0	135.7	−2.4	136.3	−4.9	134.0	−7.6	134.7	−10.0
139.0	9.8	139.8	7.3	140.8	5.0	139.2	2.5	140.0	0.0	140.7	−2.6	138.8	−5.1	139.7	−7.5	140.4	−9.9
146.0	10.1	144.6	7.5	145.5	4.9	143.9	2.2	145.0	0.0	146.0	−2.3	144.2	−5.1	145.0	−7.5	145.8	−10.0
150.6	9.9	149.4	7.5	150.6	5.2	148.9	2.4	150.0	0.0	151.0	−2.5	149.4	−4.9	150.3	−7.3	151.2	−9.9
155.5	9.8	154.2	7.3	155.3	5.0	153.9	2.4	155.0	0.0	156.0	−2.5	154.5	−5.0	155.3	−7.6	153.7	−10.1
160.5	10.2	159.2	7.7	159.7	5.1	159.0	2.5	160.0	0.0	161.0	−2.6	159.5	−5.2	160.7	−7.4	159.9	−10.0
165.3	10.0	164.0	7.4	165.1	4.8	164.0	2.7	165.0	0.0	166.0	−2.7	164.8	−4.8	165.7	−7.5	164.2	−10.2
170.2	10.2	169.0	7.5	170.1	4.9	168.7	2.2	170.0	0.0	171.3	−2.2	169.8	−4.9	170.8	−7.7	169.6	−9.9
175.2	9.9	174.1	7.7	175.1	5.0	173.7	2.2	175.0	0.0	176.3	−2.2	174.8	−5.0	175.9	−7.7	174.7	−9.9
180.3	9.9	179.1	7.7	180.1	5.0	178.7	2.2	180.0	0.0	181.3	−2.2	179.8	−5.0	180.9	−7.7	179.7	−9.9
185.3	9.9	184.1	7.7	185.2	5.0	183.7	2.2	185.0	0.0	186.3	−2.2	184.9	−5.0	185.9	−7.7	184.8	−9.9
190.4	9.9	189.2	7.7	190.3	4.9	188.7	2.2	190.0	0.0	191.3	−2.2	189.8	−4.9	191.0	−7.6	189.6	−10.3
195.8	9.7	194.3	7.5	195.2	4.8	194.0	2.6	195.0	0.0	196.0	−2.6	194.9	−4.8	196.0	−7.4	194.7	−10.0
200.9	10.0	199.3	7.4	200.5	5.2	199.0	2.6	200.0	0.0	201.0	−2.5	199.7	−5.3	200.8	−7.7	199.5	−10.2
206.3	10.1	204.7	7.6	205.5	5.0	204.0	2.5	205.0	0.0	206.0	−2.5	204.7	−5.0	205.9	−7.3	204.5	−9.8
208.8	9.9	209.7	7.3	210.6	4.9	209.0	2.4	210.0	0.0	210.8	−2.4	209.4	−5.1	210.6	−7.5	209.4	−9.9
214.9	10.0	215.0	7.5	215.9	5.1	214.0	2.3	215.0	0.0	216.1	−2.2	214.4	−4.9	215.4	−7.5	214.0	−10.1
219.6	9.9	220.3	7.5	221.2	5.1	219.3	2.6	220.0	0.0								

CATALOGUE OF 21-CM LINE PROFILES

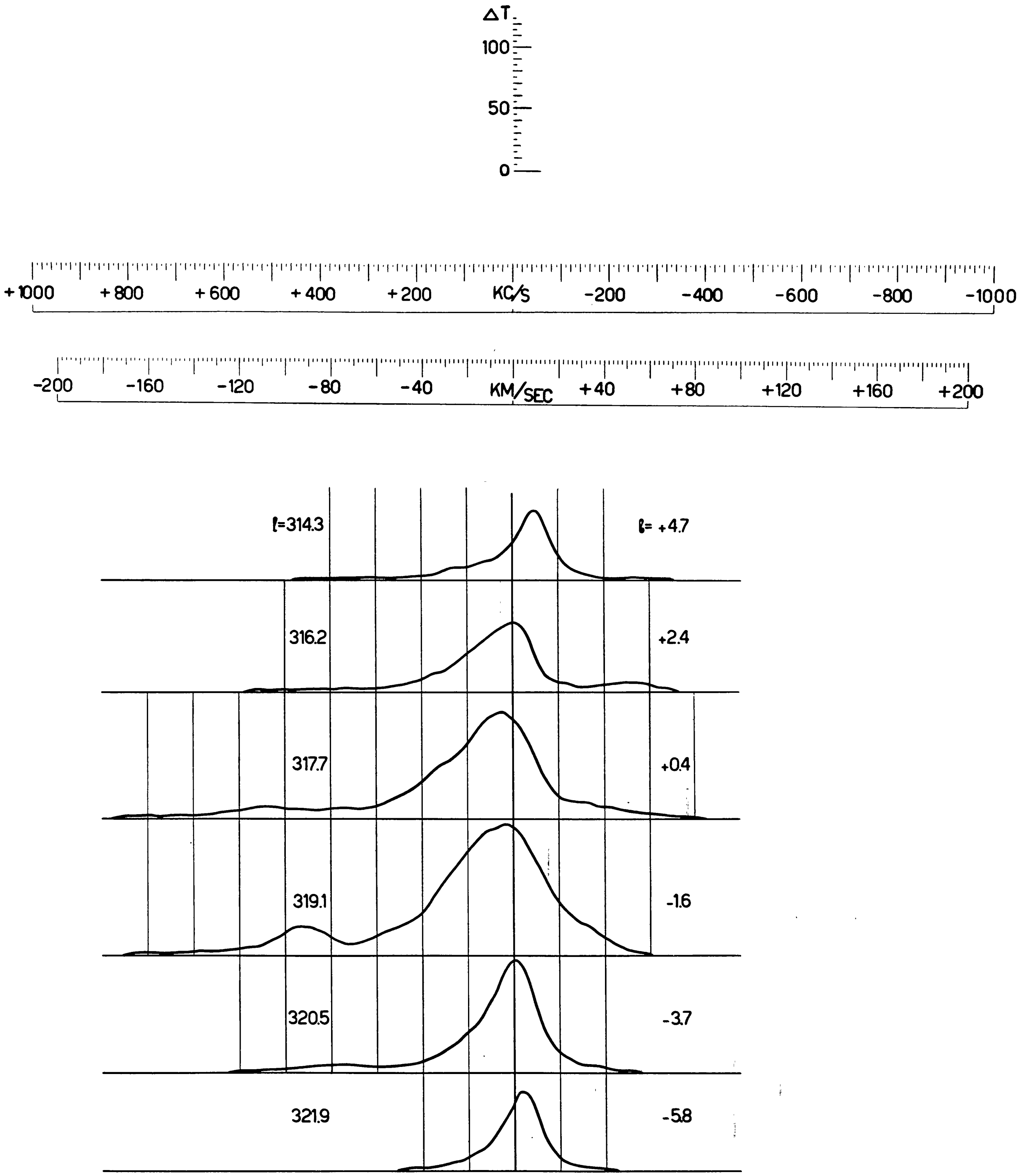

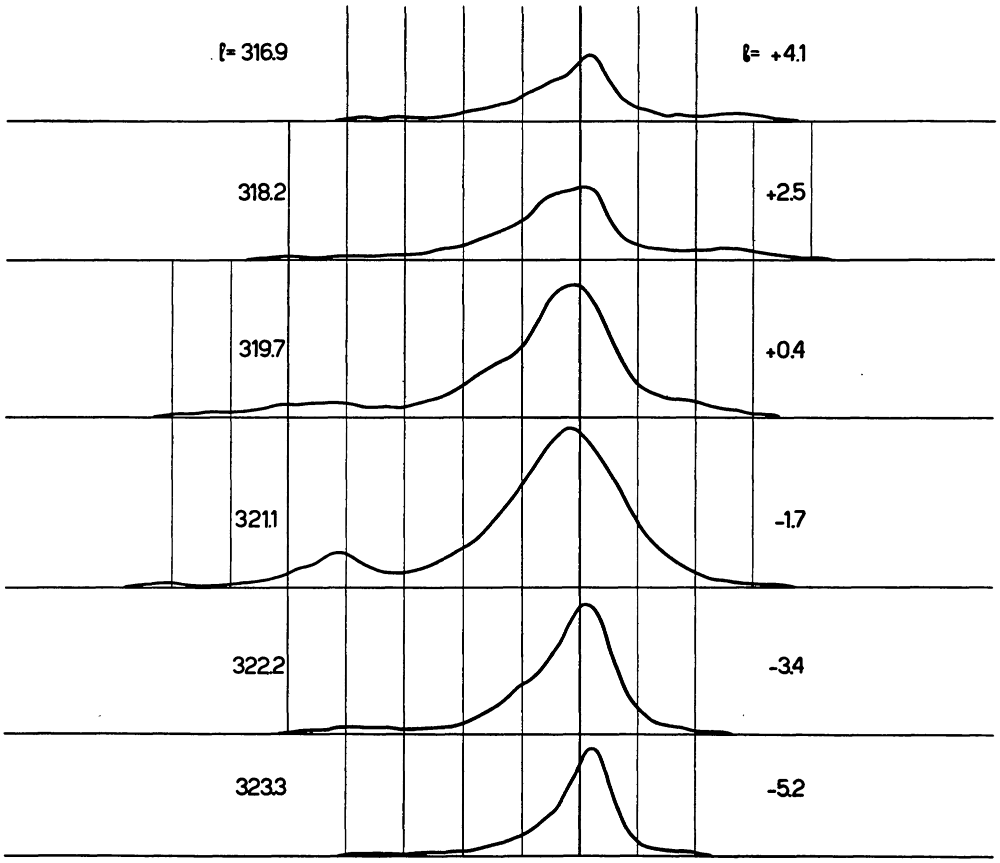
l= 316.9
b= +4.1
318.2
+2.5
319.7
+0.4
321.1
-1.7
322.2
-3.4
323.3
-5.2

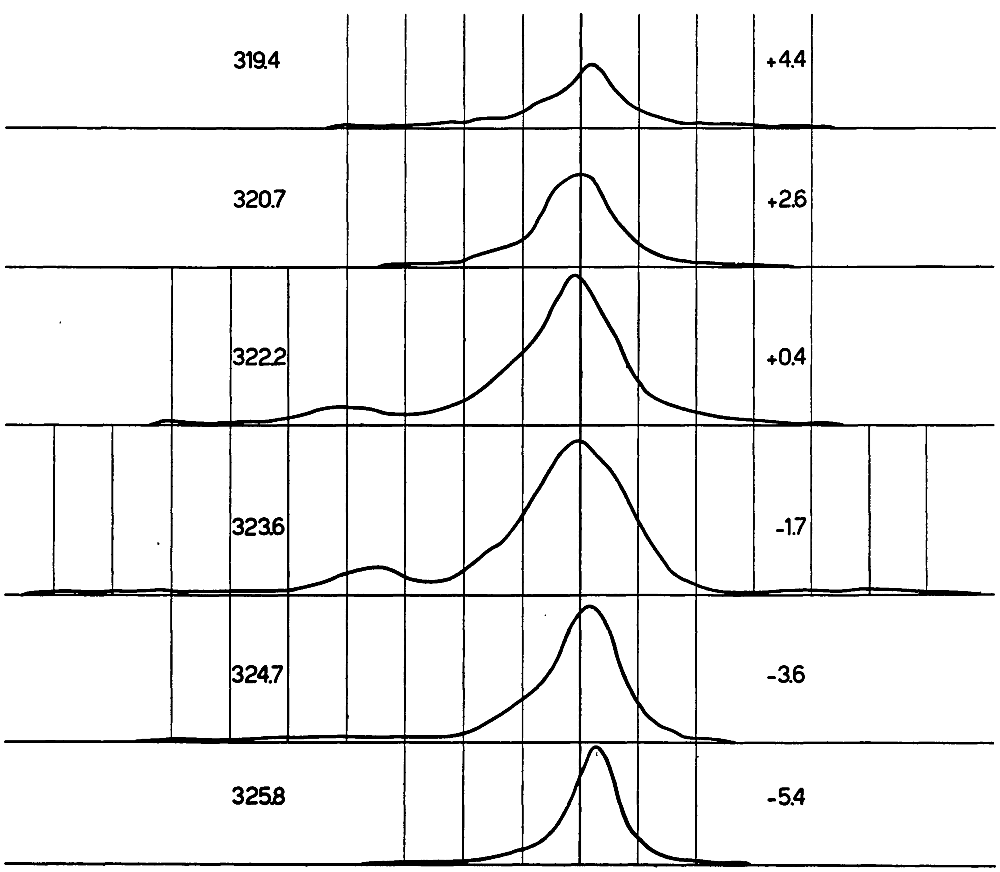
319.4
+4.4
320.7
+2.6
322.2
+0.4
323.6
-1.7
324.7
-3.6
325.8
-5.4

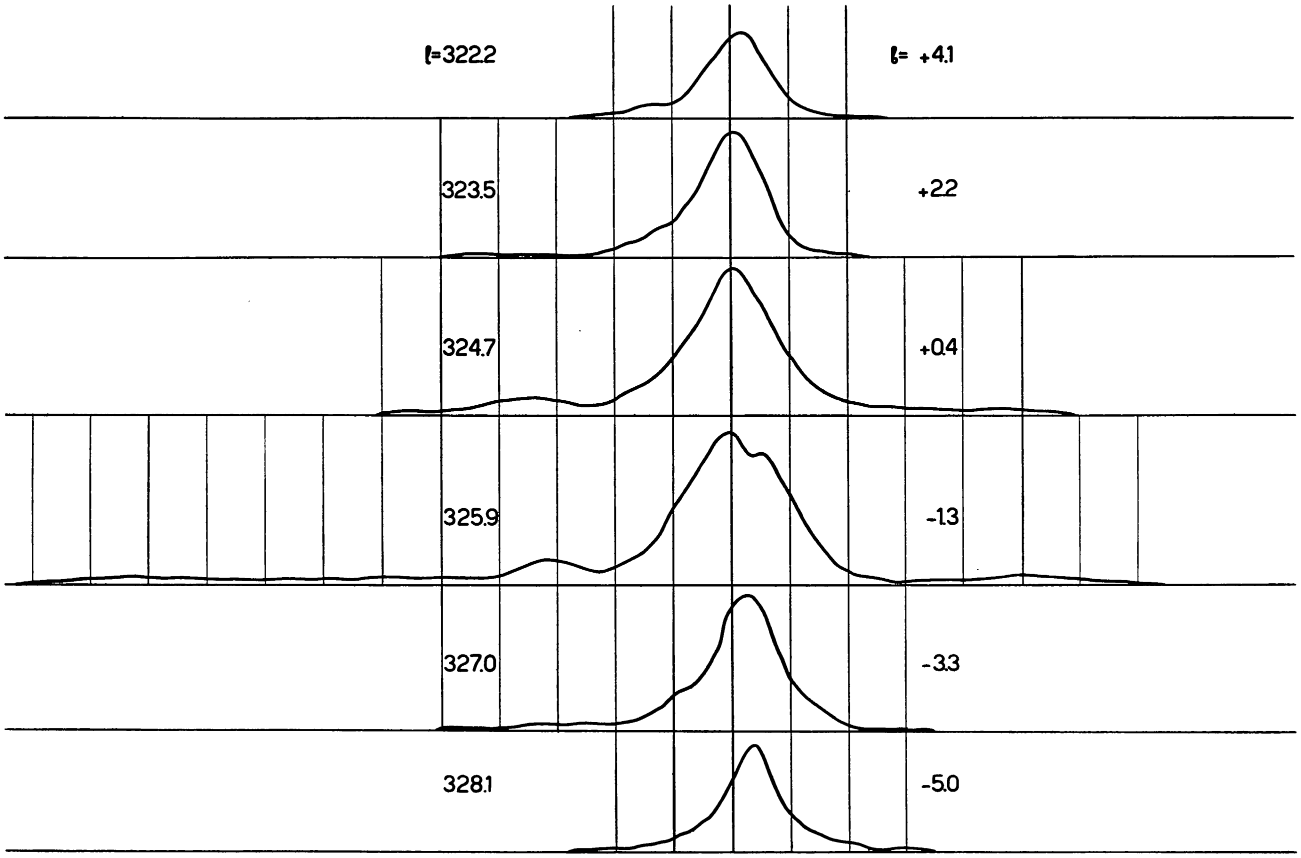
l=322.2 b= +4.1
323.5 +2.2
324.7 +0.4
325.9 -1.3
327.0 -3.3
328.1 -5.0

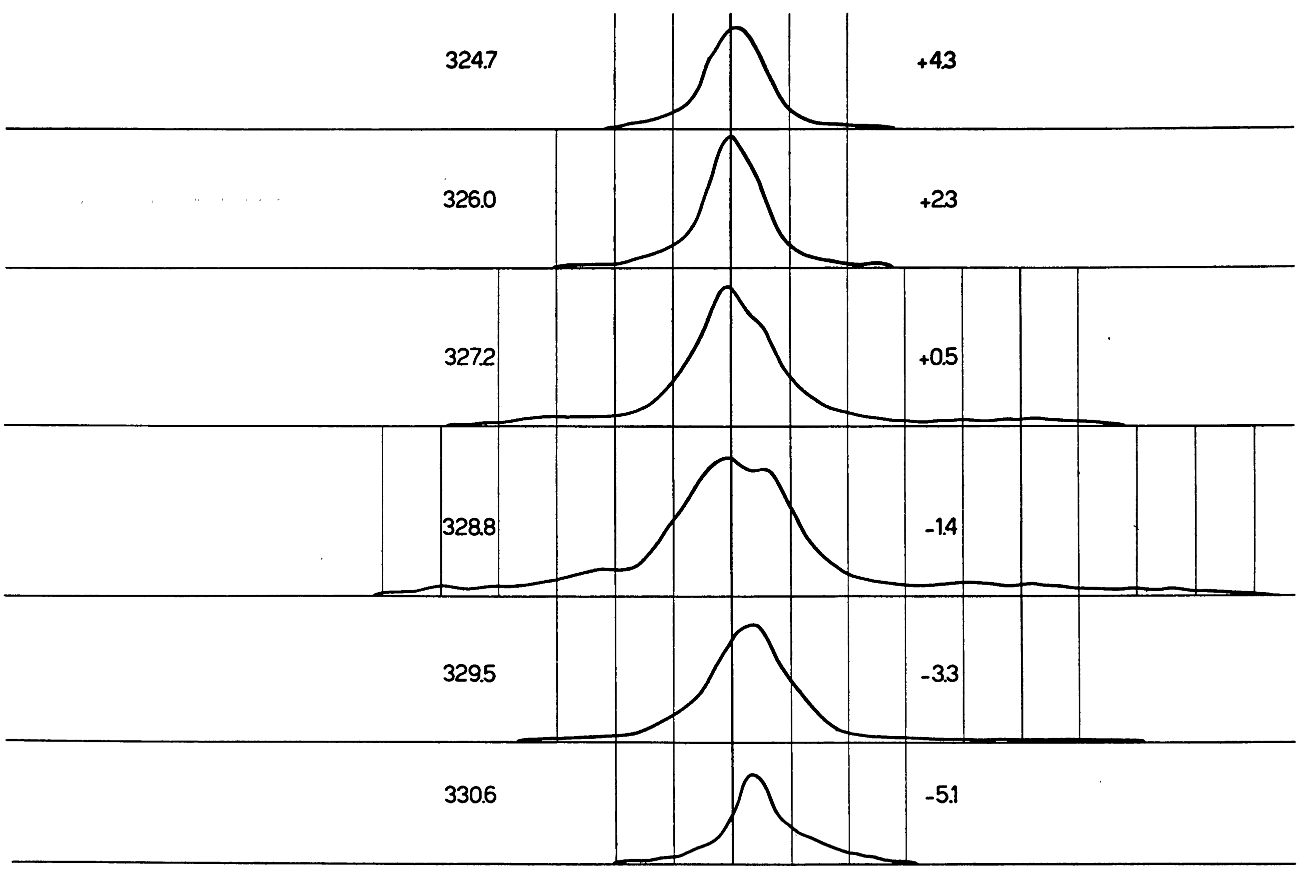
324.7 +4.3
326.0 +2.3
327.2 +0.5
328.8 -1.4
329.5 -3.3
330.6 -5.1

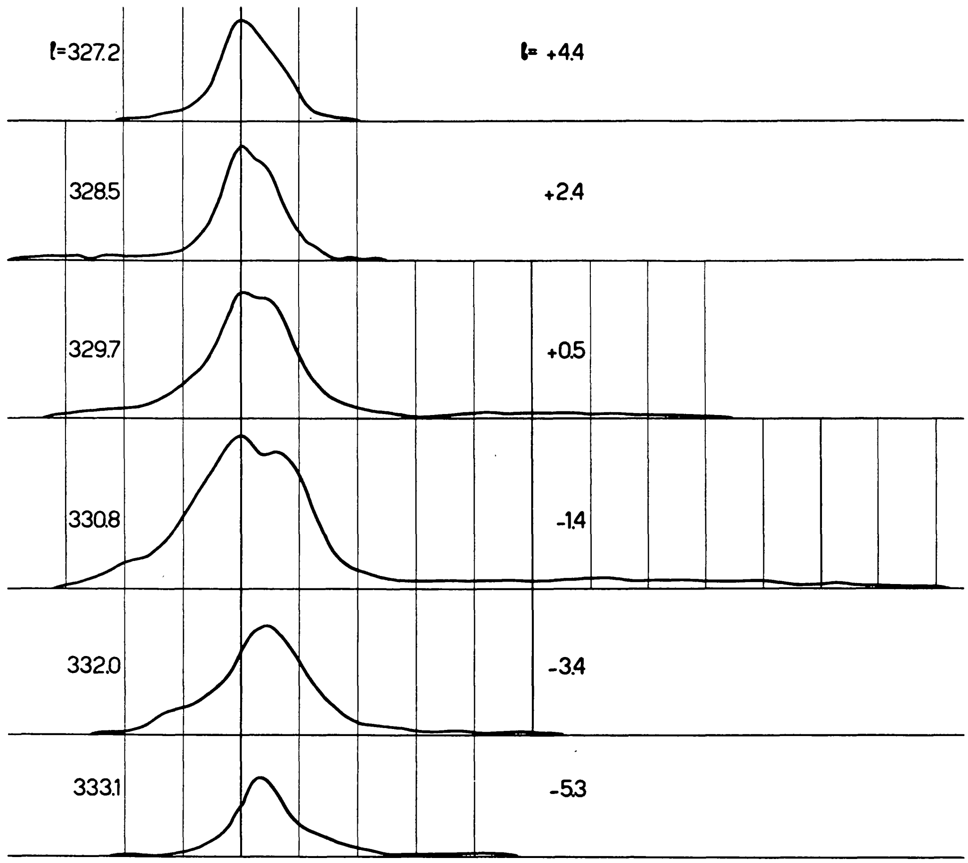
l=327.2
b= +4.4
328.5
+2.4
329.7
+0.5
330.8
-1.4
332.0
-3.4
333.1
-5.3

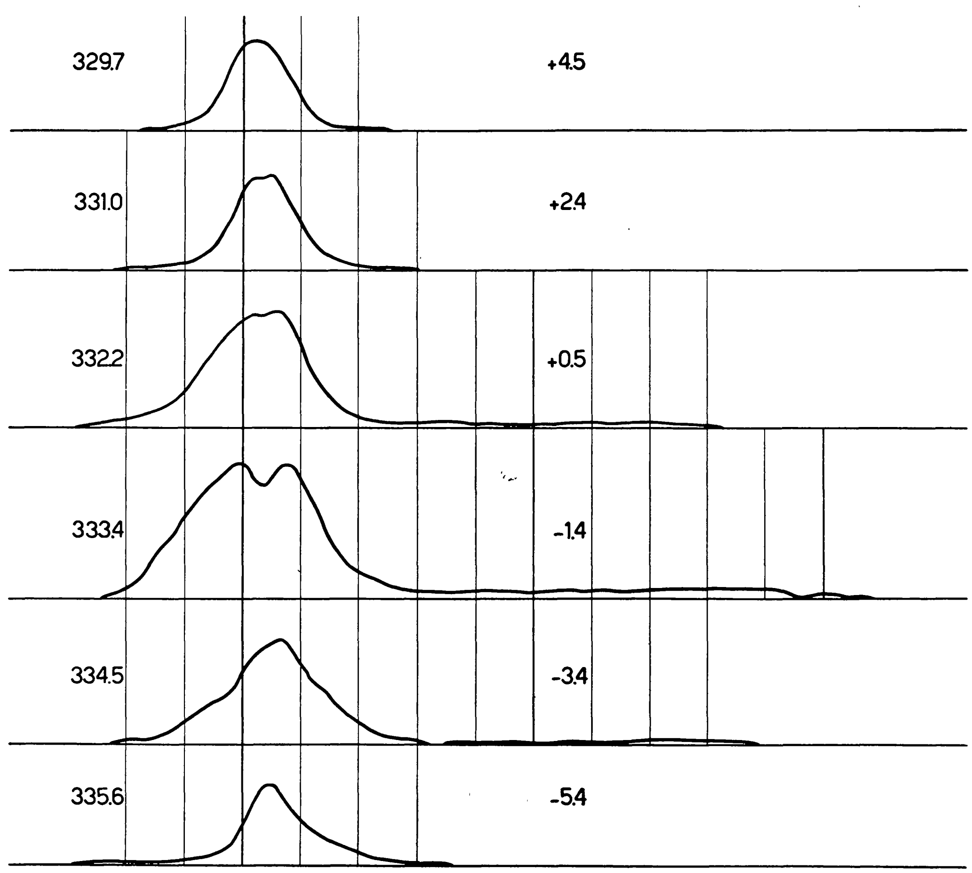
329.7
+4.5
331.0
+2.4
332.2
+0.5
333.4
-1.4
334.5
-3.4
335.6
-5.4

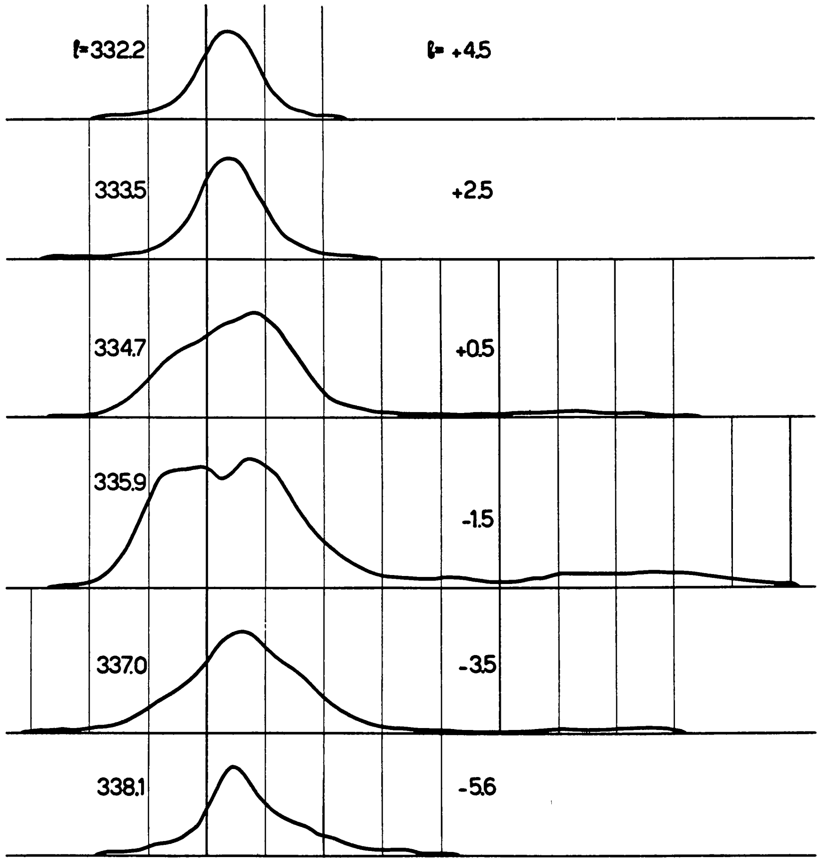
l=332.2
b= +4.5
333.5
+2.5
334.7
+0.5
335.9
-1.5
337.0
-3.5
338.1
-5.6

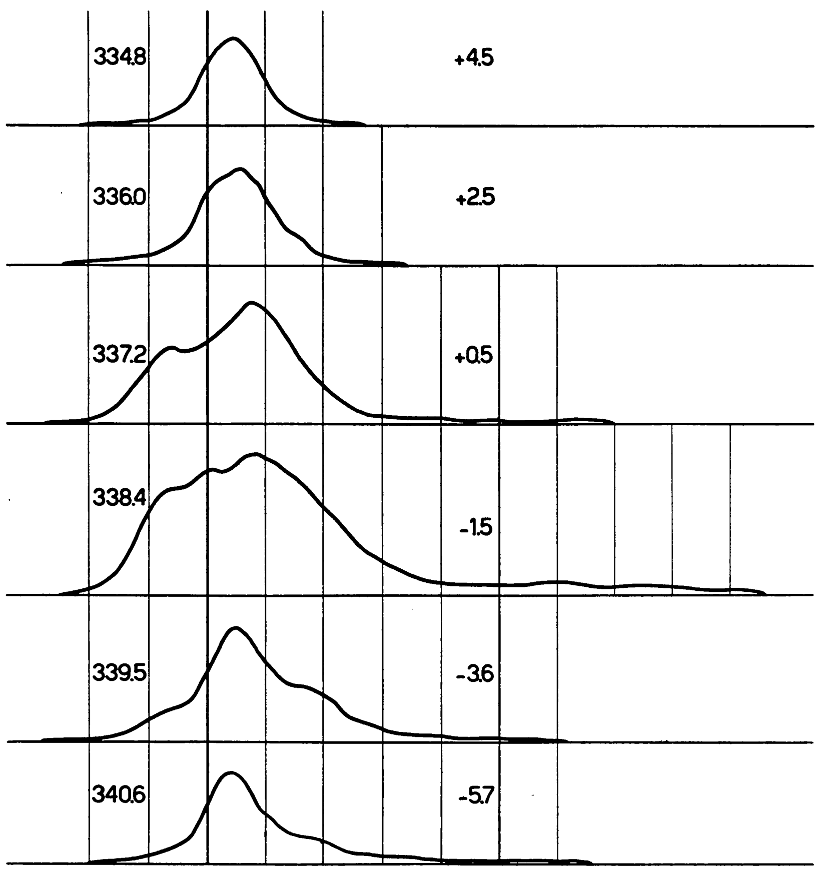
334.8
+4.5
336.0
+2.5
337.2
+0.5
338.4
-1.5
339.5
-3.6
340.6
-5.7

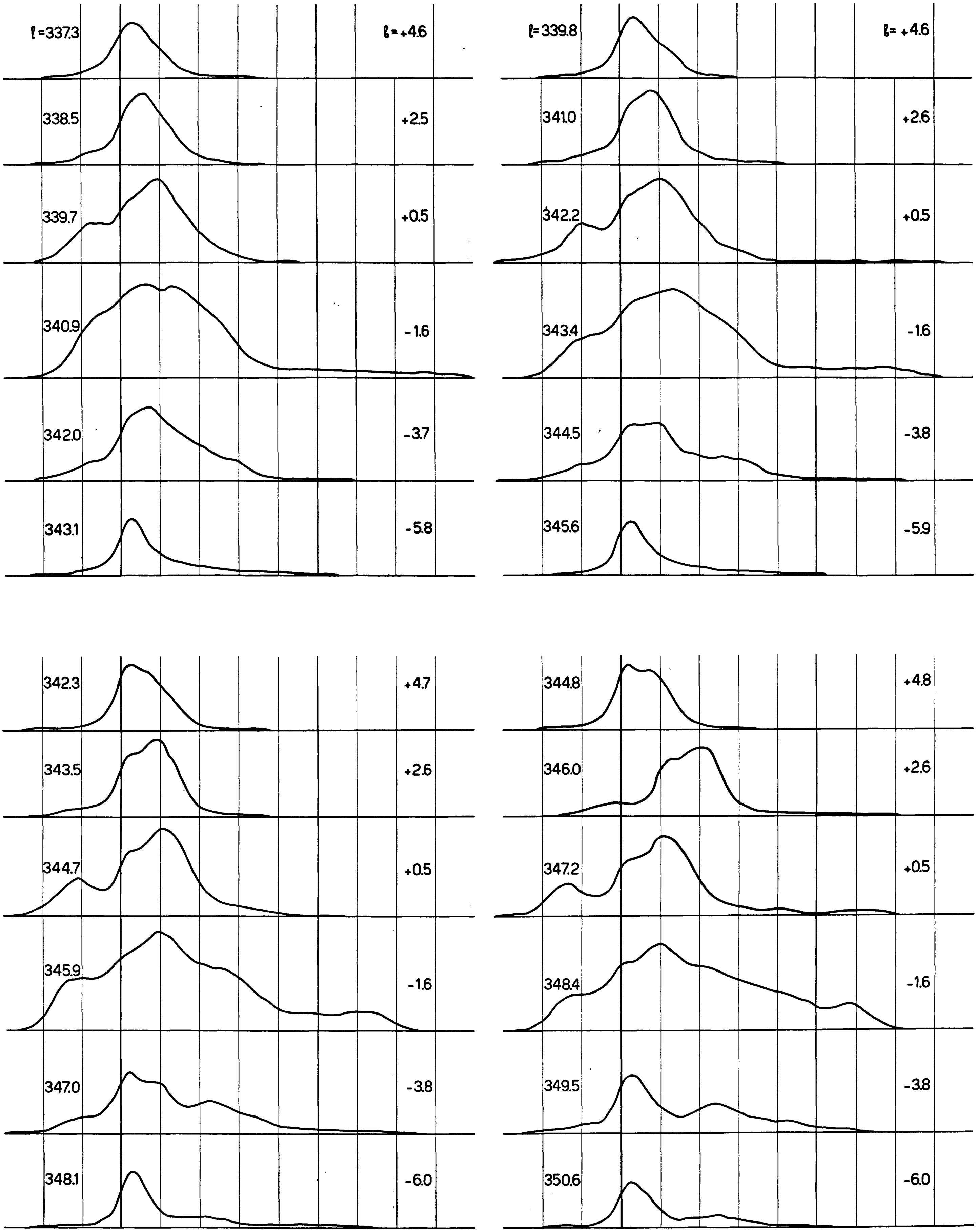

l=337.3
b=+4.6
338.5
+2.5
339.7
+0.5
340.9
-1.6
342.0
-3.7
343.1
-5.8
l=339.8
b=+4.6
341.0
+2.6
342.2
+0.5
343.4
-1.6
344.5
-3.8
345.6
-5.9
342.3
+4.7
343.5
+2.6
344.7
+0.5
345.9
-1.6
347.0
-3.8
348.1
-6.0
344.8
+4.8
346.0
+2.6
347.2
+0.5
348.4
-1.6
349.5
-3.8
350.6
-6.0

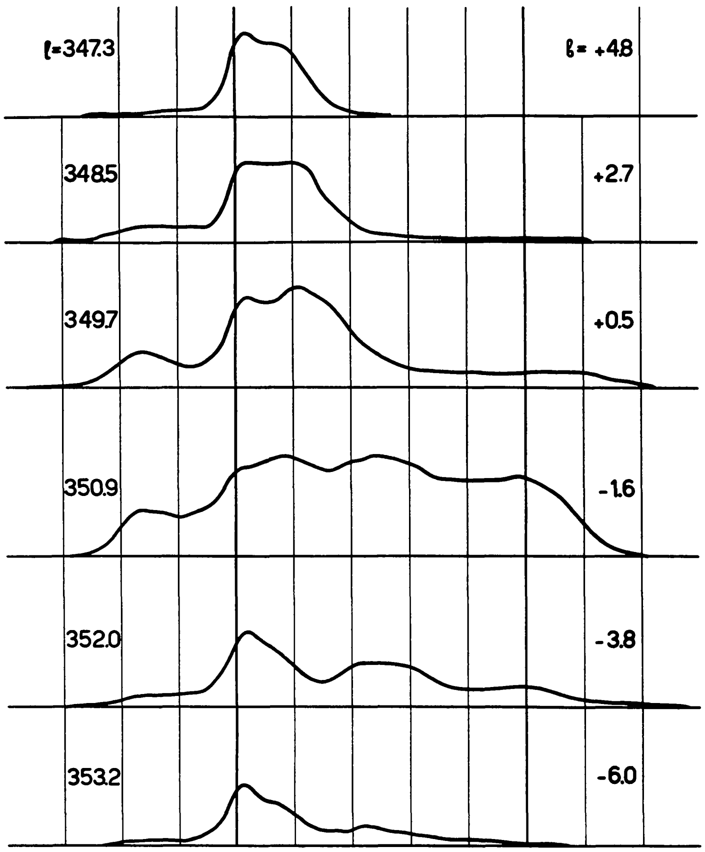
l=347.3
b= +4.8
348.5
+2.7
349.7
+0.5
350.9
-1.6
352.0
-3.8
353.2
-6.0

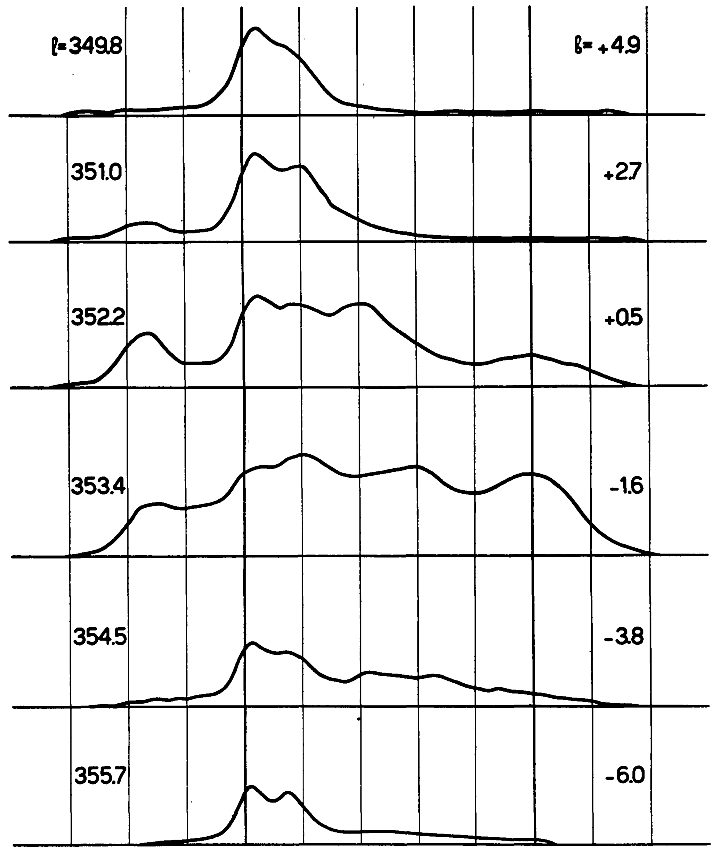
l=349.8
b= +4.9
351.0
+2.7
352.2
+0.5
353.4
-1.6
354.5
-3.8
355.7
-6.0

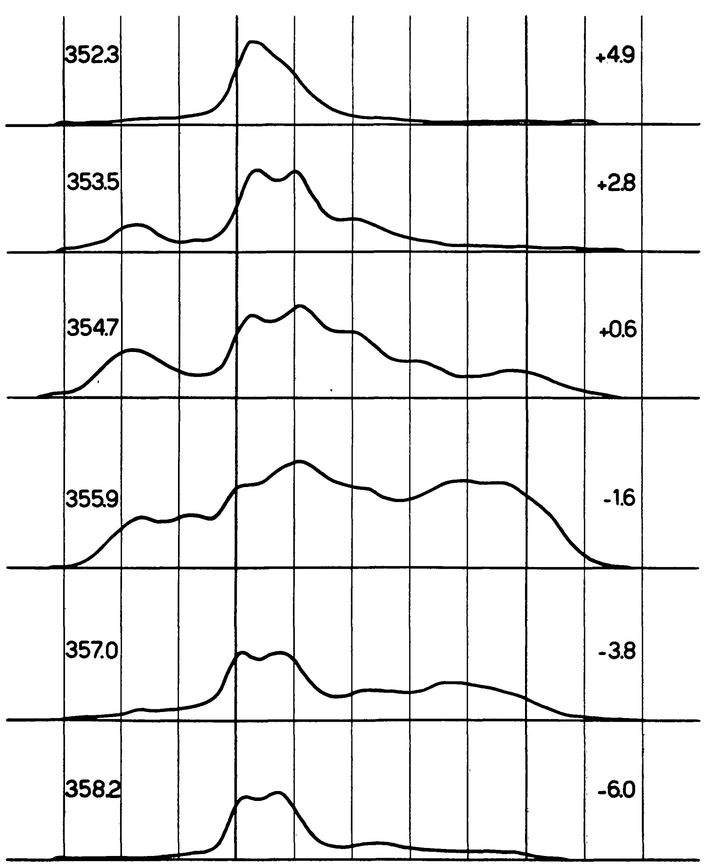
352.3
+4.9
353.5
+2.8
354.7
+0.6
355.9
-1.6
357.0
-3.8
358.2
-6.0

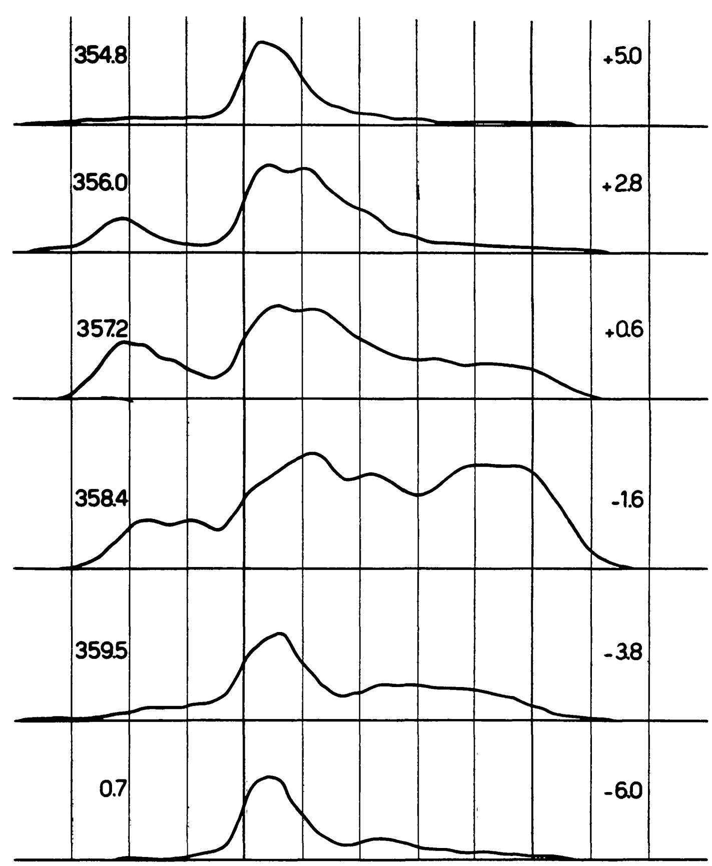
354.8
+5.0
356.0
+2.8
357.2
+0.6
358.4
-1.6
359.5
-3.8
0.7
-6.0

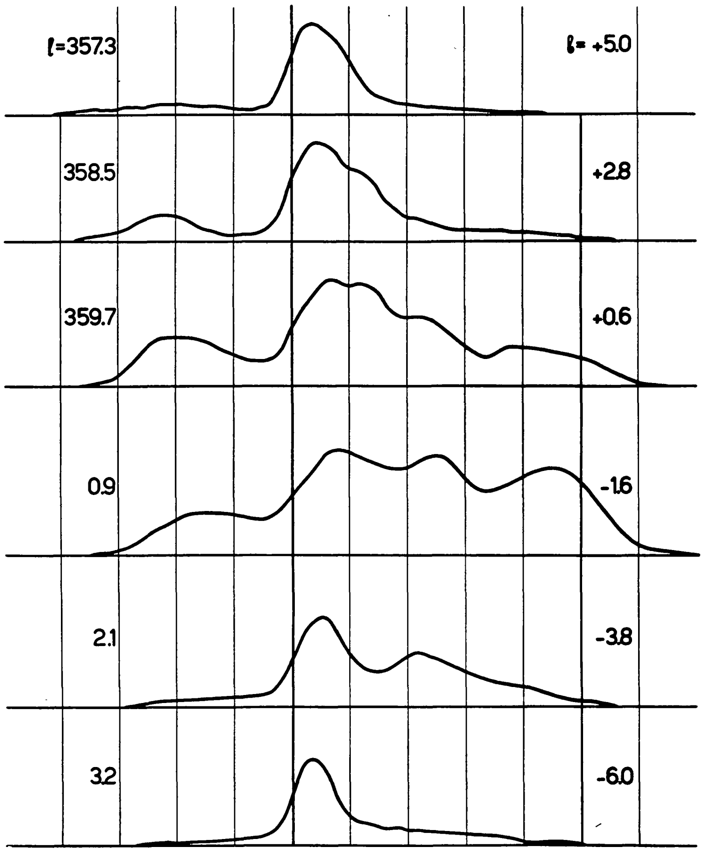

l=357.3
b= +5.0
358.5
+2.8
359.7
+0.6
0.9
-1.6
2.1
-3.8
3.2
-6.0

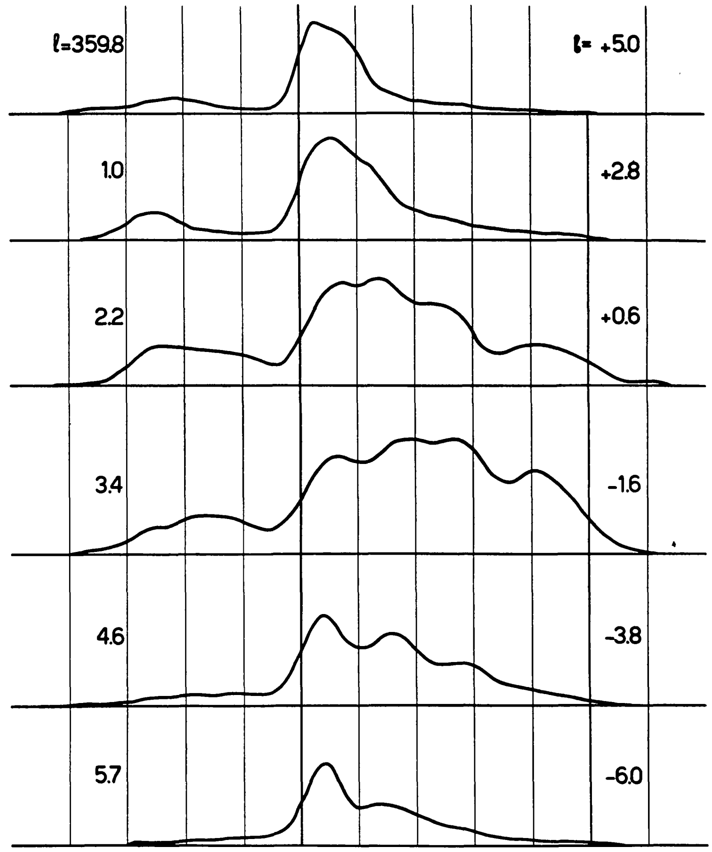

l=359.8
b= +5.0
1.0
+2.8
2.2
+0.6
3.4
-1.6
4.6
-3.8
5.7
-6.0

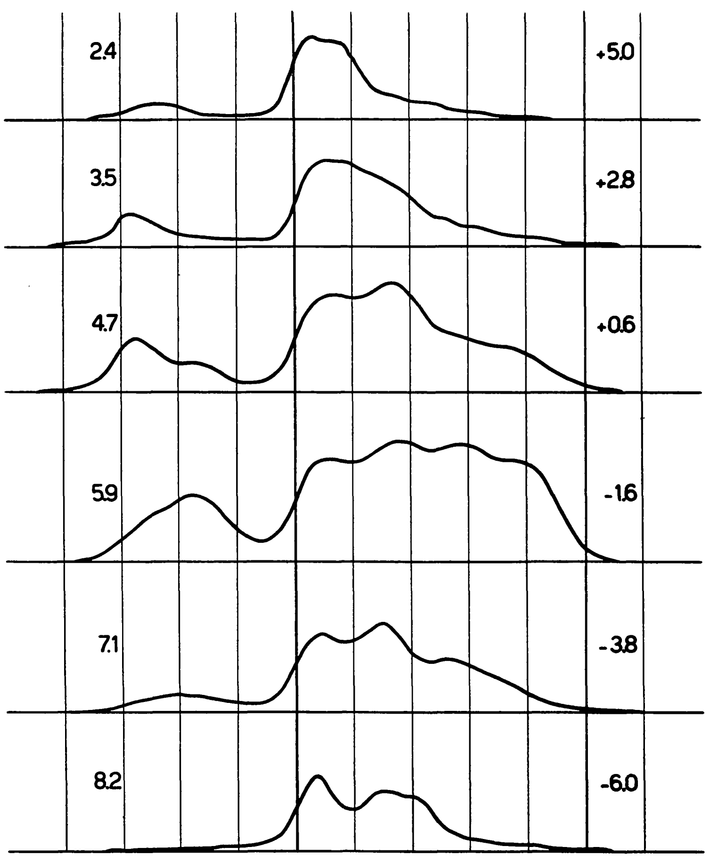

2.4
+5.0
3.5
+2.8
4.7
+0.6
5.9
-1.6
7.1
-3.8
8.2
-6.0

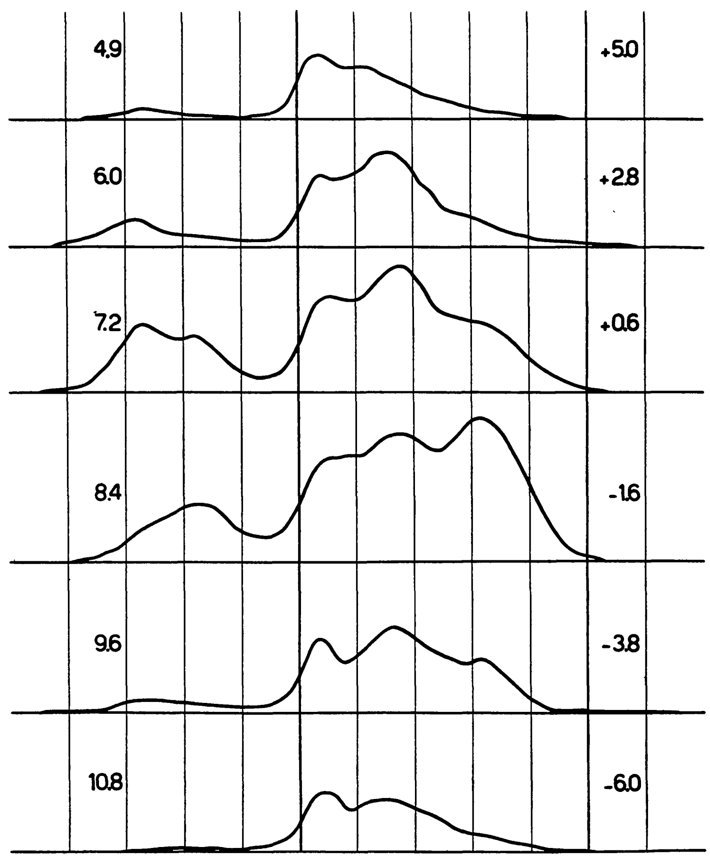

4.9
+5.0
6.0
+2.8
7.2
+0.6
8.4
-1.6
9.6
-3.8
10.8
-6.0

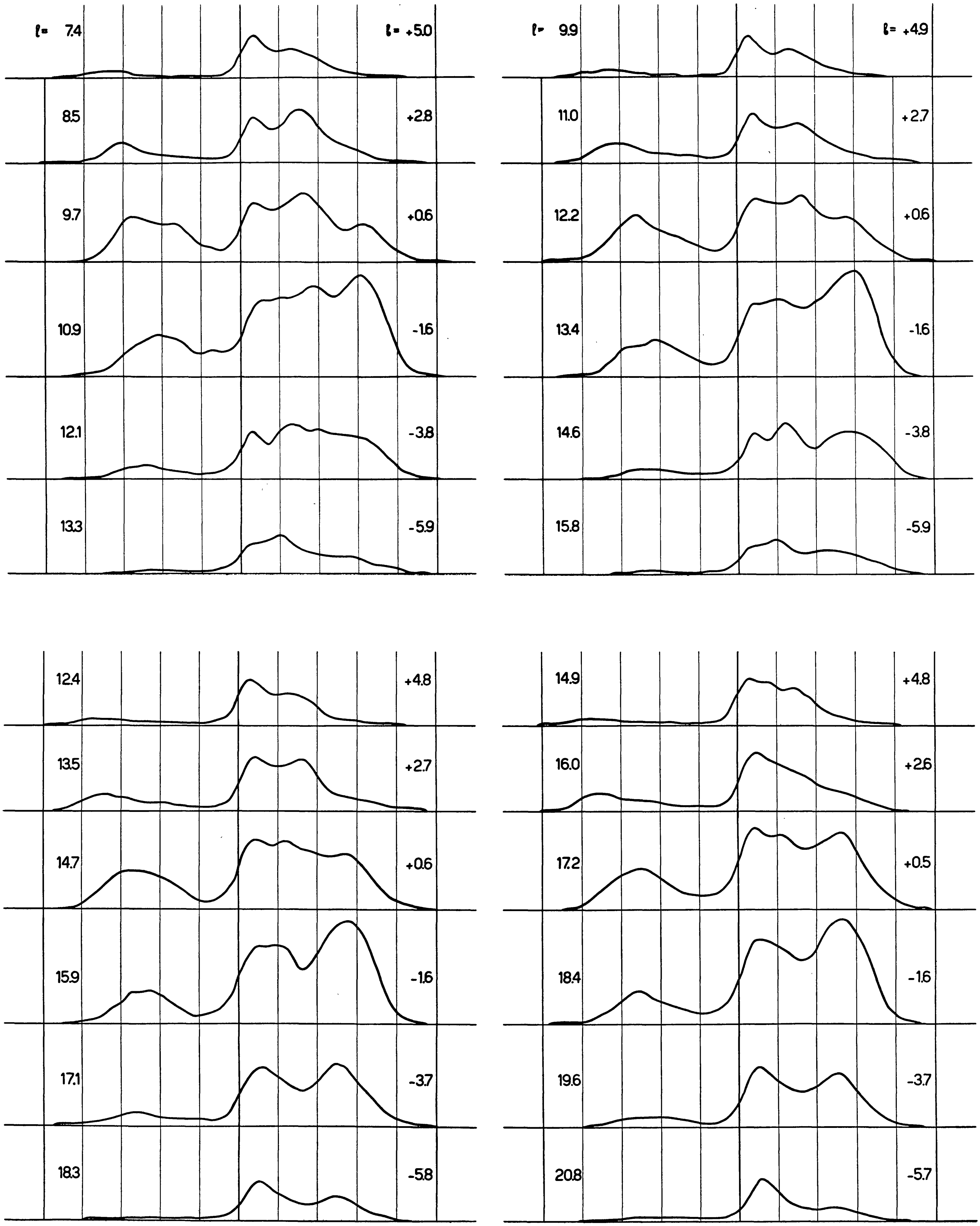
l= 7.4
b= +5.0
8.5
+2.8
9.7
+0.6
10.9
-1.6
12.1
-3.8
13.3
-5.9
l= 9.9
b= +4.9
11.0
+2.7
12.2
+0.6
13.4
-1.6
14.6
-3.8
15.8
-5.9
12.4
+4.8
13.5
+2.7
14.7
+0.6
15.9
-1.6
17.1
-3.7
18.3
-5.8
14.9
+4.8
16.0
+2.6
17.2
+0.5
18.4
-1.6
19.6
-3.7
20.8
-5.7

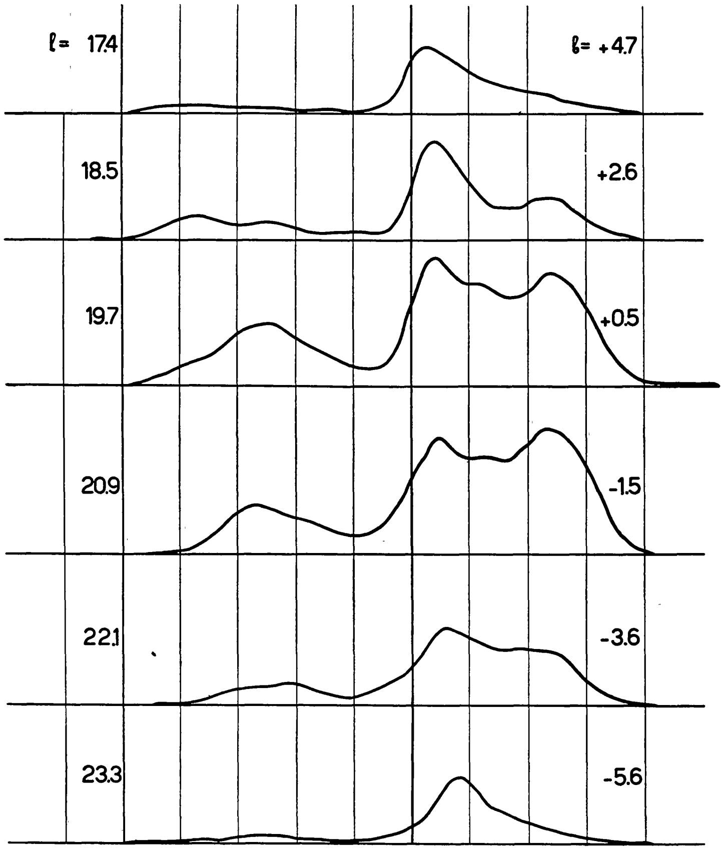
l= 17.4
b= +4.7
18.5
+2.6
19.7
+0.5
20.9
-1.5
22.1
-3.6
23.3
-5.6

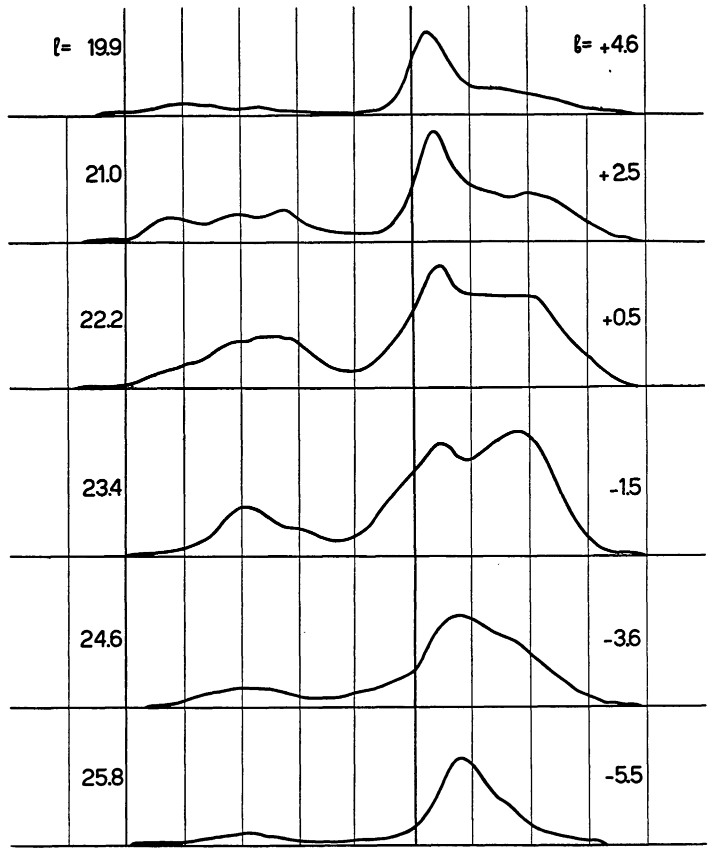
l= 19.9
b= +4.6
21.0
+2.5
22.2
+0.5
23.4
-1.5
24.6
-3.6
25.8
-5.5

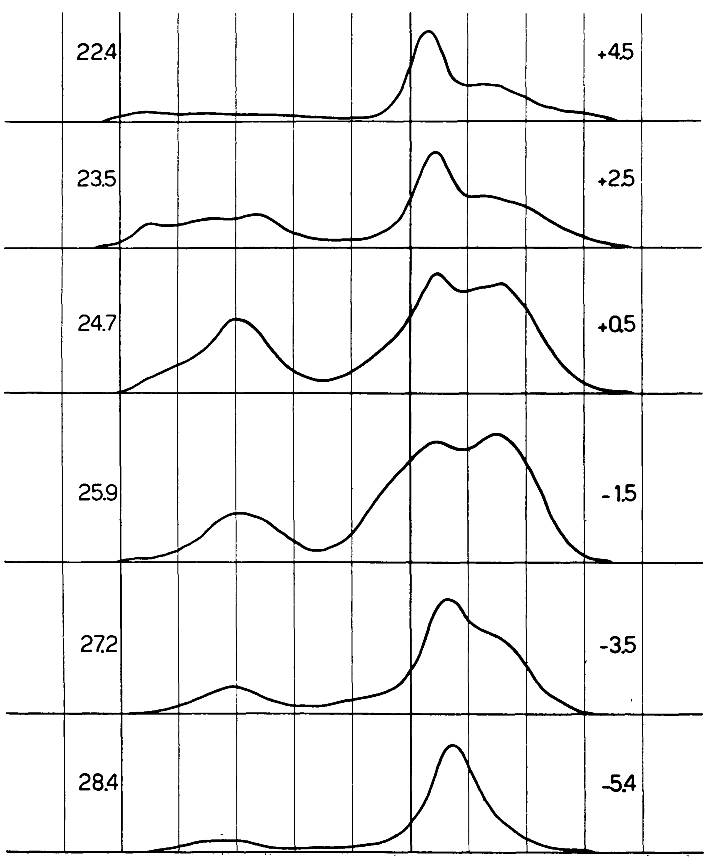
22.4
+4.5
23.5
+2.5
24.7
+0.5
25.9
-1.5
27.2
-3.5
28.4
-5.4

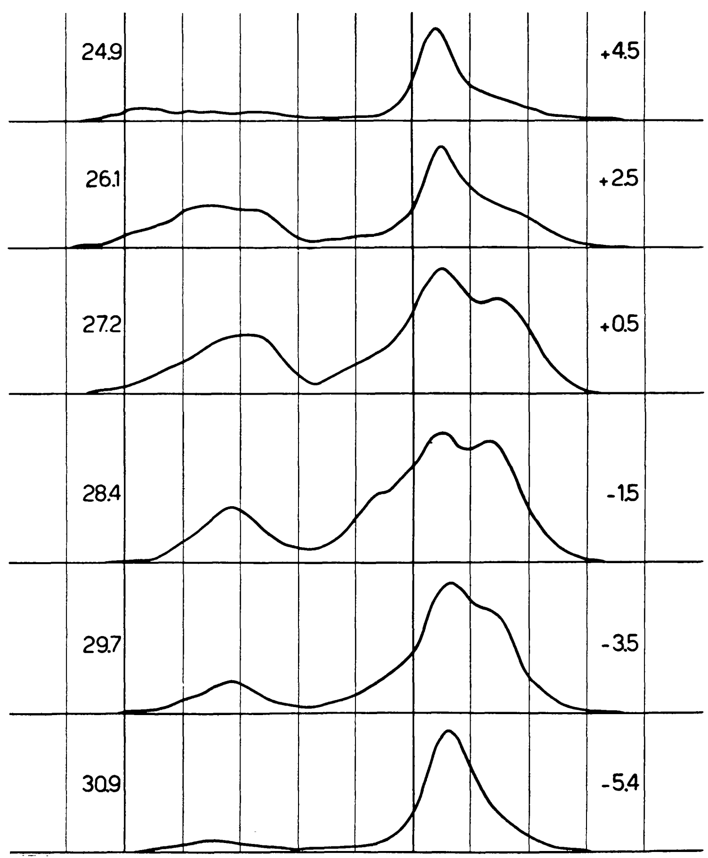
24.9
+4.5
26.1
+2.5
27.2
+0.5
28.4
-1.5
29.7
-3.5
30.9
-5.4

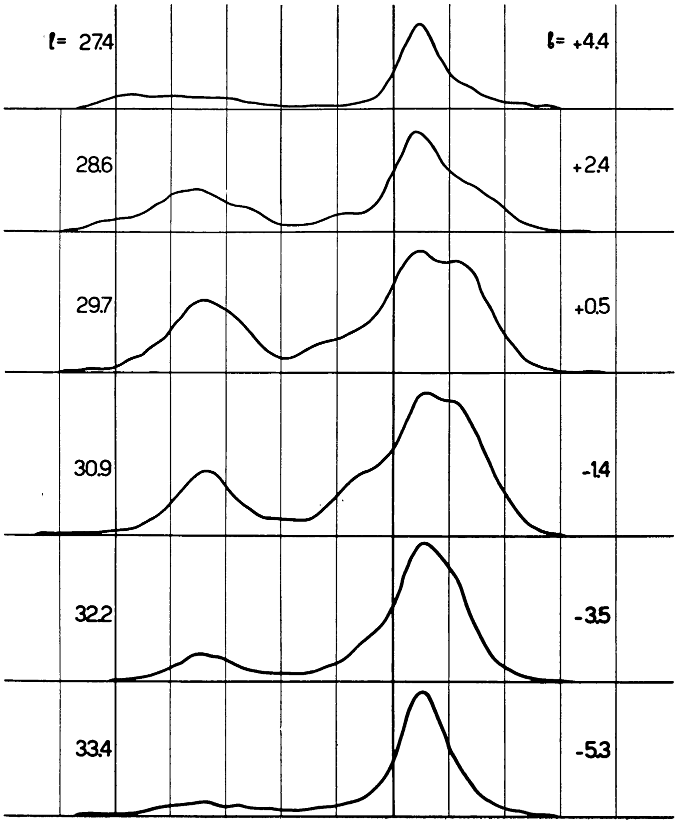
l= 27.4
b= +4.4
28.6
+2.4
29.7
+0.5
30.9
-1.4
32.2
-3.5
33.4
-5.3

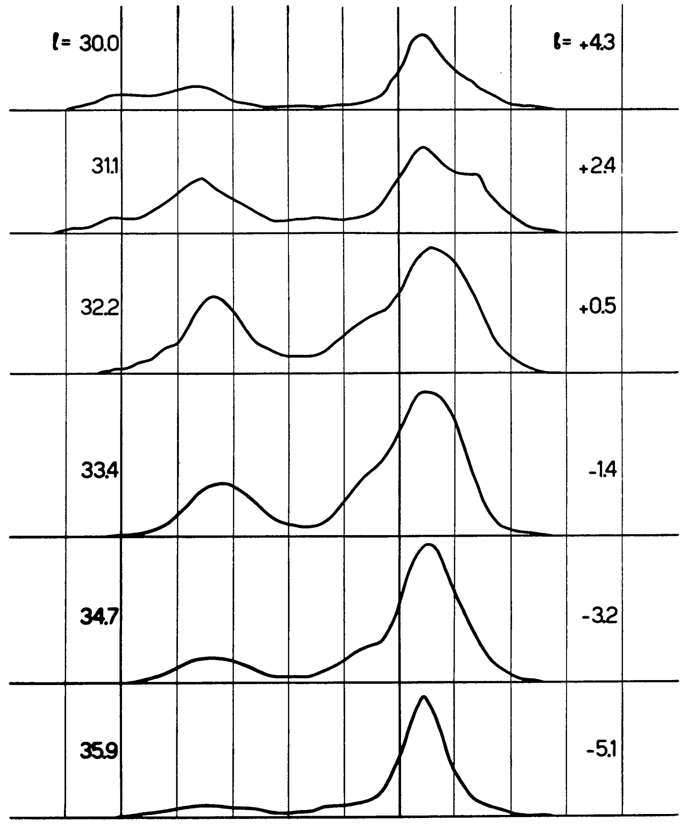
l= 30.0
b= +4.3
31.1
+2.4
32.2
+0.5
33.4
-1.4
34.7
-3.2
35.9
-5.1

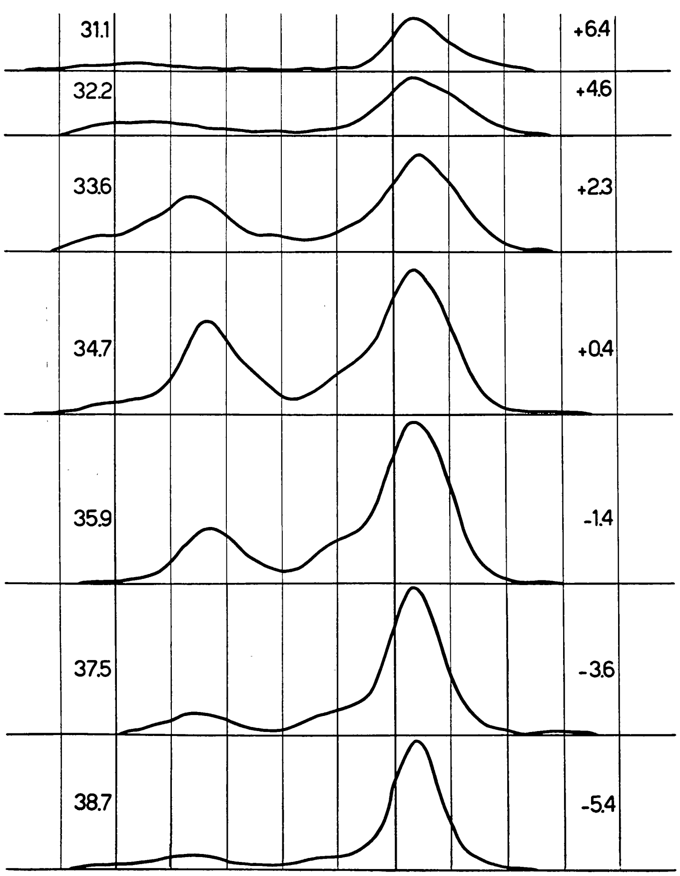
31.1
+6.4
32.2
+4.6
33.6
+2.3
34.7
+0.4
35.9
-1.4
37.5
-3.6
38.7
-5.4

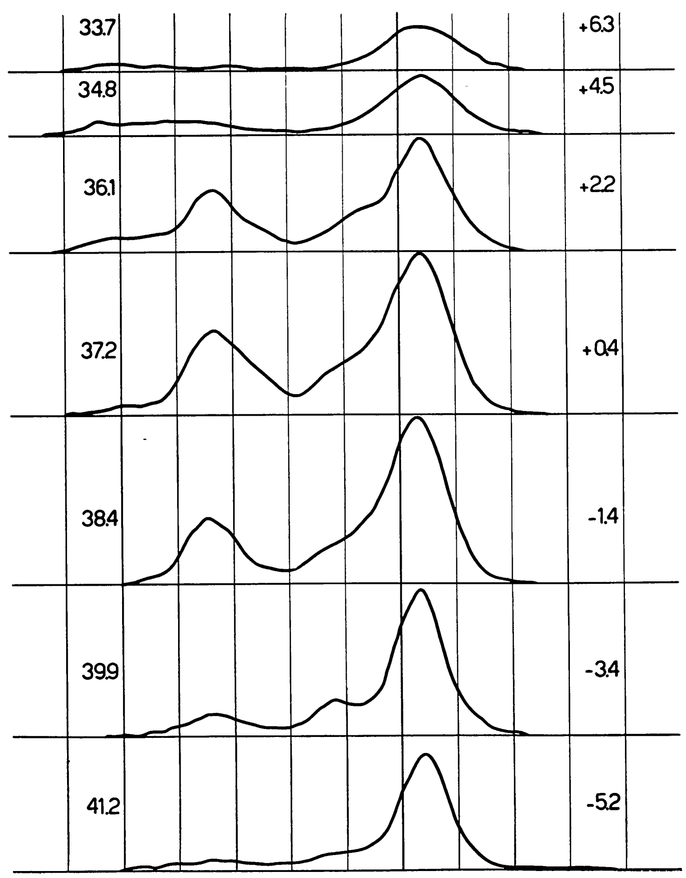
33.7
+6.3
34.8
+4.5
36.1
+2.2
37.2
+0.4
38.4
-1.4
39.9
-3.4
41.2
-5.2

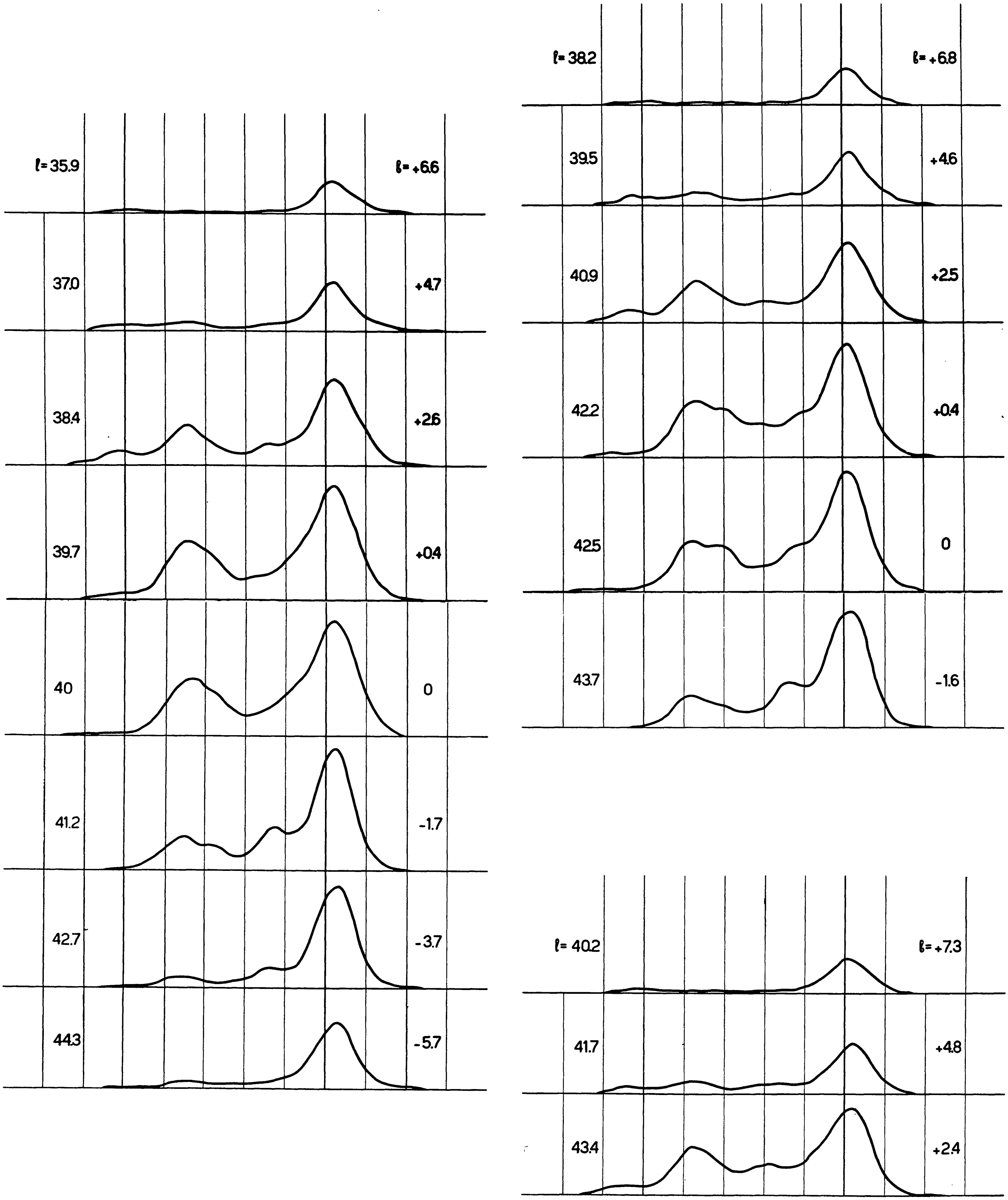
l= 35.9
b= +6.6
37.0
+4.7
38.4
+2.6
39.7
+0.4
40
0
41.2
-1.7
42.7
-3.7
44.3
-5.7
l= 38.2
b= +6.8
39.5
+4.6
40.9
+2.5
42.2
+0.4
42.5
0
43.7
-1.6
l= 40.2
b= +7.3
41.7
+4.8
43.4
+2.4

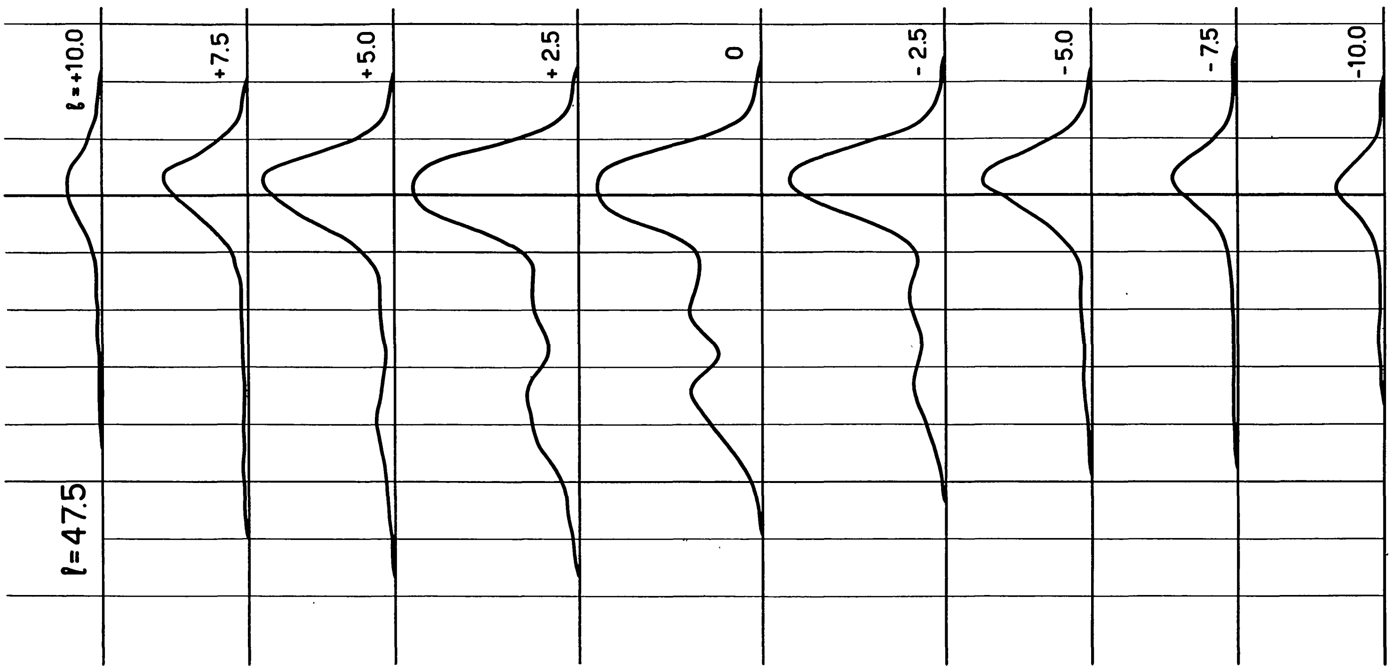

l=+10.0
+7.5
+5.0
+2.5
0
-2.5
-5.0
-7.5
-10.0
l=47.5

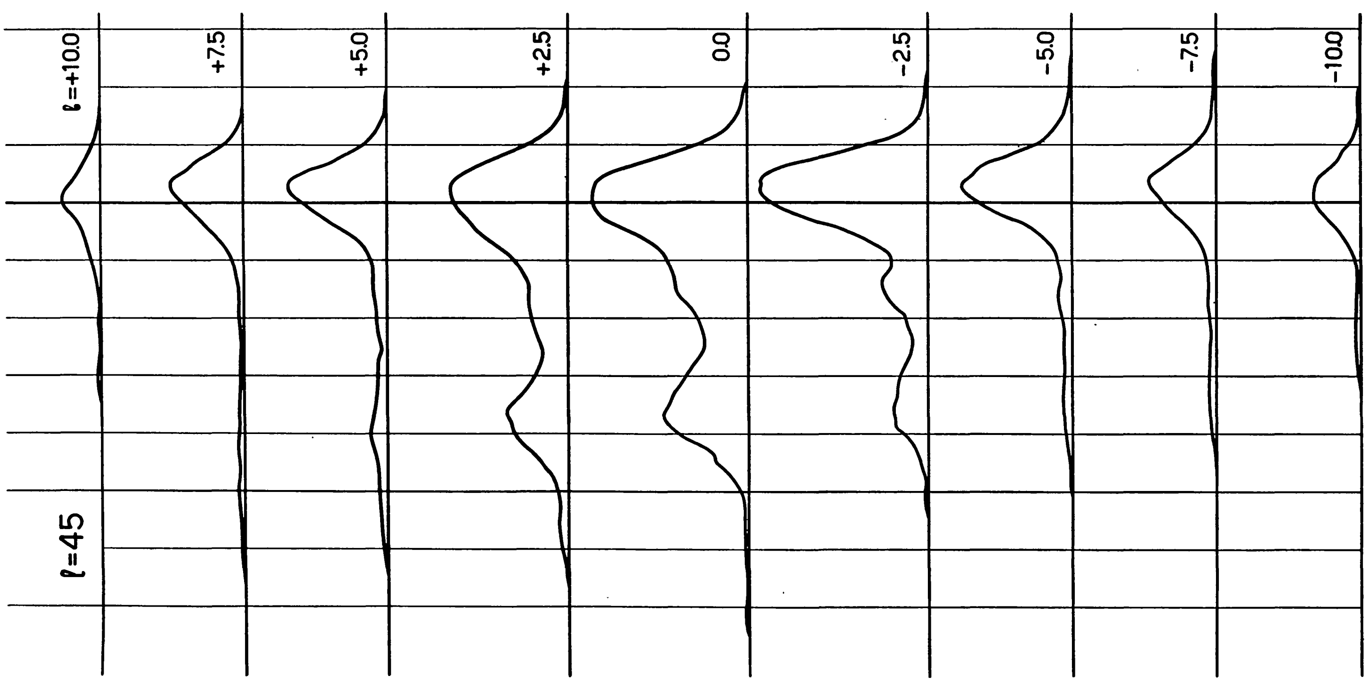

l=+10.0
+7.5
+5.0
+2.5
0.0
-2.5
-5.0
-7.5
-10.0
l=45

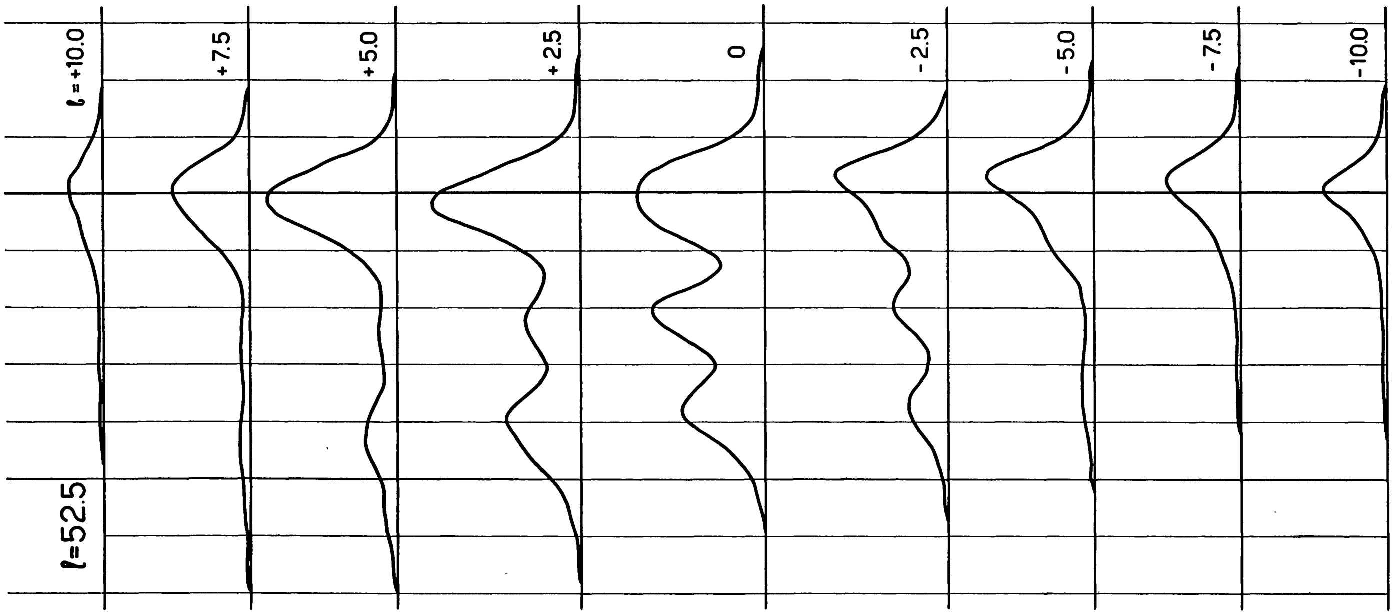
l=52.5
b=+10.0
+7.5
+5.0
+2.5
0
-2.5
-5.0
-7.5
-10.0

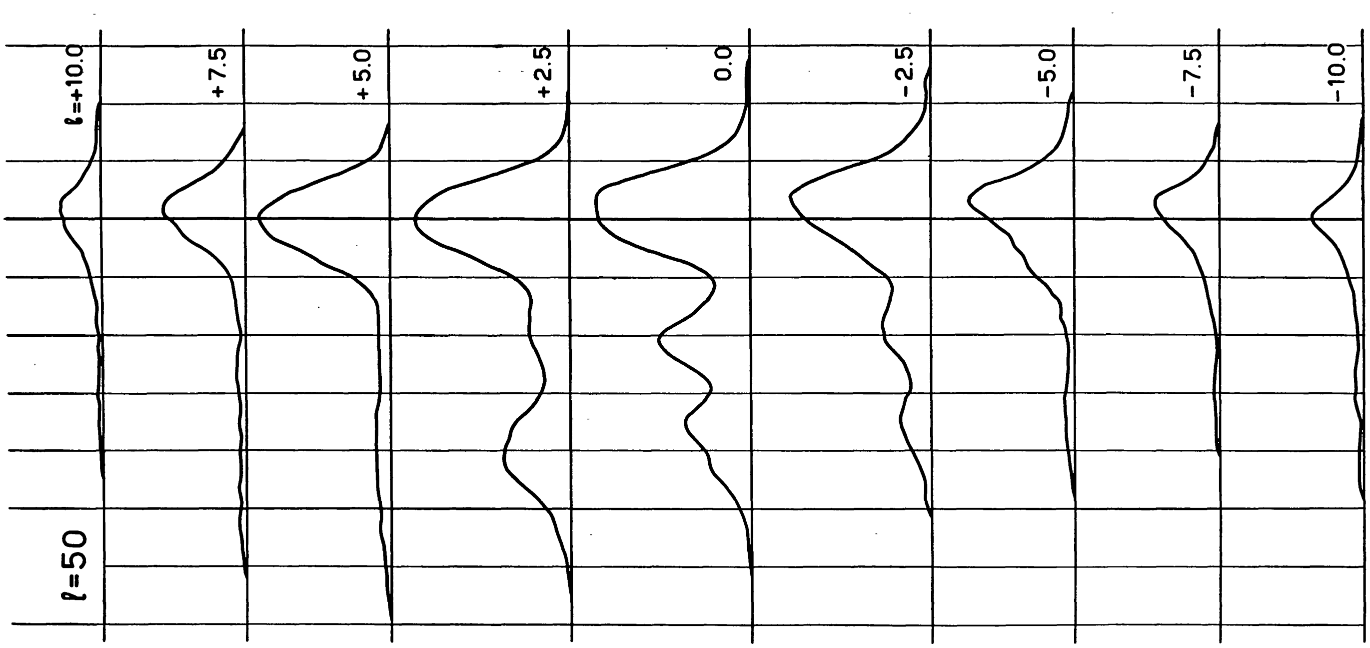
l=50
b=+10.0
+7.5
+5.0
+2.5
0.0
-2.5
-5.0
-7.5
-10.0

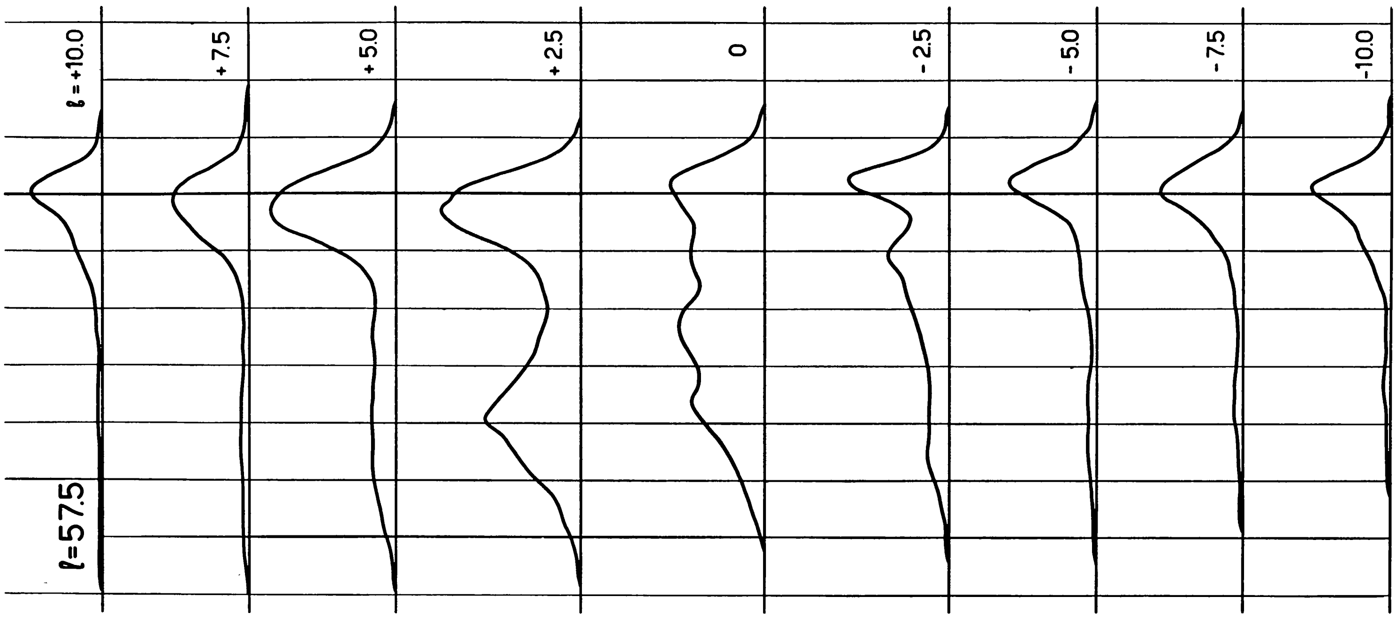
l=57.5
l = +10.0
+ 7.5
+ 5.0
+ 2.5
0
- 2.5
- 5.0
- 7.5
-10.0

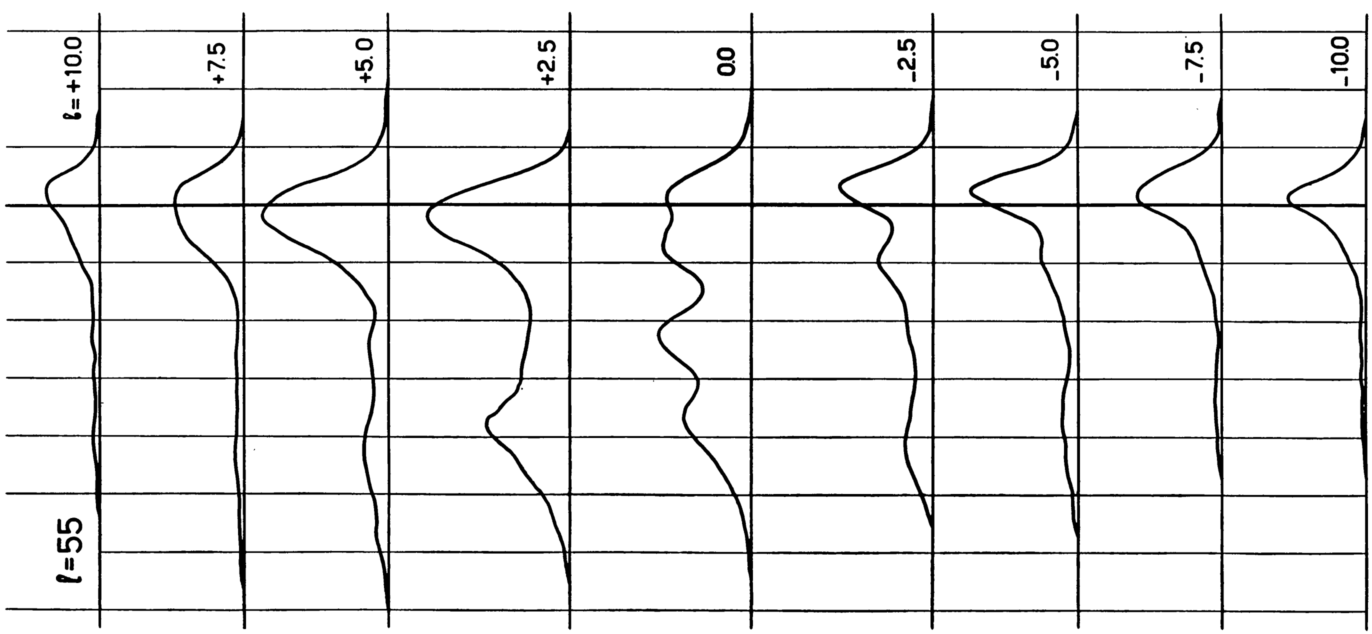
l=55
l = +10.0
+7.5
+5.0
+2.5
0.0
-2.5
-5.0
-7.5
-10.0

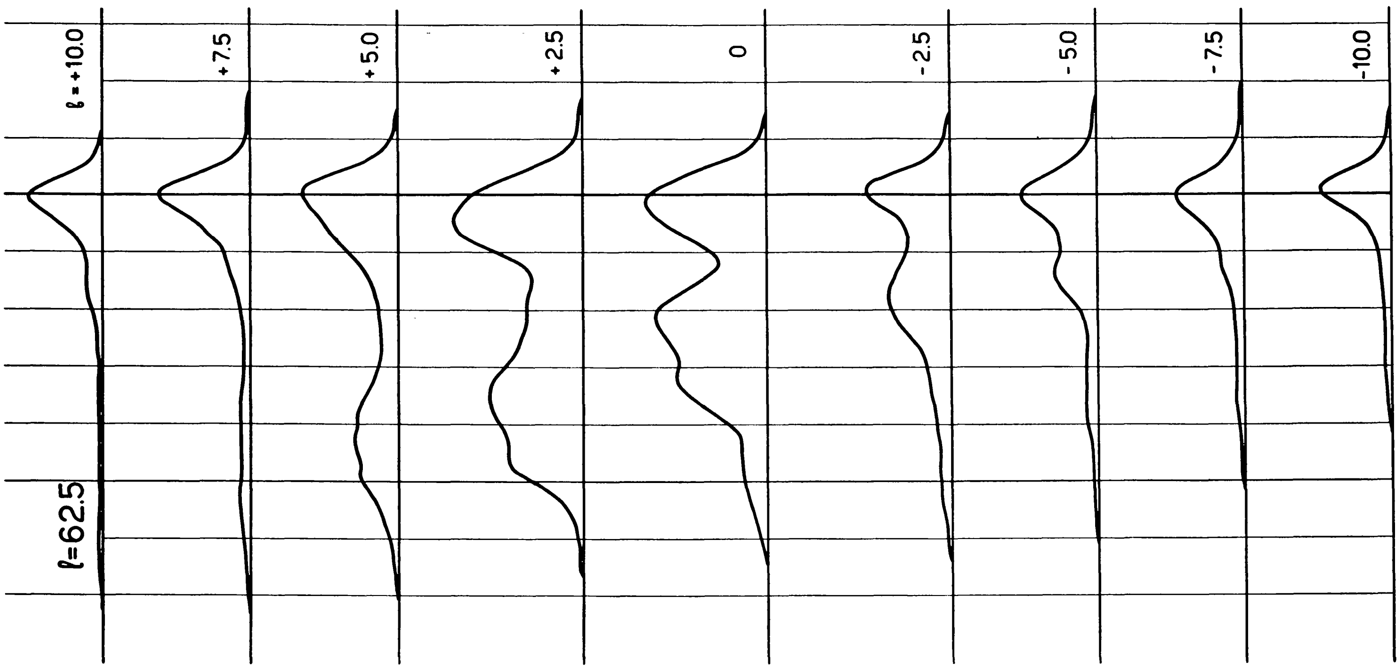
l=62.5
b=+10.0
+7.5
+5.0
+2.5
0
-2.5
-5.0
-7.5
-10.0

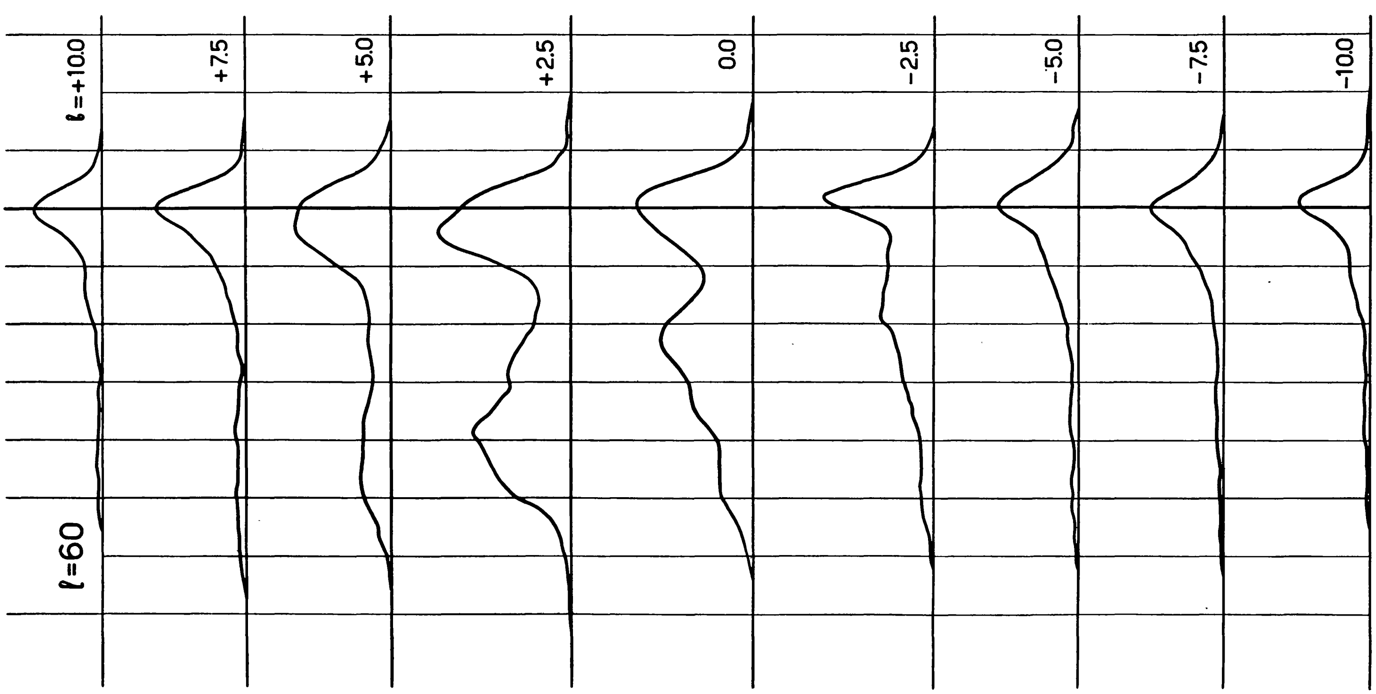
l=60
b=+10.0
+7.5
+5.0
+2.5
0.0
-2.5
-5.0
-7.5
-10.0

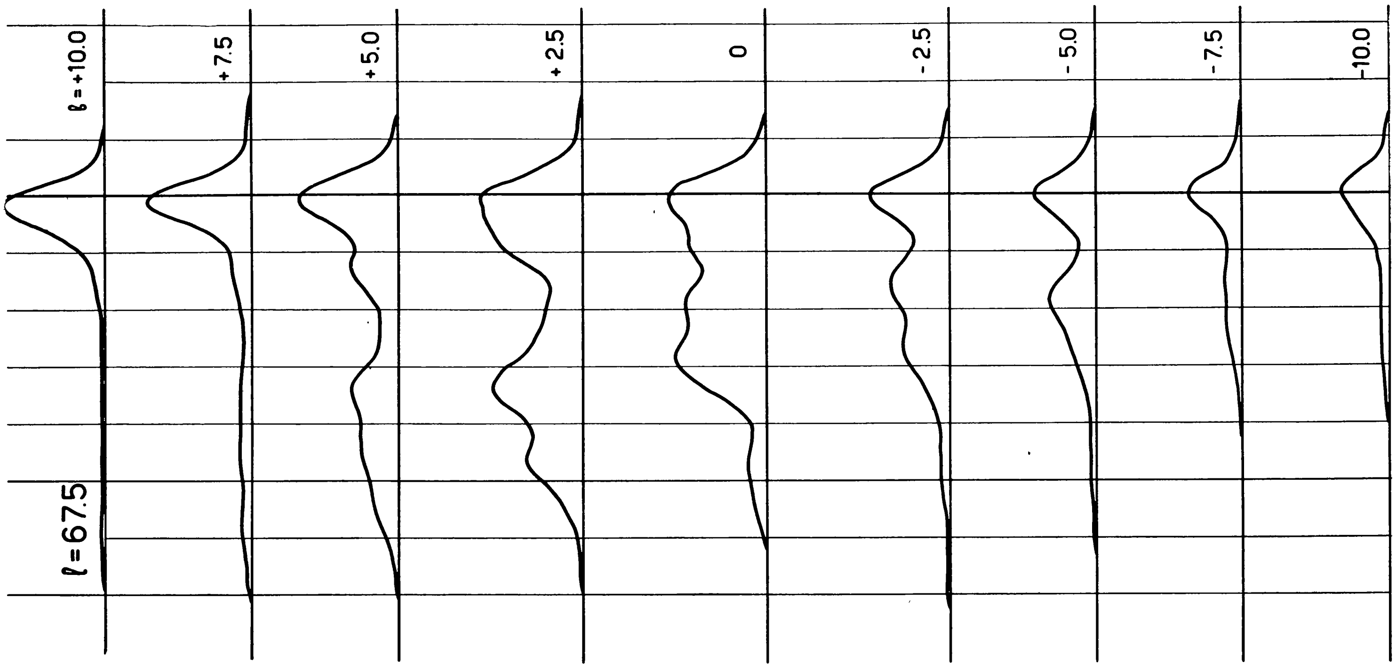
b = +10.0
+7.5
+5.0
+2.5
0
-2.5
-5.0
-7.5
-10.0
l = 67.5

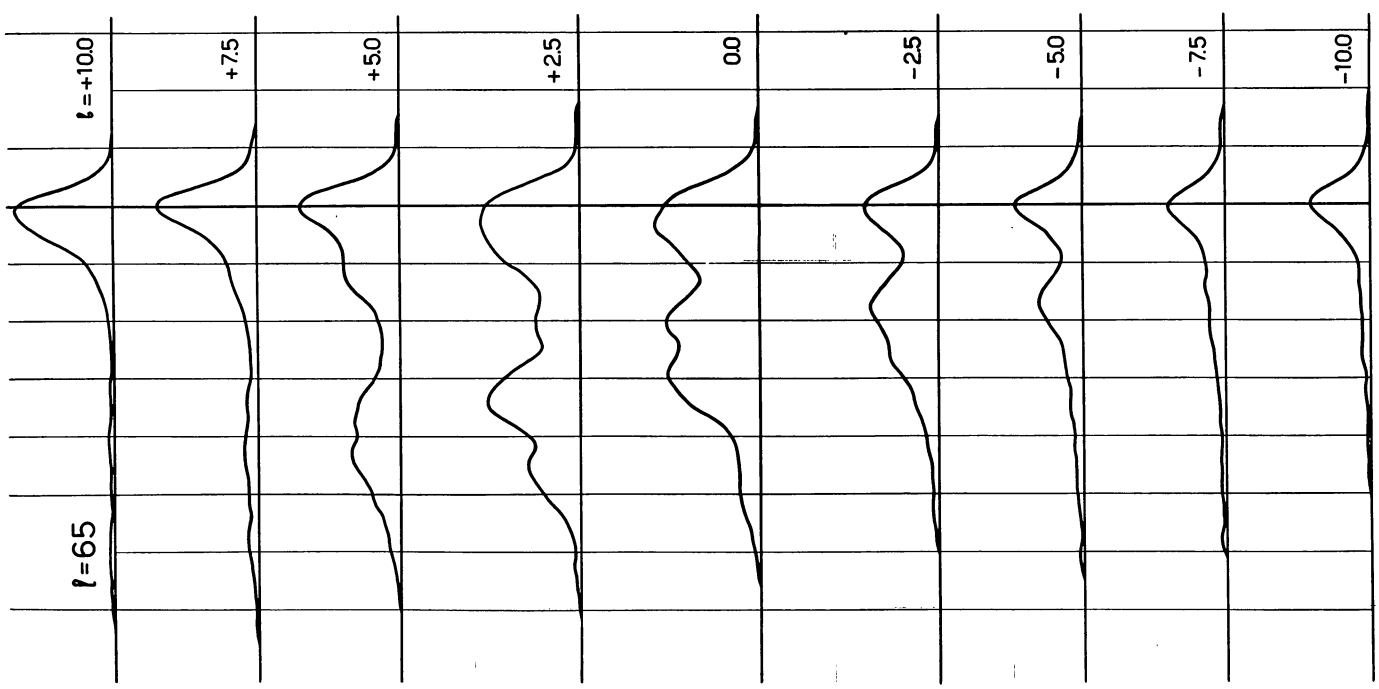
b = +10.0
+7.5
+5.0
+2.5
0.0
-2.5
-5.0
-7.5
-10.0
l = 65

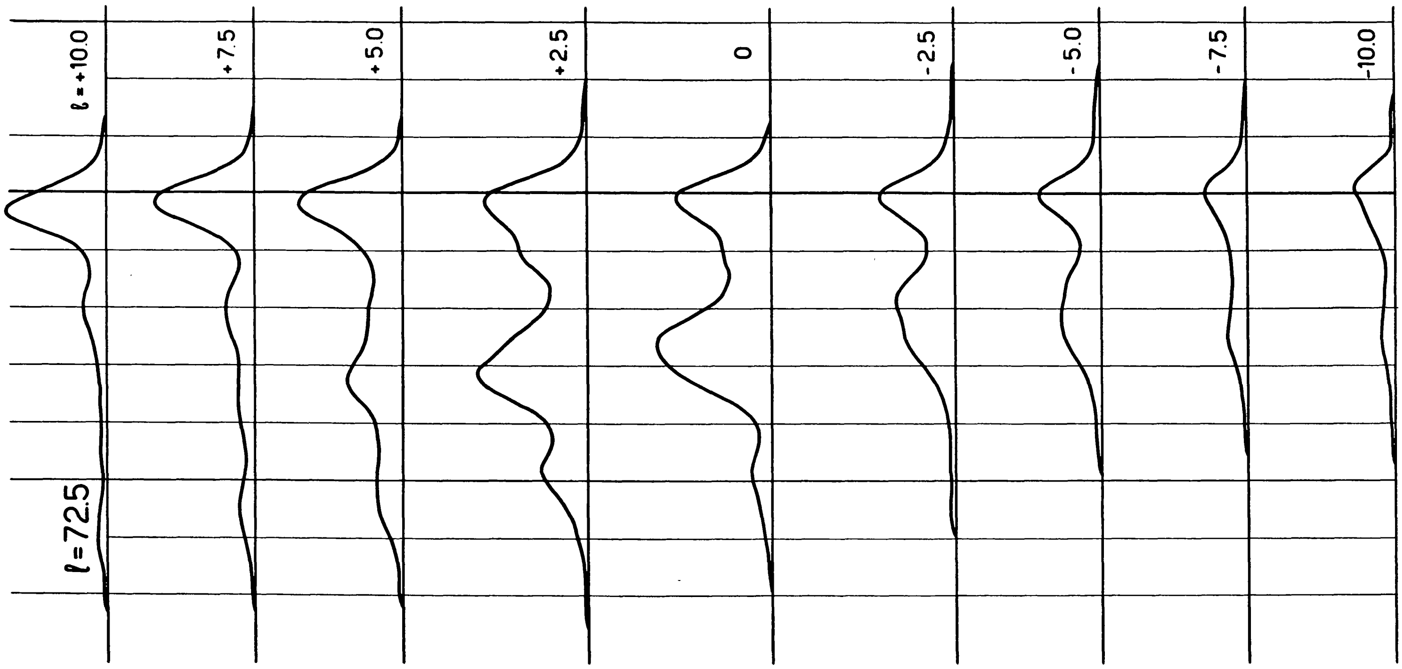
ℓ = +10.0
+7.5
+5.0
+2.5
0
-2.5
-5.0
-7.5
-10.0
ℓ=72.5

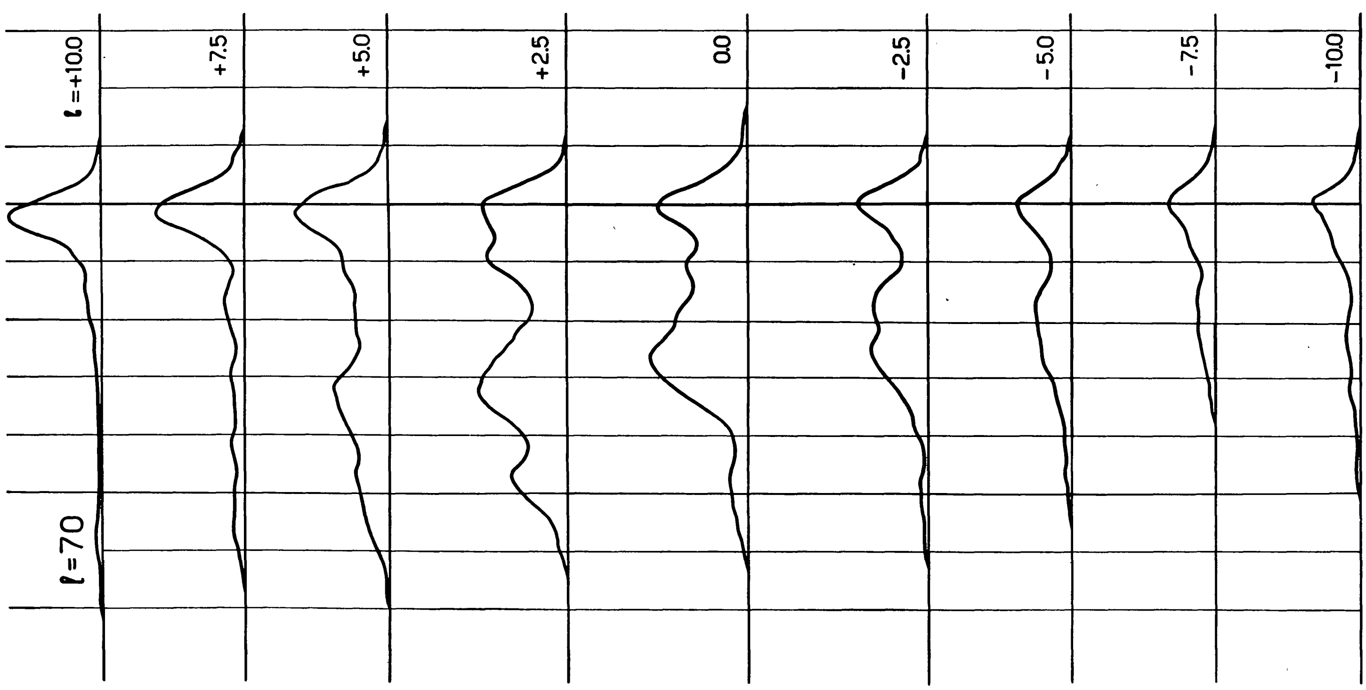
ℓ = +10.0
+7.5
+5.0
+2.5
0.0
-2.5
-5.0
-7.5
-10.0
ℓ=70

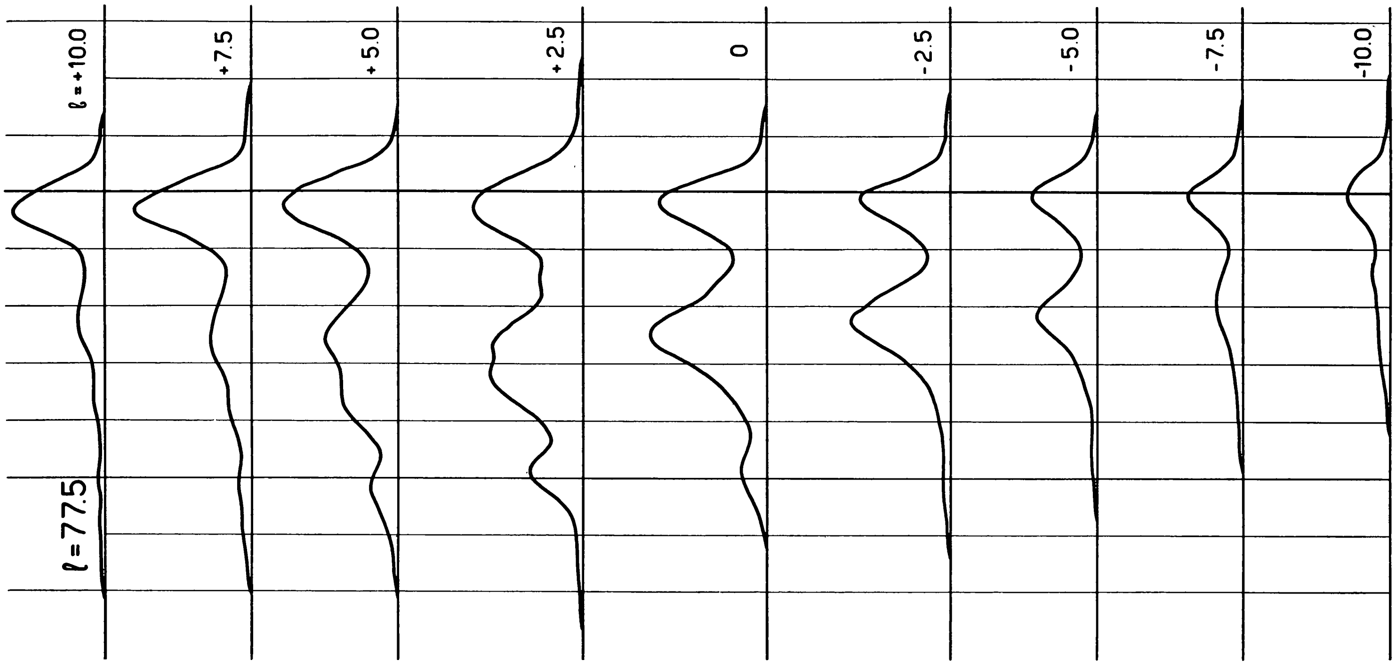
b = +10.0
+7.5
+5.0
+2.5
0
-2.5
-5.0
-7.5
-10.0
l = 77.5

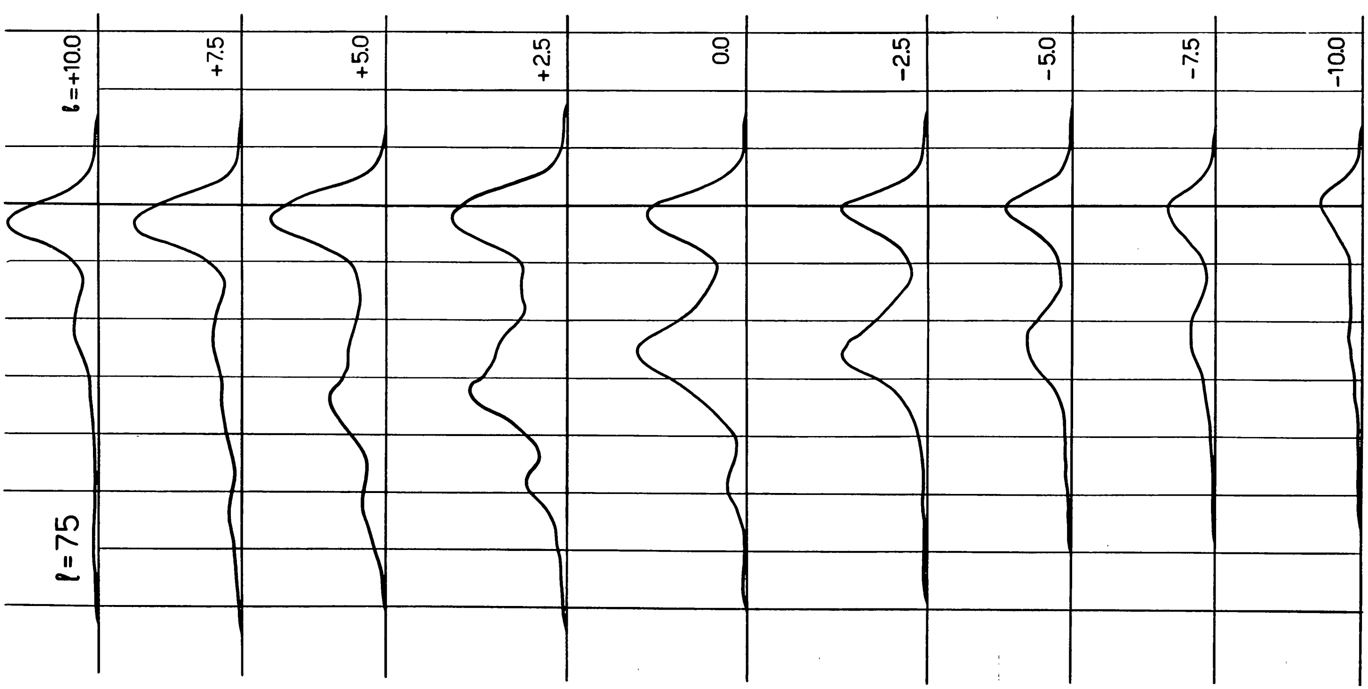
b = +10.0
+7.5
+5.0
+2.5
0.0
-2.5
-5.0
-7.5
-10.0
l = 75

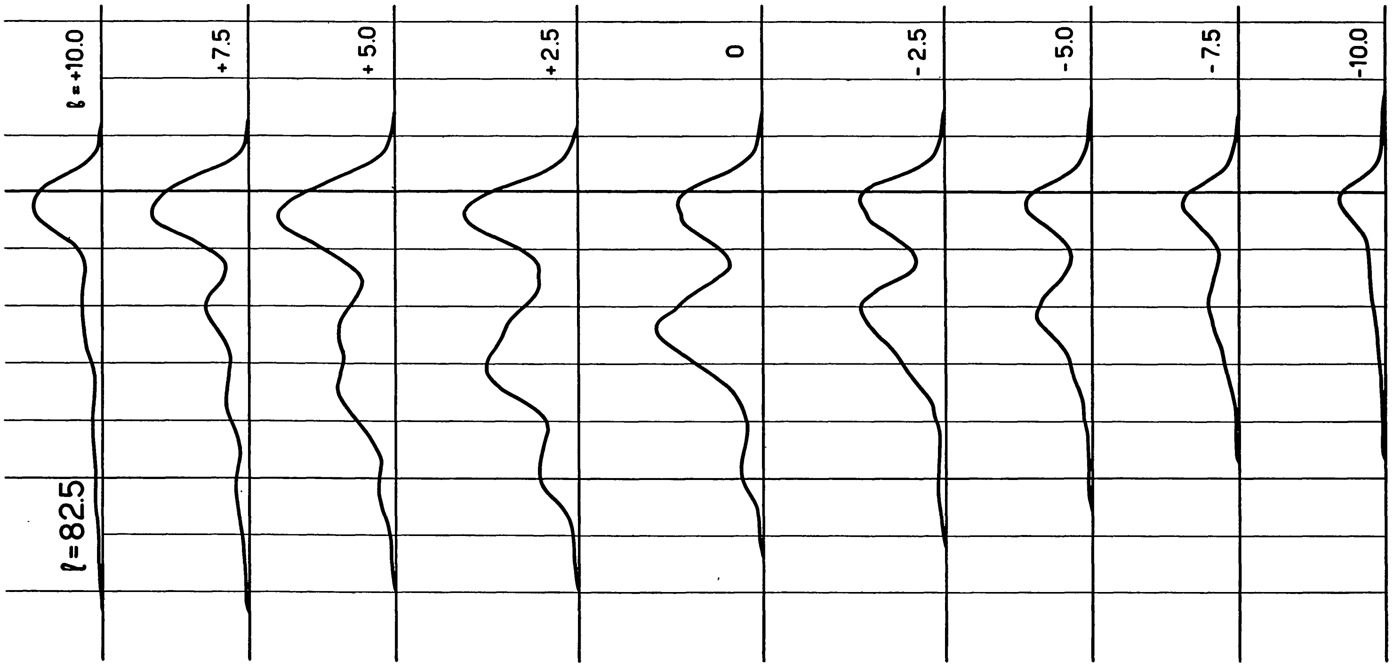

b = +10.0
+7.5
+5.0
+2.5
0
-2.5
-5.0
-7.5
-10.0
l = 82.5

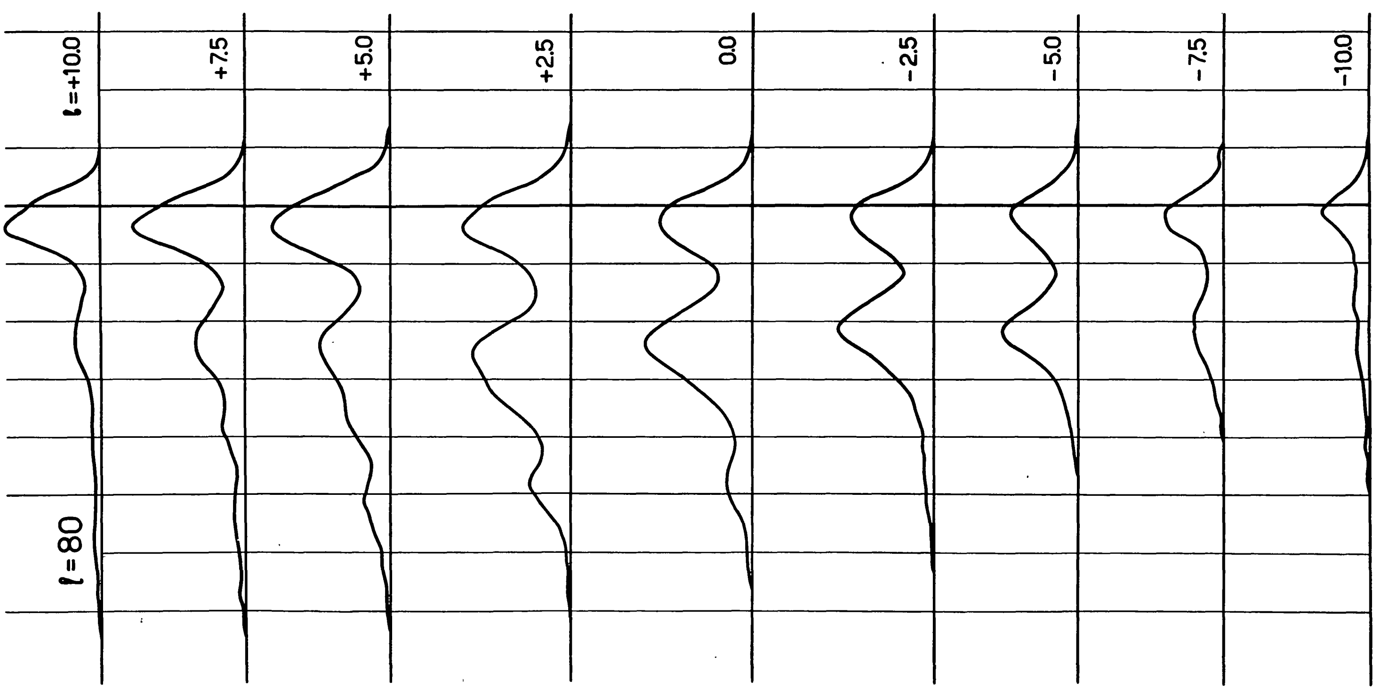

b = +10.0
+7.5
+5.0
+2.5
0.0
-2.5
-5.0
-7.5
-10.0
l = 80

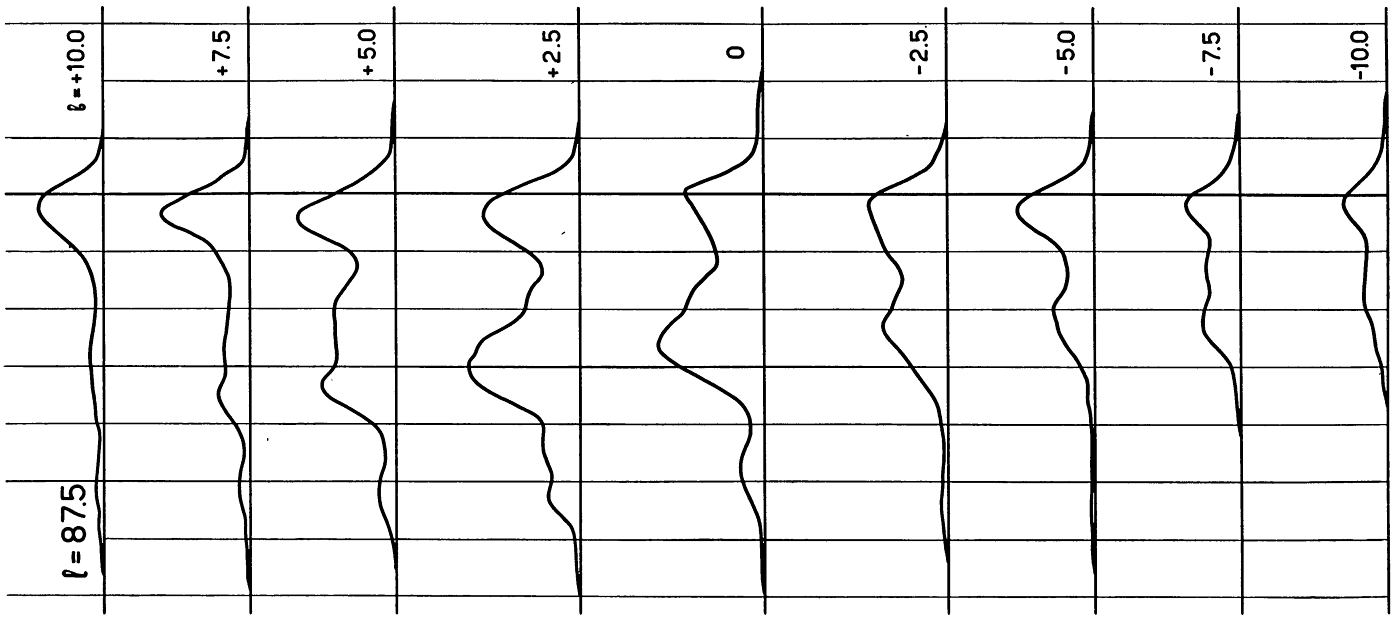

l = 87.5
b = +10.0
+7.5
+5.0
+2.5
0
-2.5
-5.0
-7.5
-10.0

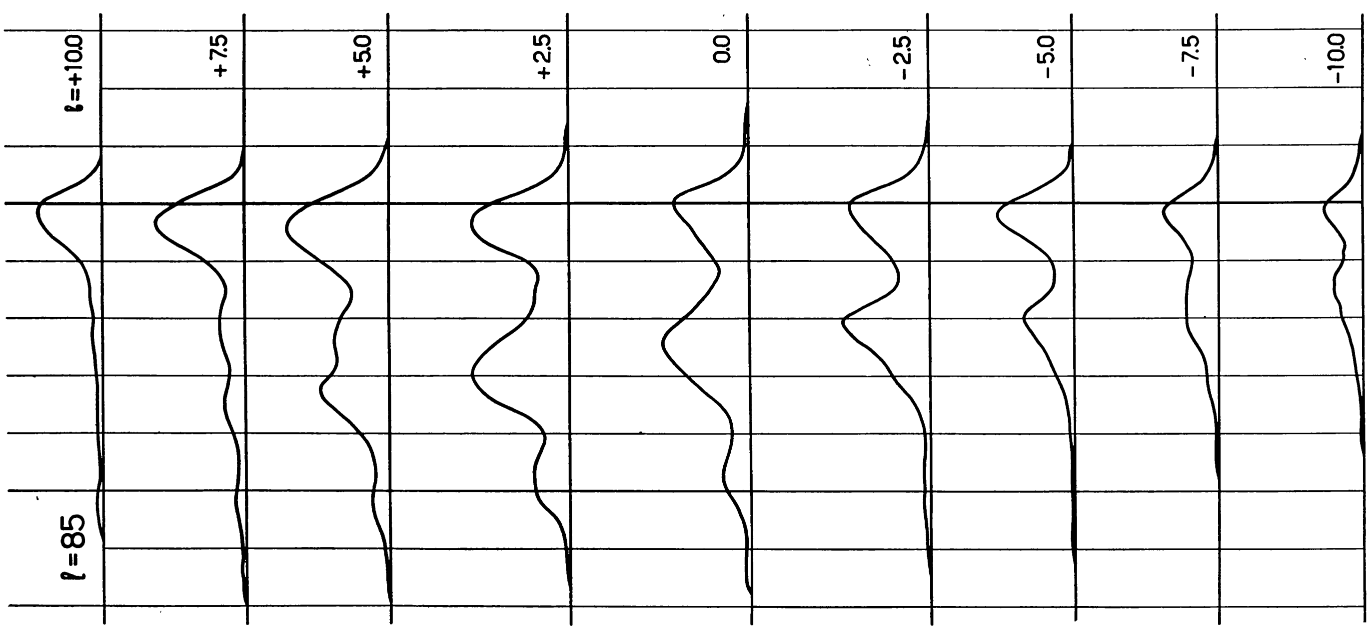

l = 85
b = +10.0
+7.5
+5.0
+2.5
0.0
-2.5
-5.0
-7.5
-10.0

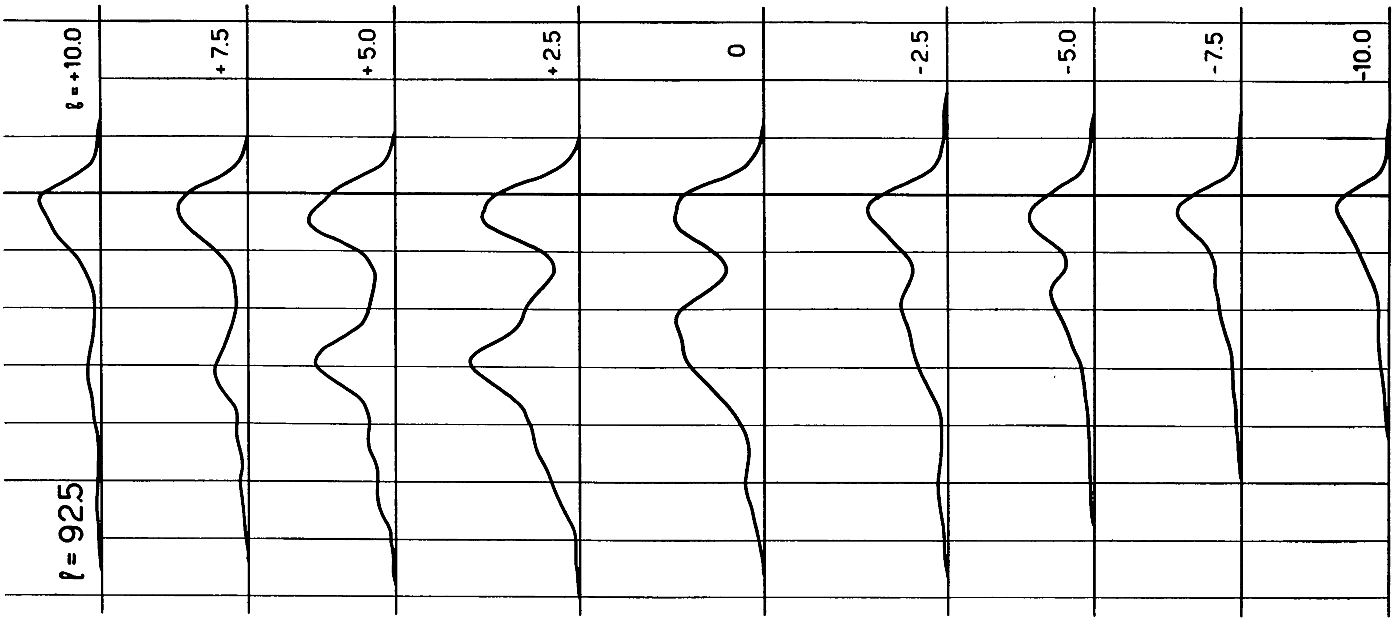
b = +10.0
+7.5
+5.0
+2.5
0
-2.5
-5.0
-7.5
-10.0
l = 92.5


b = +10.0
+7.5
+5.0
+2.5
0.0
-2.5
-5.0
-7.5
-10.0
l = 90

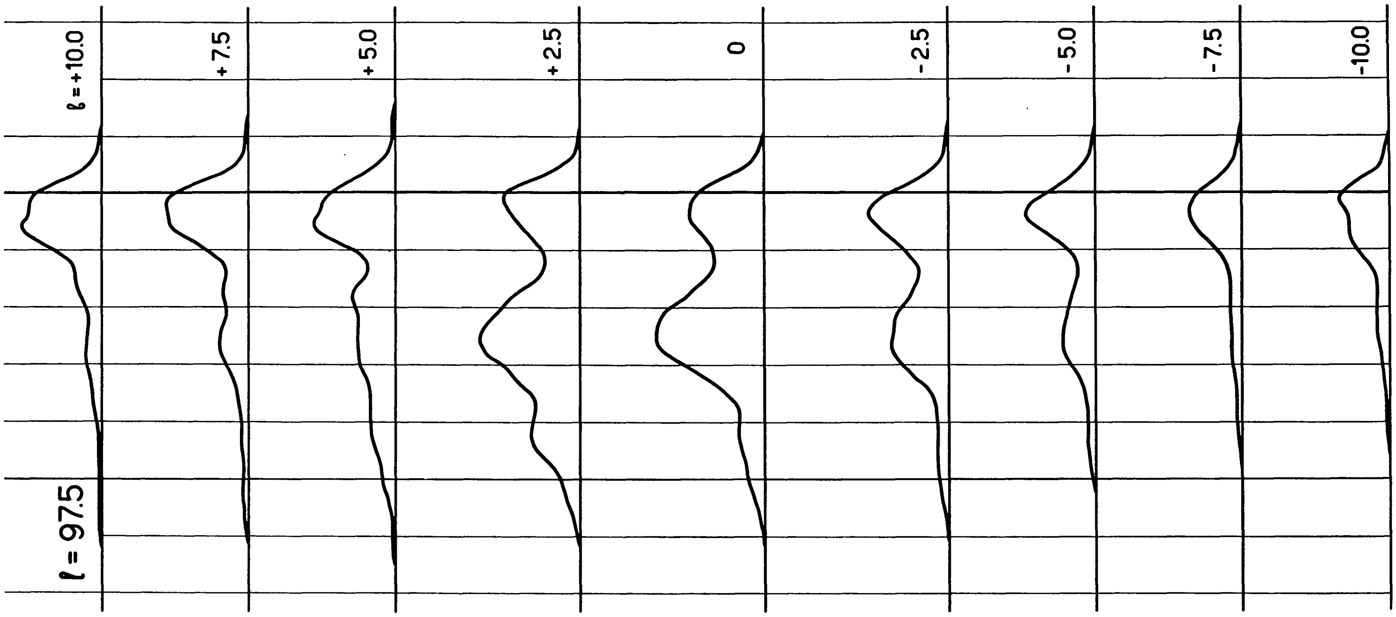
l = +10.0
+7.5
+5.0
+2.5
0
-2.5
-5.0
-7.5
-10.0
l = 97.5

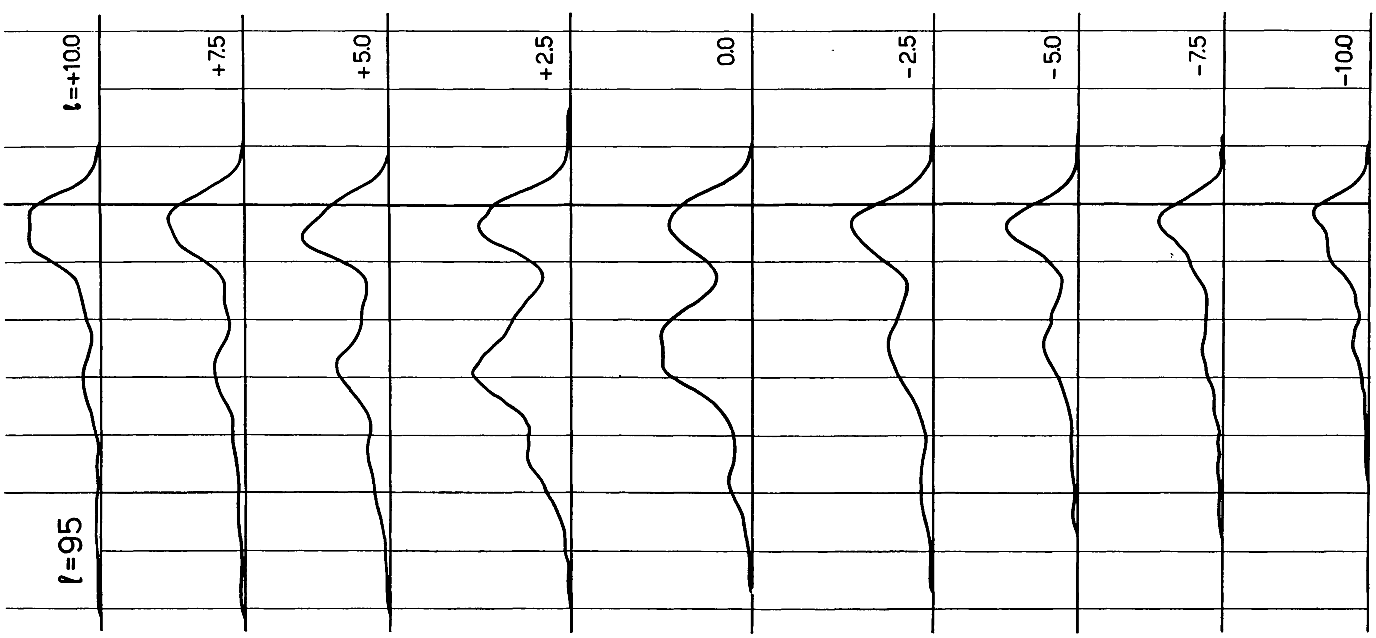
l = +10.0
+7.5
+5.0
+2.5
0.0
-2.5
-5.0
-7.5
-10.0
l = 95

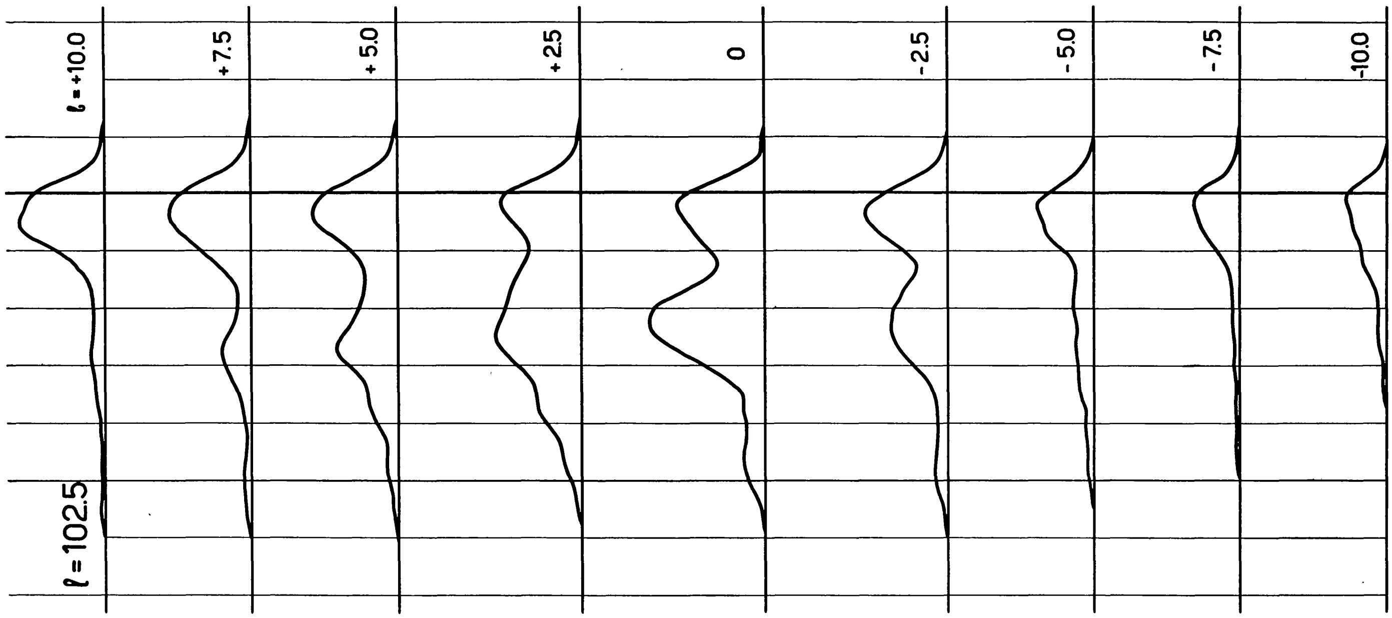
b = +10.0
+7.5
+5.0
+2.5
0
-2.5
-5.0
-7.5
-10.0
l = 102.5

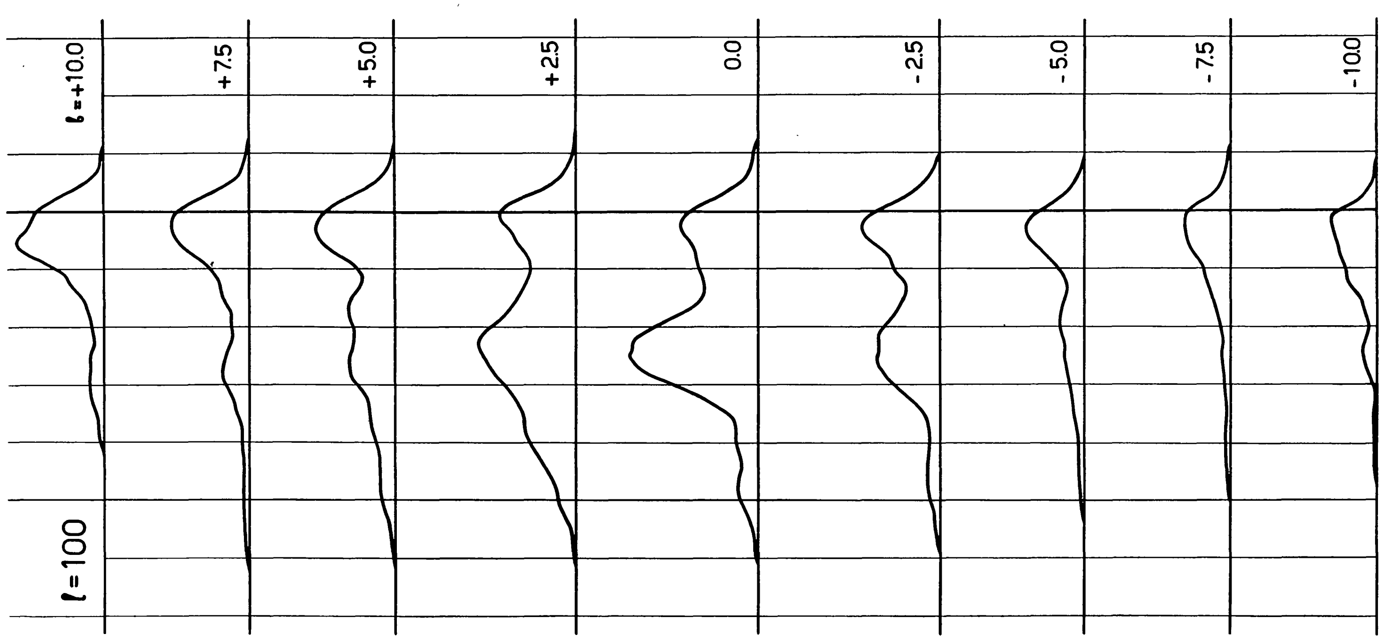
b = +10.0
+7.5
+5.0
+2.5
0.0
-2.5
-5.0
-7.5
-10.0
l = 100

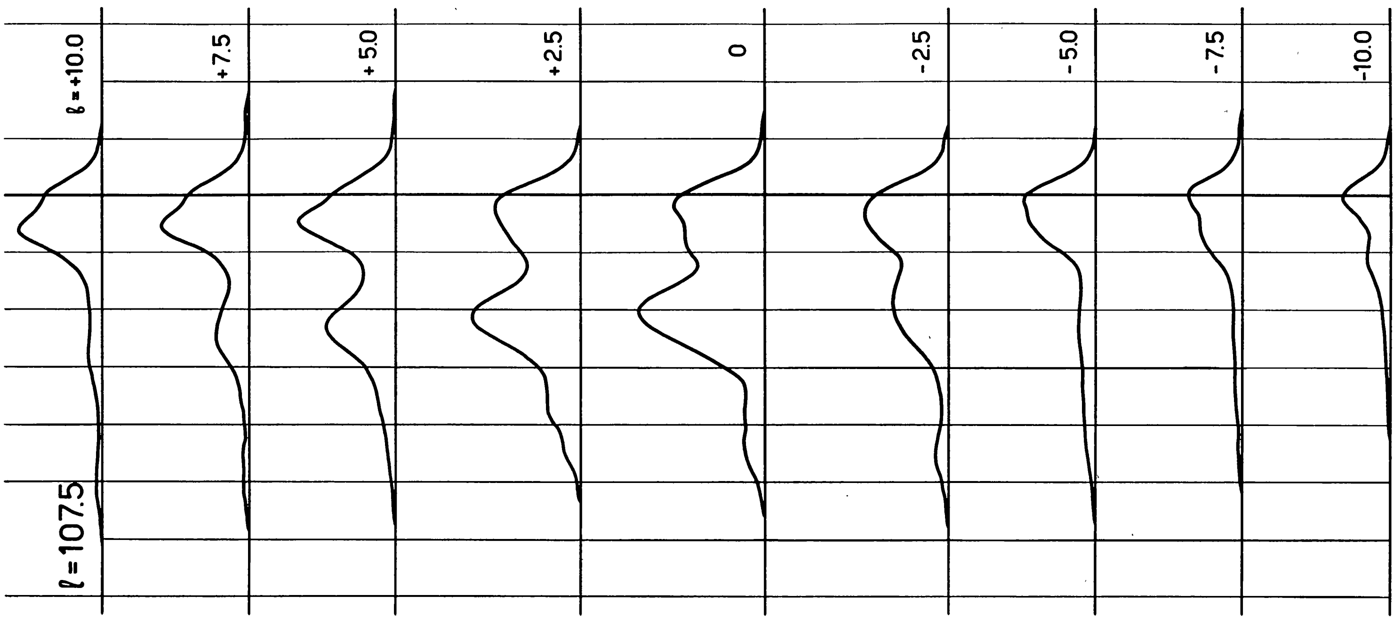
b = +10.0
+7.5
+5.0
+2.5
0
-2.5
-5.0
-7.5
-10.0
l = 107.5

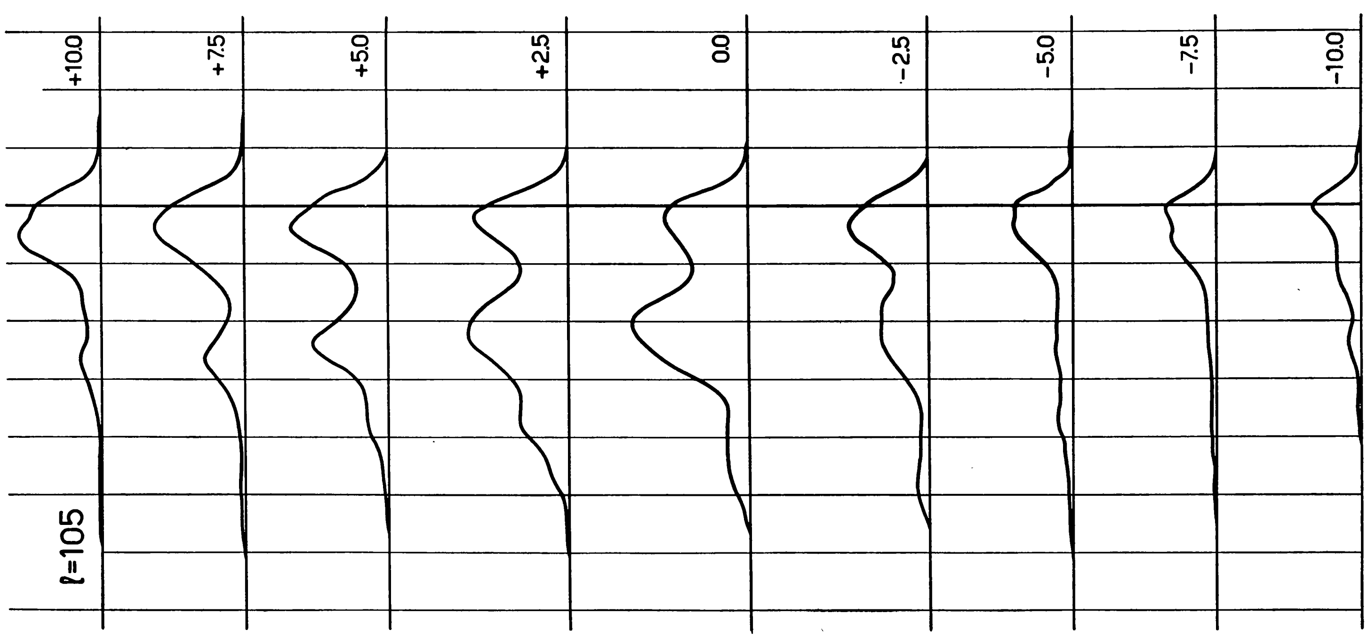
+10.0
+7.5
+5.0
+2.5
0.0
-2.5
-5.0
-7.5
-10.0
l = 105

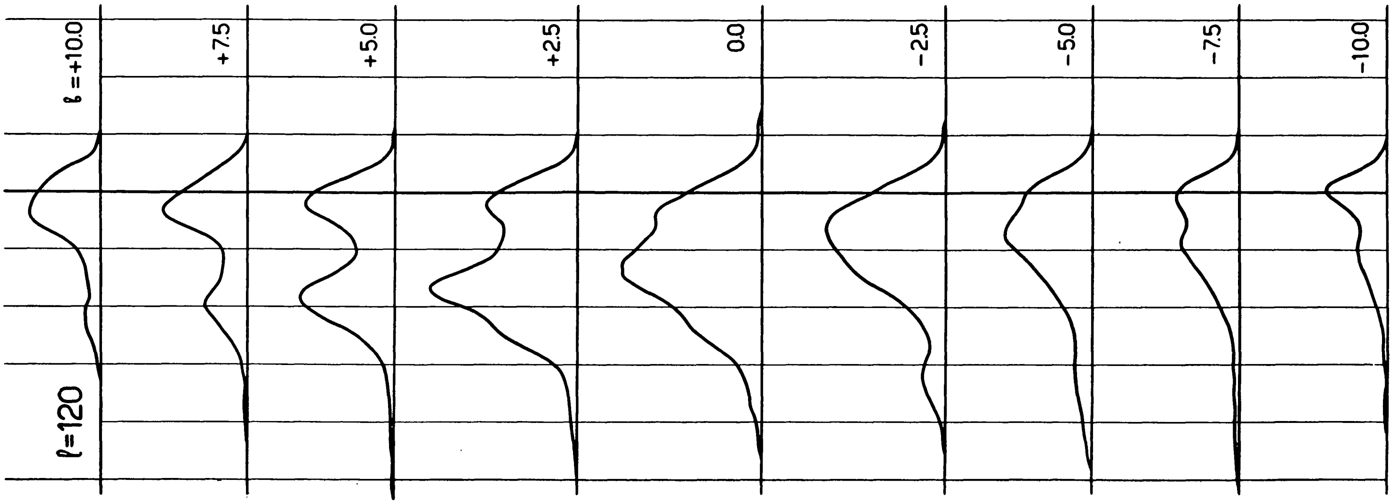
b = +10.0
+7.5
+5.0
+2.5
0.0
−2.5
−5.0
−7.5
−10.0
l = 120

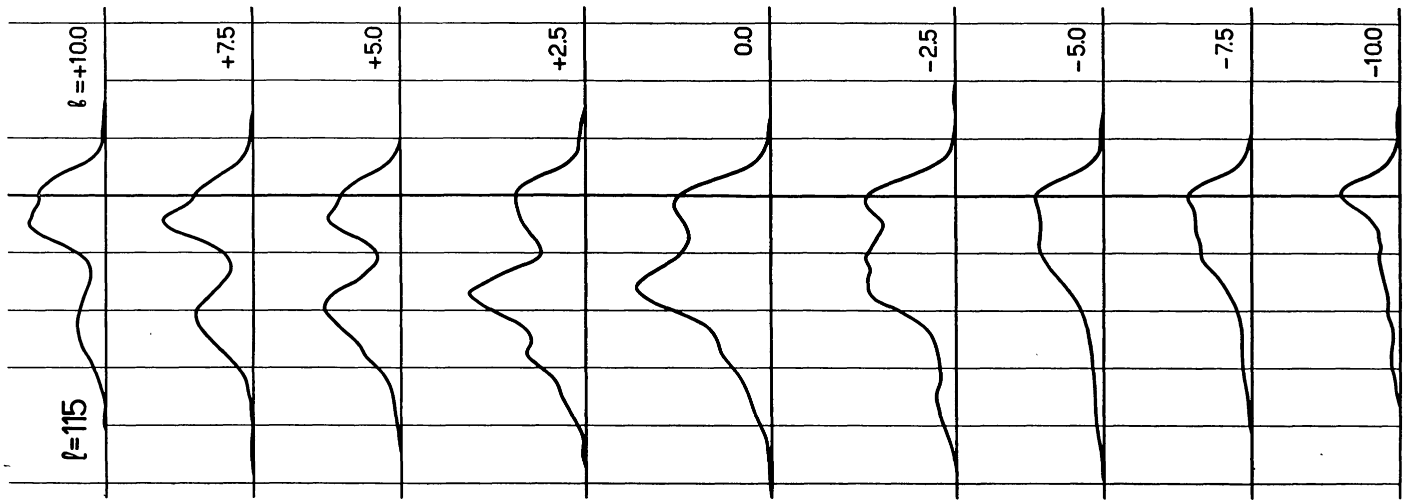
b = +10.0
+7.5
+5.0
+2.5
0.0
−2.5
−5.0
−7.5
−10.0
l = 115

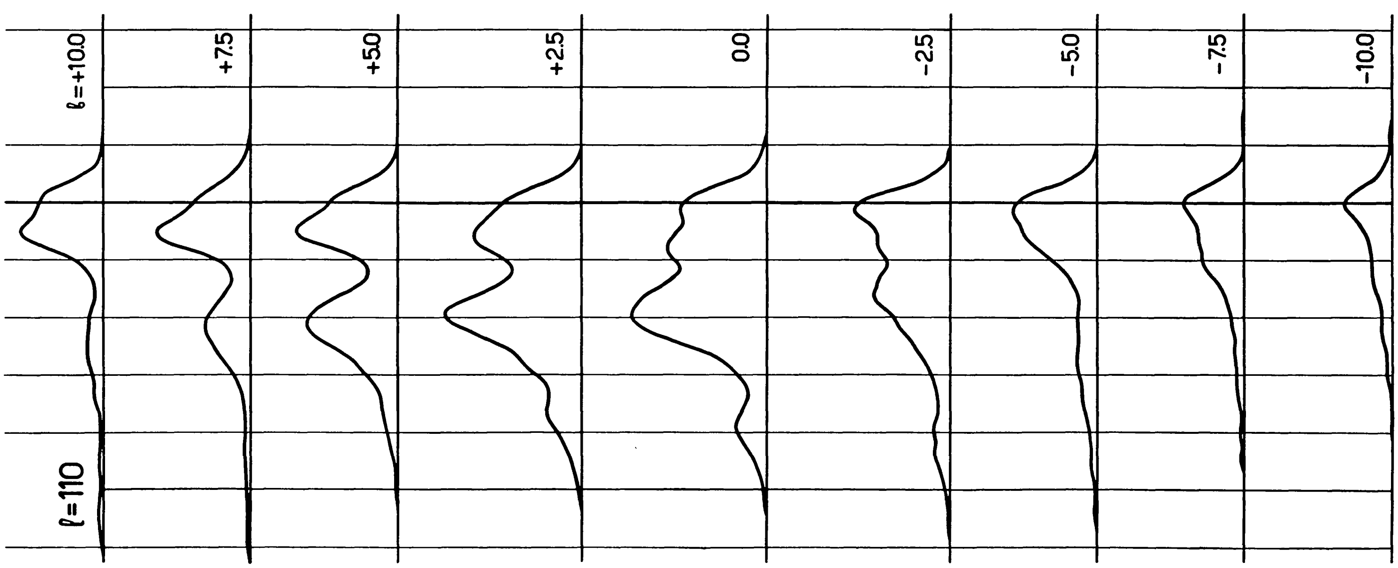
b = +10.0
+7.5
+5.0
+2.5
0.0
−2.5
−5.0
−7.5
−10.0
l = 110

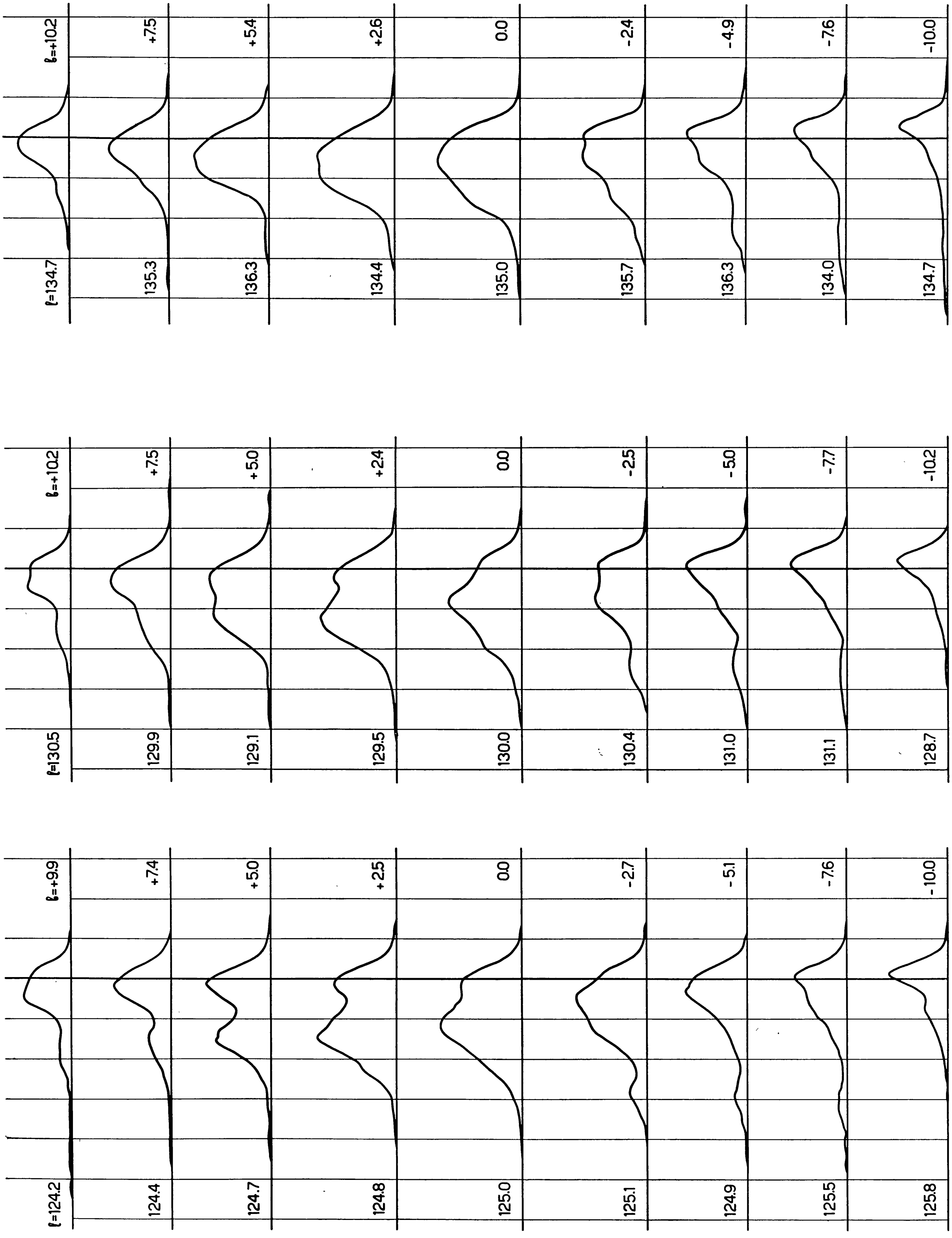
b=+10.2
+7.5
+5.4
+2.6
0.0
-2.4
-4.9
-7.6
-10.0
l=134.7
135.3
136.3
134.4
135.0
135.7
136.3
134.0
134.7
b=+10.2
+7.5
+5.0
+2.4
0.0
-2.5
-5.0
-7.7
-10.2
l=130.5
129.9
129.1
129.5
130.0
130.4
131.0
131.1
128.7
b=+9.9
+7.4
+5.0
+2.5
0.0
-2.7
-5.1
-7.6
-10.0
l=124.2
124.4
124.7
124.8
125.0
125.1
124.9
125.5
125.8

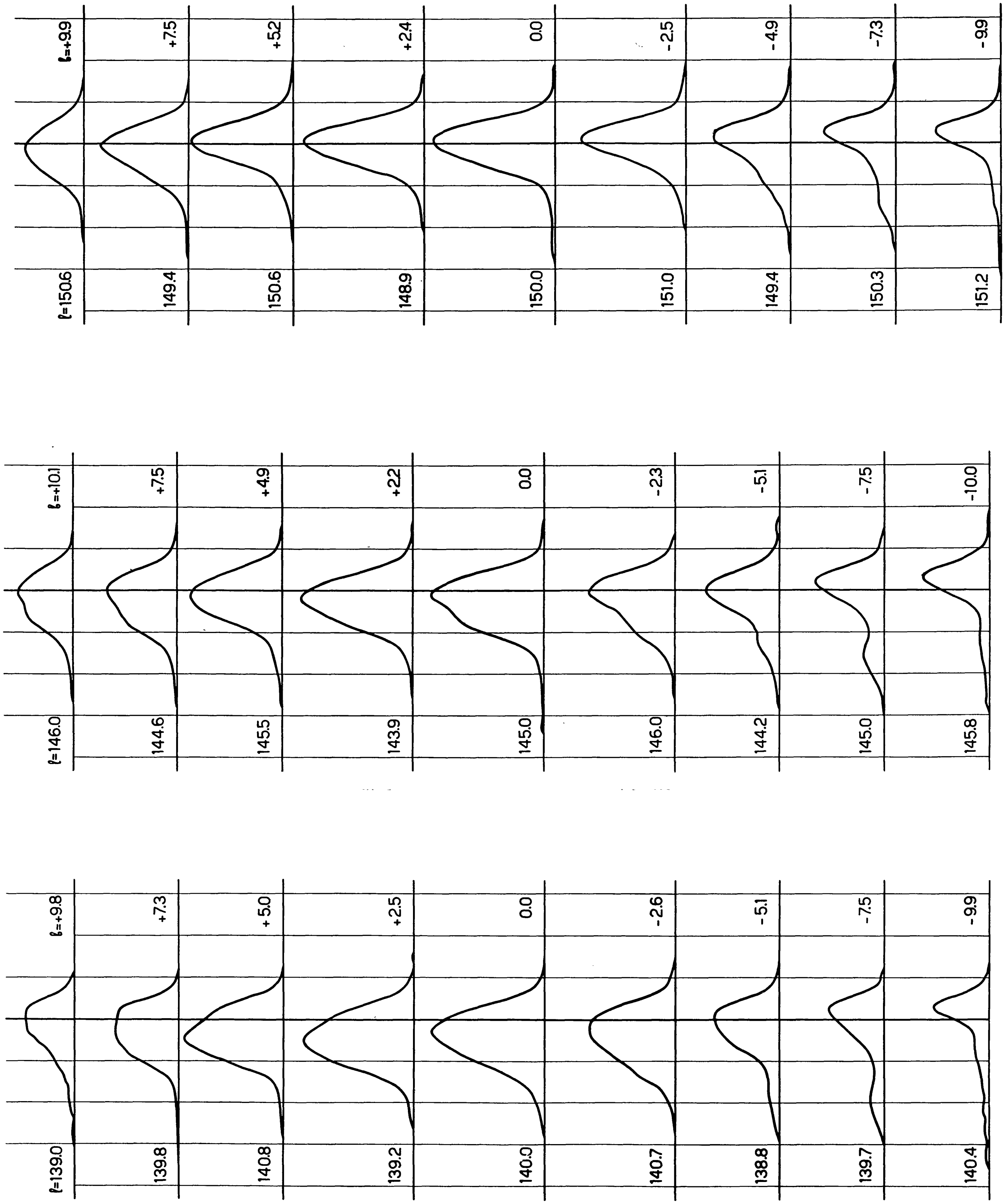
b=+9.9
+7.5
+5.2
+2.4
0.0
-2.5
-4.9
-7.3
-9.9
l=150.6
149.4
150.6
148.9
150.0
151.0
149.4
150.3
151.2
b=+10.1
+7.5
+4.9
+2.2
0.0
-2.3
-5.1
-7.5
-10.0
l=146.0
144.6
145.5
143.9
145.0
146.0
144.2
145.0
145.8
b=+9.8
+7.3
+5.0
+2.5
0.0
-2.6
-5.1
-7.5
-9.9
l=139.0
139.8
140.8
139.2
140.0
140.7
138.8
139.7
140.4

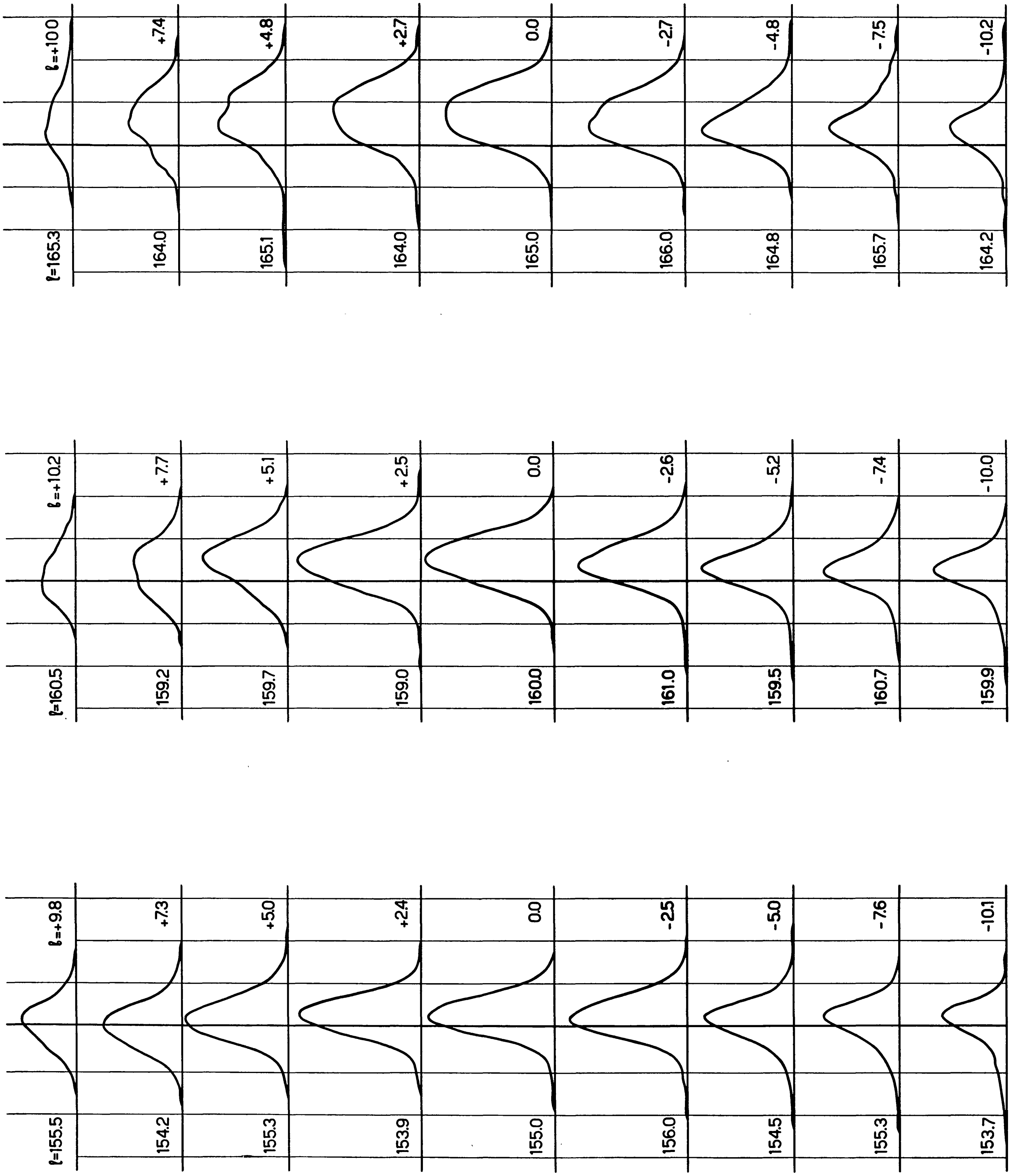
l=+10.0
+7.4
+4.8
+2.7
0.0
-2.7
-4.8
-7.5
-10.2
l=165.3
164.0
165.1
164.0
165.0
166.0
164.8
165.7
164.2
l=+10.2
+7.7
+5.1
+2.5
0.0
-2.6
-5.2
-7.4
-10.0
l=160.5
159.2
159.7
159.0
160.0
161.0
159.5
160.7
159.9
l=+9.8
+7.3
+5.0
+2.4
0.0
-2.5
-5.0
-7.6
-10.1
l=155.5
154.2
155.3
153.9
155.0
156.0
154.5
155.3
153.7

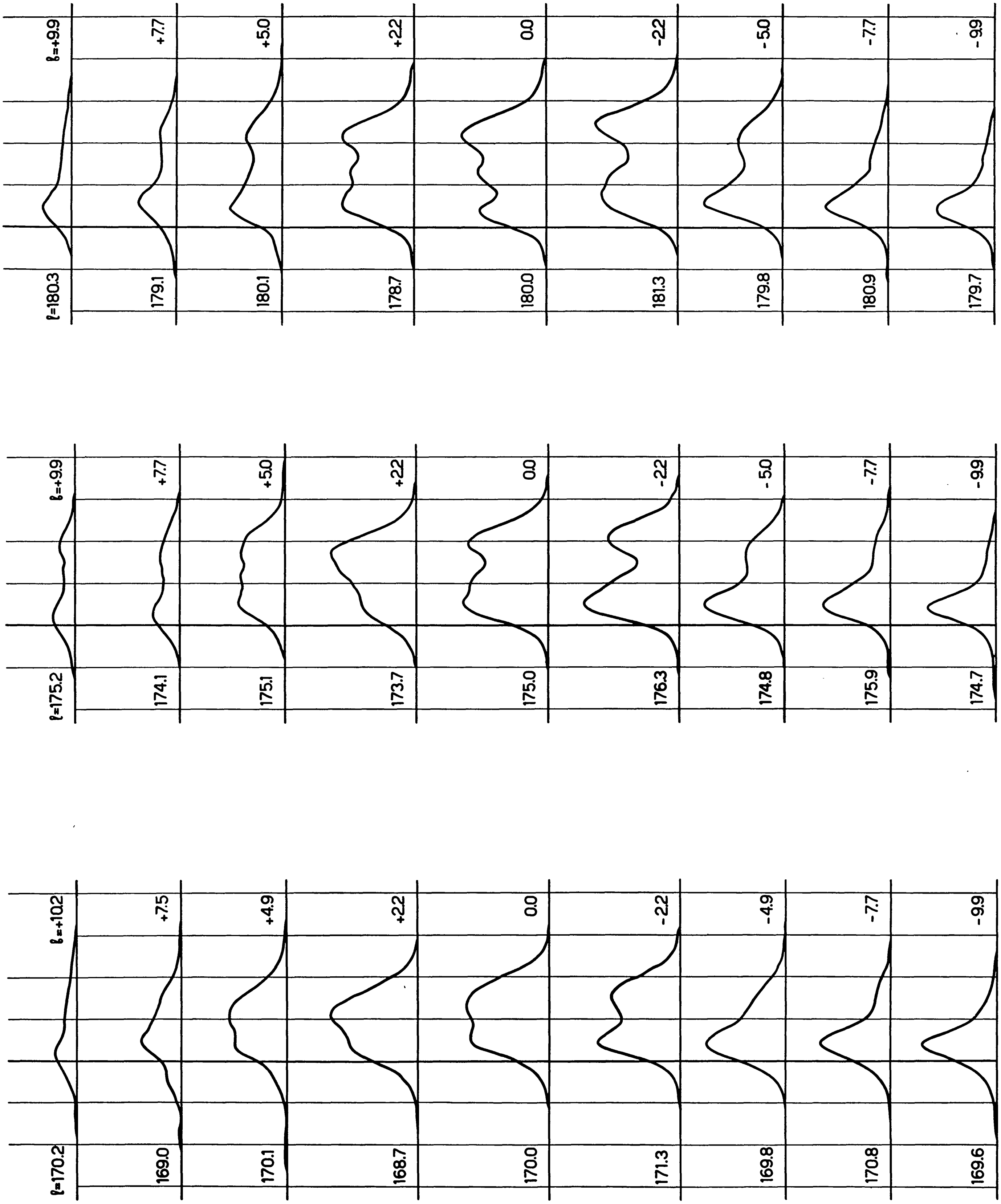

b=+9.9
+7.7
+5.0
+2.2
0.0
-2.2
-5.0
-7.7
-9.9
ℓ=180.3
179.1
180.1
178.7
180.0
181.3
179.8
180.9
179.7
b=+9.9
+7.7
+5.0
+2.2
0.0
-2.2
-5.0
-7.7
-9.9
ℓ=175.2
174.1
175.1
173.7
175.0
176.3
174.8
175.9
174.7
b=+10.2
+7.5
+4.9
+2.2
0.0
-2.2
-4.9
-7.7
-9.9
ℓ=170.2
169.0
170.1
168.7
170.0
171.3
169.8
170.8
169.6

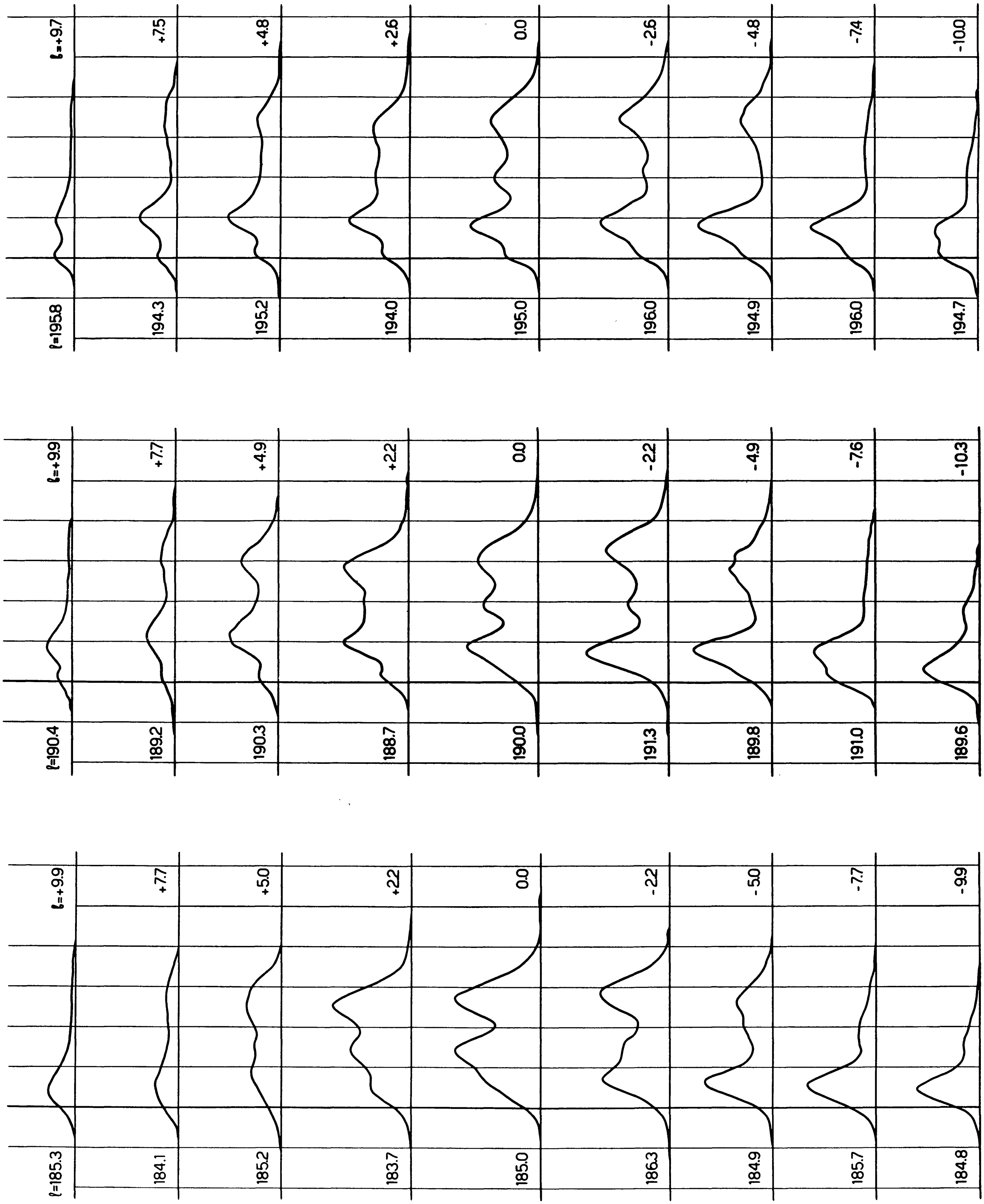
b=+9.7
+7.5
+4.8
+2.6
0.0
-2.6
-4.8
-7.4
-10.0
l=195.8
194.3
195.2
194.0
195.0
196.0
194.9
196.0
194.7
b=+9.9
+7.7
+4.9
+2.2
0.0
-2.2
-4.9
-7.6
-10.3
l=190.4
189.2
190.3
188.7
190.0
191.3
189.8
191.0
189.6
b=+9.9
+7.7
+5.0
+2.2
0.0
-2.2
-5.0
-7.7
-9.9
l=185.3
184.1
185.2
183.7
185.0
186.3
184.9
185.7
184.8

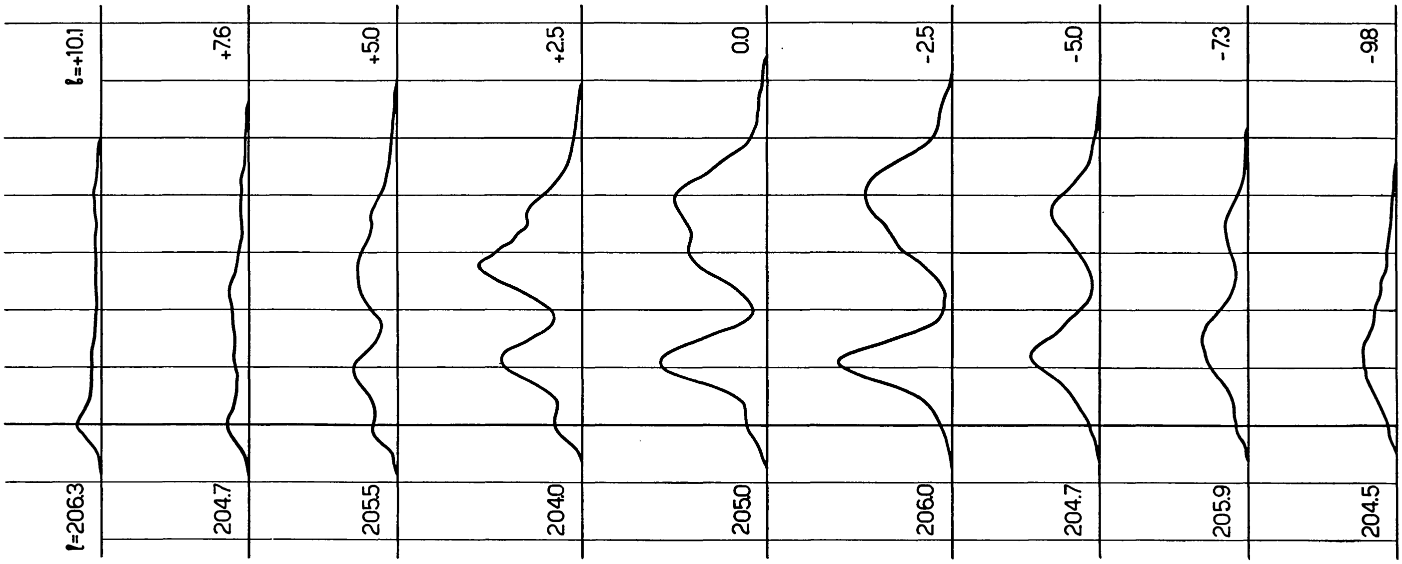
b=+10.1
+7.6
+5.0
+2.5
0.0
-2.5
-5.0
-7.3
-9.8
l=206.3
204.7
205.5
204.0
205.0
206.0
204.7
205.9
204.5

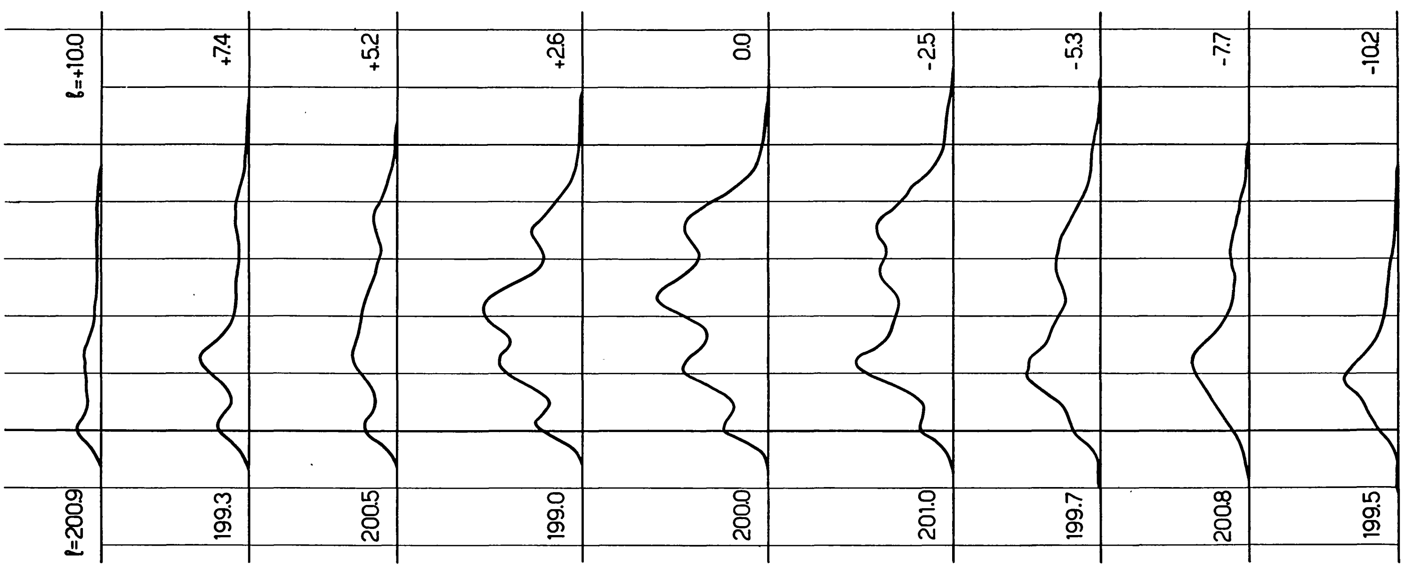
b=+10.0
+7.4
+5.2
+2.6
0.0
-2.5
-5.3
-7.7
-10.2
l=200.9
199.3
200.5
199.0
200.0
201.0
199.7
200.8
199.5

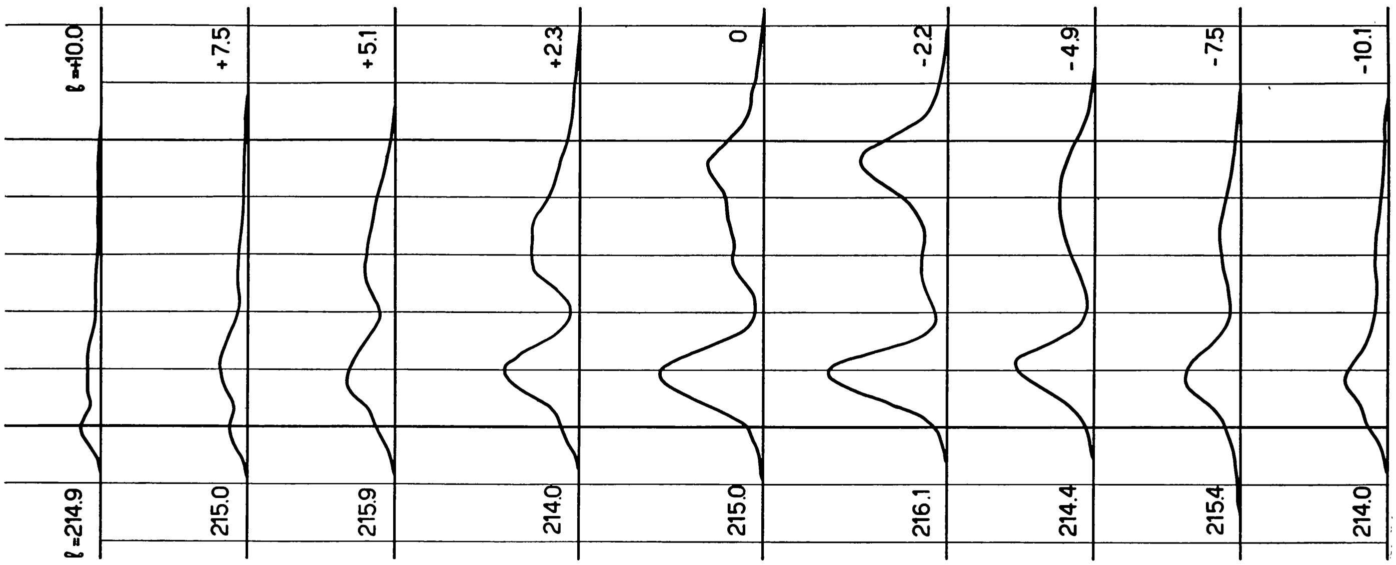
b =+10.0
+7.5
+5.1
+2.3
0
-2.2
-4.9
-7.5
-10.1
l =214.9
215.0
215.9
214.0
215.0
216.1
214.4
215.4
214.0

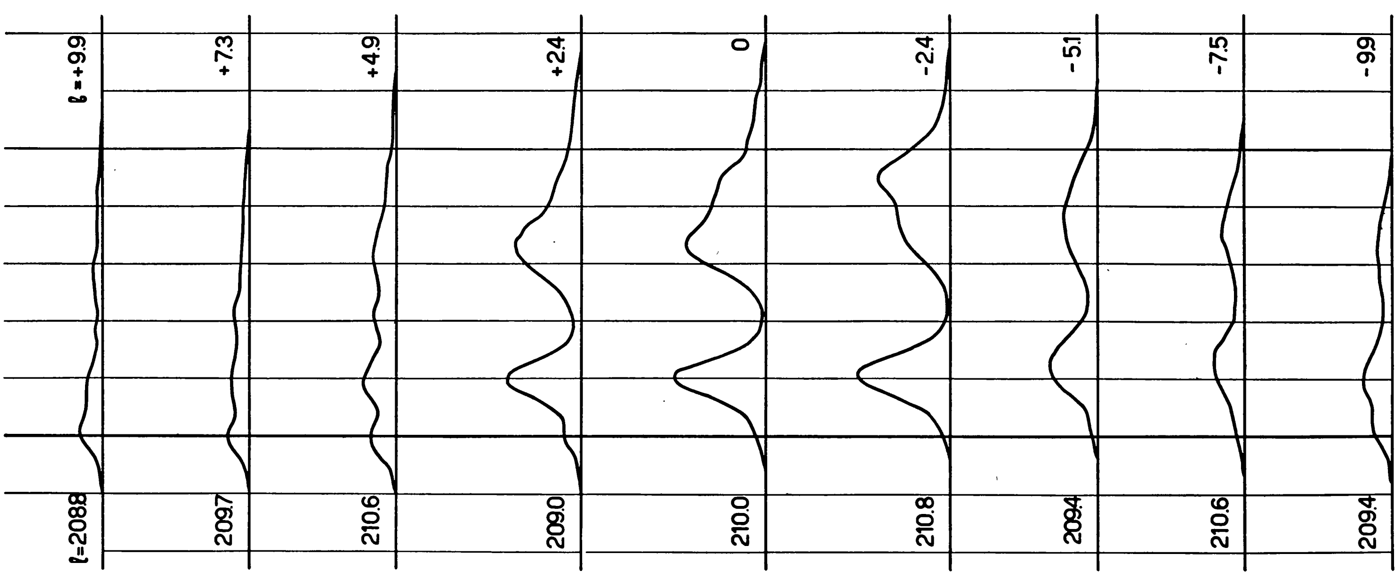
b =+9.9
+7.3
+4.9
+2.4
0
-2.4
-5.1
-7.5
-9.9
l=208.8
209.7
210.6
209.0
210.0
210.8
209.4
210.6
209.4

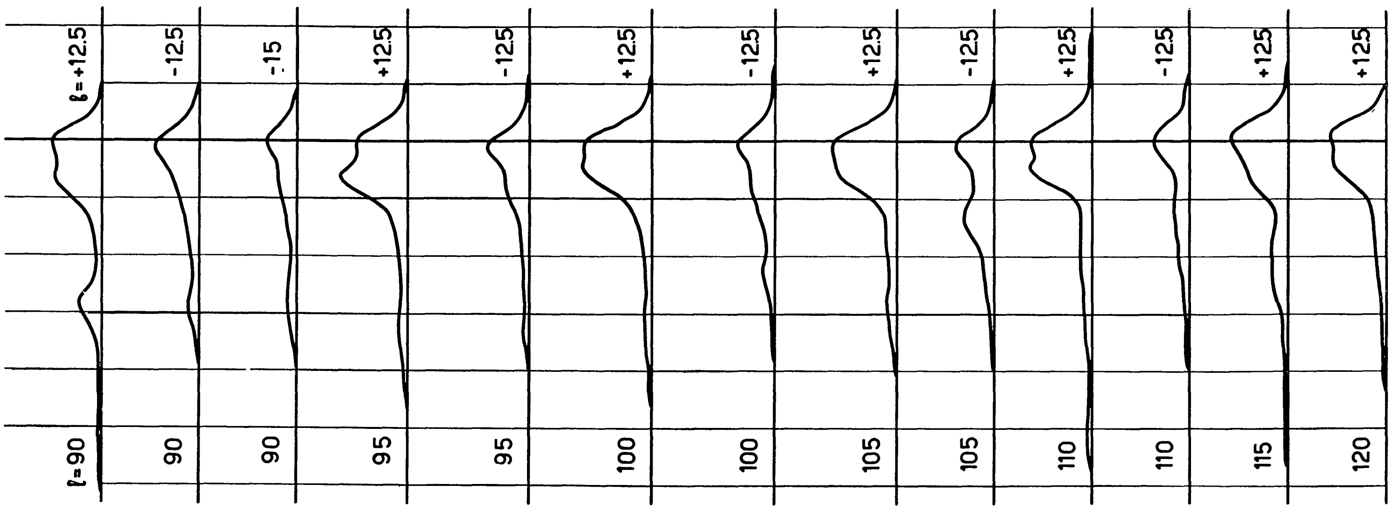

l=90 b=+12.5
90 -12.5
90 -15
95 +12.5
95 -12.5
100 +12.5
100 -12.5
105 +12.5
105 -12.5
110 +12.5
110 -12.5
115 +12.5
120 +12.5

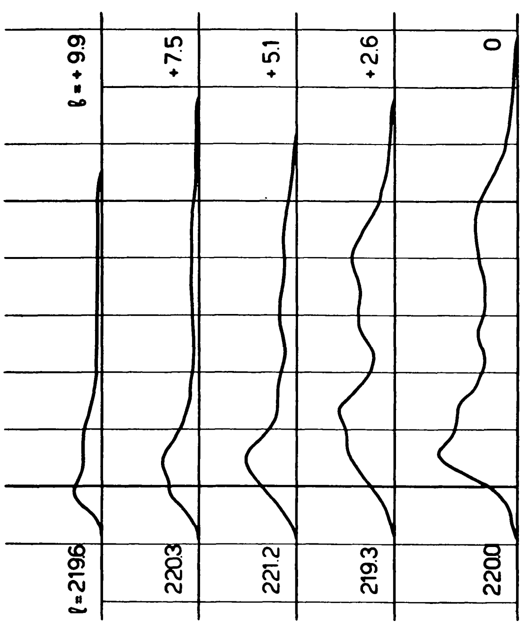

l=219.6 b=+9.9
220.3 +7.5
221.2 +5.1
219.3 +2.6
220.0 0

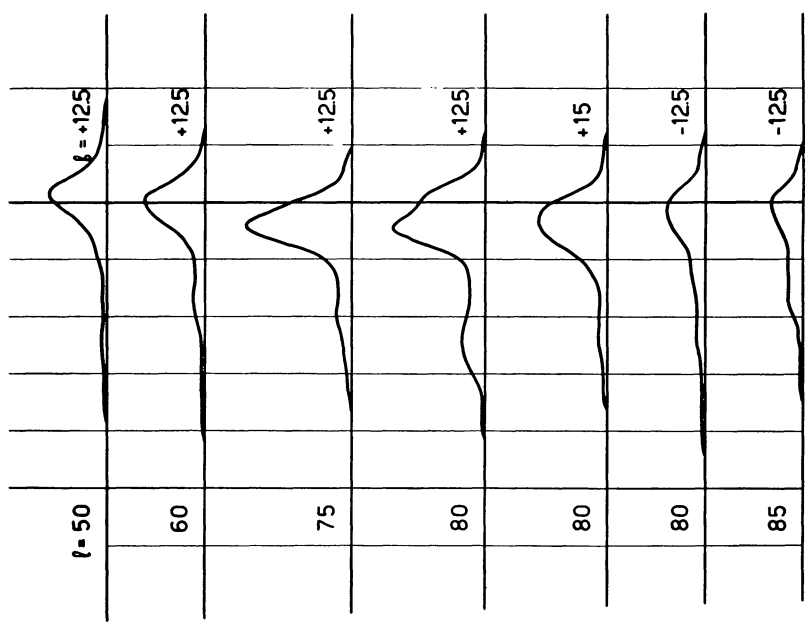

l=50 b=+12.5
60 +12.5
75 +12.5
80 +12.5
80 +15
80 -12.5
85 -12.5

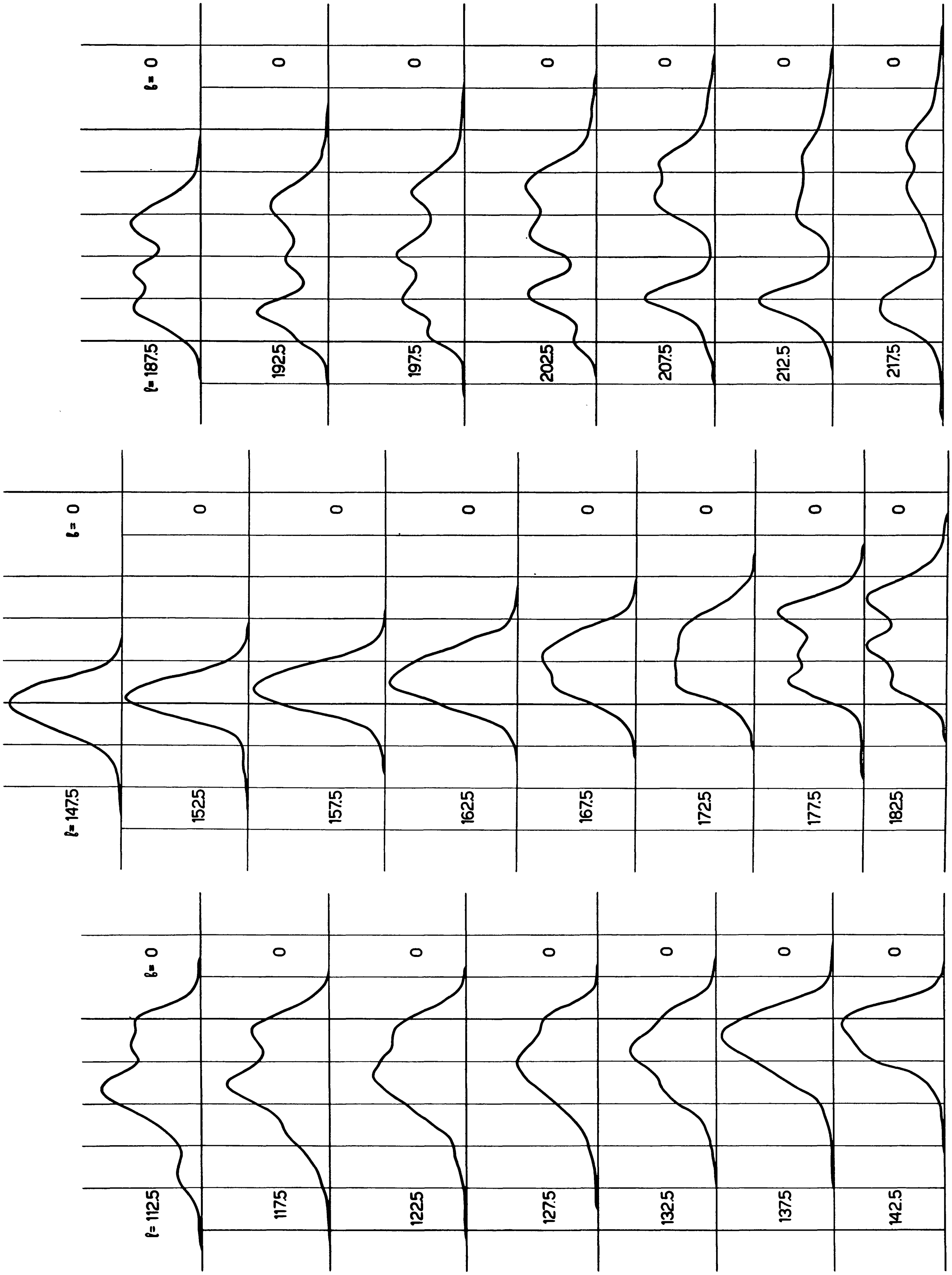
b = 0
l = 187.5
192.5
197.5
202.5
207.5
212.5
217.5
l = 147.5
152.5
157.5
162.5
167.5
172.5
177.5
182.5
l = 112.5
117.5
122.5
127.5
132.5
137.5
142.5
0